THE
PHYSICAL REVIEW
A Journal of Experimental and Theoretical Physics Established by E. L. Nichols in 1893
VOL. 50, NO. 6 SEPTEMBER 15, 1936 SECOND SERIES

On the Allowed Cone of Cosmic Radiation

G. LEMAITRE AND M. S. VALLARTA, *University of Louvain and Massachusetts Institute of Technology*
(Received July 15, 1936)

Further results of an extensive study of trajectories asymptotic to a known family of unstable periodic orbits in the earth's dipolar magnetic field, carried out by means of Bush's differential analyzer, are presented in this paper. A detailed discussion is given of our methods of determining asymptotic trajectories by means of the differential analyzer and by numerical integration of a whole family at a time; comparison of the results obtained shows the absence of systematic errors of any consequence in the mechanical integrations and exhibits the precision attained with the differential analyzer. The families of asymptotic trajectories are then analyzed systematically in order to determine the main cones for latitudes up to 30°. This leads to the theory of the azimuthal effect and a study of the region in the vicinity of the zenith.

IN a preceding paper[1] to which reference should be made for a complete statement of the problem treated here and of our methods of attack, we gave results obtained from the analysis of some three hundred asymptotic trajectories to a known family of unstable periodic orbits found by means of Bush's differential analyzer[2] and discussed fully the sections of the main allowed cones of cosmic radiation by the meridian plane, which in turn led us to the theory of the north-south asymmetry. Those results were presented at the time with reservations as far as a critical examination of their precision was concerned. We have now been able to complete the calculations announced in our preceding paper, to which we shall return below, with the result that suspected systematic errors are so small that they can well be neglected. Certain other points which were then summarily sketched will now be developed in detail; in particular we shall present here a full discussion of our method of determination of asymptotic trajectories by means of the differential analyzer and a fairly complete determination of the main allowed cones for geomagnetic latitudes up to 30°. The last two sections will be devoted to the analysis of the azimuthal effect and to a study of the region in the vicinity of the zenith.

1. The Determination of Asymptotic Trajectories by Means of Bush's Differential Analyzer

The differential equations of motion to be integrated are (reference 1, Eqs. (4), (5))

$$d^2x/d\sigma^2=(1/(2\gamma_1)^4)e^{2z}-e^{-z}+e^{-2z}\cos^2\lambda,$$
$$d^2\lambda/d\sigma^2=e^{-2z}\sin\lambda\cos\lambda-(\sin\lambda/\cos^3\lambda). \quad (1)$$

Our problem is to find the solutions of these differential equations corresponding to trajectories asymptotic to a known family of unstable periodic orbits.

[1] G. Lemaitre and M. S. Vallarta, Phys. Rev. **49**, 719 (1936).
[2] V. Bush, J. Frank. Inst. **212**, 447 (1931).

Before asymptotic trajectories can be studied, a full theory of the family of periodic orbits mentioned above must be available. The family in question was discovered by Störmer[3] who was also able to calculate two of its members by his method of numerical integration. A complete treatment of the family has been given by one of us[4] so that any one of its members can be calculated without great trouble and with high precision. While the details of these calculations would be out of place here and consequently are left for a separate paper, the results are reproduced in Fig. 1 where the small circles are the points on the periodic orbits of phase 0°, 15° 30°, ··· 90° which were computed. The equi-phase line 90°, i.e., the locus of the vertices of the periodic orbits which is important for our purpose as further discussed in a later section of this paper, has also been drawn in the figure.

Solutions of the system (1) representing the desired asymptotic trajectories and valid in the vicinity of the periodic orbits have been given by Bouckaert;[5] other methods which we have recently developed and to which we return below are now available. In order to extend these solutions to the region of low energies and high latitudes, however, recourse must be had in general either to methods of numerical integration such as the one outlined in a later section of this paper or to methods of mechanical integration such as that developed by Bush,[2] because in general the system (1) cannot be integrated in terms of known functions. Since the knowledge of several hundred asymptotic trajectories is required for a satisfactory treatment of our problem the first line of attack involves a very large amount of tedious labor while the second can still be carried through in much shorter time.

An outline of our method of determination of asymptotic trajectories by means of Bush's differential analyzer has already been published.[1] Here we add only such details as are needed for a full understanding of our line of attack and of the results obtained. A first integration of the system (1) yields

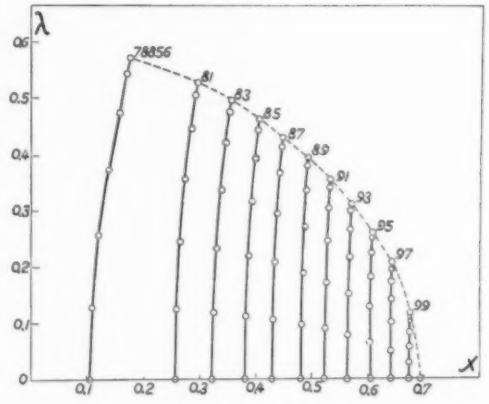

FIG. 1. The family of periodic orbits.

$$dx/d\sigma = \int ((e^{4x}/16\gamma_1^4) - e^x + \cos^2\lambda)e^{-2x}d\sigma,$$
$$d\lambda/d\sigma = \int (e^{-2x} - (1/\cos^4\lambda))\sin\lambda\cos\lambda d\sigma. \quad (2)$$

When written in the above form, suggested by S. H. Caldwell, the system (1) may be immediately set in the differential analyzer now available at the Massachusetts Institute of Technology and solved mechanically. This differential analyzer has ordinarily four input tables and six integrators, but an ingenious change in the machine connections devised for the present problem by S. H. Caldwell enables the use of the output table simultaneously as an input table so that in all five input tables and six integrators were available. Of these five input tables, two are needed to introduce in the machine the functions $e^{4x}/16\gamma_1^4 - e^x$ and e^{-2x}, and three more to introduce $\cos^2\lambda$, $1/\cos^4\lambda$ and $\sin\lambda\cos\lambda$. Of the six integrators, two are required to integrate the product of the two functions under the integral sign in each of the two equations (2), and two more to integrate the derivatives $dx/d\sigma$ and $d\lambda/d\sigma$ so as to obtain x and λ. The output table is then controlled so as to plot x as abscissa and λ as ordinate.

The scale factors are determined from the range of x and λ which it is desired to explore. For the present investigation the scales were so chosen that x could vary from -1.0 to 0.7, λ from -0.7 to 1.0, $dx/d\sigma$ and $d\lambda/d\sigma$ from -0.5 to 0.5. The limits of the last two functions were found from a study of the energy integral (reference 1, Eq. (5)).

[3] C. Störmer, Zeits. f. Astrophys. **1**, 237 (1930).
[4] G. Lemaitre, Ann. de la Soc. Sci. de Bruxelles **A54**, 194 (1935).
[5] L. Bouckaert, Ann. de la Soc. Sci. de Bruxelles **A54**, 174 (1935).

TABLE I. *Data for some of the fundamental points.*

$\gamma_1=$	1	0.87	0.90	0.93	0.96
x	μ_0	η	η	η	η
0.075	3.1587	1.166	1.022	0.850	—
0.100	3.2127	—	—	—	—
0.125	3.2829	—	—	—	—
0.150	3.3670	1.211	1.062	0.890	—
0.175	3.4647	—	—	—	—
0.200	3.5790	—	—	—	0.721
0.225	3.7114	1.281	1.133	0.959	0.738
0.250	3.8608	—	—	—	—
0.275	4.0352	—	—	—	—
0.300	4.2342	1.371	1.266	1.051	0.821

TABLE II. *Values of the initial angle for $\gamma_1=0.91$ for all equatorial runs.*

x	ν	μ	η
0.075	−0.753	3.2265	0.968
0.100	−0.531	3.2605	0.978
0.125	−0.252	3.3056	0.992
0.150	0.084	3.359	1.008
0.175	0.380	3.431	1.029
0.200	0.760	3.511	1.053
0.225	1.276	3.596	1.079
0.250	1.914	3.689	1.107
0.275	2.745	3.788	1.136
0.300	3.650	3.907	1.172

The initial conditions are introduced into the machine knowing x, λ and the initial slope $\tan\eta$. The knowledge of x and λ is sufficient to set the starting points on the input tables. To set the starting points on each one of the six integrators it is necessary to calculate the values of the functions e^{-2x},

$$e^{4x}/16\gamma_1{}^4-e^x+\cos^2\lambda, \quad e^{-2x}-1/\cos^4\lambda,$$

$$\sin\lambda\cos\lambda, \quad dx/d\sigma \quad \text{and} \quad d\lambda/d\sigma.$$

The first four are computed from the known values of x and λ, the last two from the initial inclination η by the relations

$$dx/d\sigma=P^{\frac{1}{2}}\cos\eta; \quad d\lambda/d\sigma=P^{\frac{1}{2}}\sin\eta, \qquad (3)$$

where P is given by Eq. (5).[1]

For the efficient operation of the machine it is important that the calculations described above be carried out rapidly and accurately. For this purpose master sheets were prepared in advance giving the value of the required functions from $x=-0.125$ to $x=0.350$ by intervals of 0.025 along the equator where P reduces to $e^{2x}/16\gamma_1{}^4-(e^{-x}-1)^2$ and for every degree of latitude along the line $\theta=0$ where $P=e^{2x}/16\gamma_1{}^4$.

As already mentioned in our preceding paper,[1] for convenience trajectories were always started either from the equator or from the line $\theta=0$. Once the master sheets are ready it is easy to calculate the initial conditions while the machine is tracing a trajectory, i.e., in the interval of a few minutes.

As already mentioned in our preceding paper one method for the determination of asymptotic trajectories consists in choosing a point on the equator within the periodic orbit and the initial slope arbitrarily. The initial conditions having been set on the machine, a trajectory is started in the direction towards the periodic orbit; the initial slope is then adjusted until the trajectory neither intersects nor falls short of the periodic orbit. More precisely let us suppose that the initial slope has been estimated not too far from the correct value, and assume for the sake of exemplification that the trajectory cuts through the periodic orbit. The initial angle is then increased by equal amounts, say of 0.008 radian until the trajectory falls decidedly short of the periodic orbit. The angle is then decreased by steps of 0.004 radian until the trajectory again cuts through, then increased by steps of 0.002 until the latter falls short, then again decreased by steps of 0.001 until it cuts through. In this way it is usually possible to determine the critical angle for an asymptotic orbit within around 0.001 radian by making from five to ten trials, each one taking from four to six minutes. That the critical angle is actually determined by this method with a precision of a few thousandths of a radian is confirmed by independent calculations of asymptotic trajectories to be more fully discussed in a later section of this paper.

In order to be free from the need of finding the critical angle for every equatorial point in the manner outlined in the preceding paragraph a method of interpolation was devised which permits the calculation of critical angles at intermediate points once the values at certain fundamental points have been ascertained. Let $\epsilon=1-\gamma_1$ and let

$$\mu_0=\lim_{\gamma_1\to 1}(\eta/\epsilon^{\frac{1}{2}}), \qquad (4)$$

η being the initial critical angle for a given value of x. The quantity μ_0 may be calculated from

TABLE III. *Initial conditions for various values of γ_1 and values of $x<0.075$ along the equator.*

γ_1 $=x$	0.87 η	0.89 η	0.91 η	0.93 η	0.95 η
−0.100	—	—	—	—	0.780
−0.075	—	—	—	0.890	0.747
−0.050	—	—	0.981	0.866	0.721
−0.025	—	—	0.965	0.852	0.707
0	1.160	1.050	0.957	0.840	0.703
0.025	1.155	1.050	0.956	0.840	0.705
0.050	1.163	1.055	0.960	0.842	0.711

Bouckaert's formulas[5] for values of x greater than about 0.1 and is given in Table I above. Let now μ be the corresponding quantity for $\gamma_1 \neq 1$. We have

$$\mu = \eta/\epsilon^{\frac{1}{3}}, \tag{5}$$

where η is now determined by the trajectories traced by the differential analyzer as outlined above. Let us place

$$\mu = \mu_0 - \nu\epsilon. \tag{6}$$

Our process of interpolation consists in finding η for certain fundamental points and then calculating ν from it by the use of the formulas written above; ν is then plotted to an appropriate scale as a function of γ_1 for each chosen value of x through which we desire to have an asymptotic trajectory. For interpolated points ν is determined from these plots knowing x and γ_1, μ is then calculated and finally η. Table I gives the data for some of the fundamental points.

As an example of the use of the method of interpolation we give in Table II the values of the initial angle for $\gamma_1=0.91$ for all equatorial runs.

Similar tables were prepared for all other values of γ_1 which were studied (reference 1, p. 722). In all over one hundred asymptotic trajectories starting from equatorial points were thus determined. In order to verify interpolated values a few trajectories were continued as far as the periodic orbit with very satisfactory results. That the precision of interpolated trajectories is as high as that of trajectories through fundamental points will be shown in the next section.

For points on the equator for which μ_0 cannot be calculated from Bouckaert's formulas, i.e., for very small and for negative values of x, the initial angle was determined from the condition that an asymptotic trajectory must be tangent to the envelope of the asymptotic family which was known from those asymptotic trajectories already found. As a further verification the trajectories were continued in some cases as far as the periodic orbit, but because of the sharpness of the turns when such asymptotic orbits oscillate in the vicinity of the periodic orbit the ordinary condition for an asymptotic trajectory cannot be ascertained with precision by means of the differential analyzer. As an example we give in Table III the initial conditions for a few of the values of γ_1 we have studied and values of $x<0.075$ along the equator.

As regards asymptotic trajectories starting from the line $\theta=0$ the procedure was similar to that described above: the criterion determining an asymptotic trajectory was that it must be tangent to the envelope of the asymptotic family. The interpolation was made directly on the initial angle, the procedure being to plot to an appropriate scale η as a function of λ for each value of γ_1 from a few fundamental points and then to read off from the plot the value of η for intermediate values of λ. Curves showing the relation between the critical angle and the latitude for all values of γ_1 along the line $\theta=0$ have already been published (Fig. 5, reference 1). As an example the values of the critical angle for fundamental points corresponding to $\gamma_1=0.85$ are given in Table IV:

Examples of families of asymptotic trajectories are given in Fig. 2. In this figure portions of trajectories intercepted by the earth are shown dotted, i.e., for these portions a parallel to the λ-axis cuts a preceding part of the trajectory.

TABLE IV. *Values of the critical angle for fundamental points for $\gamma_1=0.85$.*

λ (deg.)	η	η_1
−23	2.170	—
−20	—	2.326
0	1.253	1.885
5	1.140	—
10	1.035	—
15	0.915	1.451
20	0.794	1.235
25	0.603	0.975
26	0.562	0.915
27	0.523	0.830
28	0.515	0.750
29	—	0.600

A few trajectories of the third kind and a self-reversing doubly asymptotic trajectory with self-reversal point T_2 (cf. reference 1, sec. 4, Fig. 4) are clearly seen.

2. Precision of Asymptotic Trajectories

In this section we present an outline of a method of calculation of asymptotic trajectories which we have developed recently in order to investigate systematic errors in the trajectories found by means of the differential analyzer. The details are reserved for a paper to appear shortly in the Annales de la Société Scientifique de Bruxelles. It will be seen that systematic errors in asymptotic trajectories determined by means of the differential analyzer are small enough that they can well be neglected, except for very high latitudes, and that the precision attained throughout is very satisfactory.

The family of asymptotic trajectories is represented by a trigonometrical series in $\omega\sigma+\varphi$, where $2\pi/\omega$ is the period and φ the arbitrary phase of the periodic orbit. We have

$$x=\sum_k[y_k(\sigma)\sin k(\omega\sigma+\varphi) +z_k(\sigma)\cos k(\omega\sigma+\varphi)] \quad (7)$$

and a similar expression for λ with amplitudes μ, ν in which k takes even integral values in the expansion for x and odd values in that for λ. The asymptotic behavior of $y(\sigma)$ and $z(\sigma)$ is exhibited by the expression for z_k:

$$z_k(\sigma)=z_k+z_k'e^{\Omega\sigma}+z_k''e^{2\Omega\sigma}+\cdots, \quad (8)$$

where z_k, z_k', z_k'' are numerical coefficients of which the first corresponds to the periodic orbit. The variational equation then yields a set of linear and homogeneous equations the determinant of which must vanish. This condition, i.e., the "secular equation," determines the real characteristic exponent Ω. We have thus computed the first and second order terms in $e^{\Omega\sigma}$. The second order term of z_0 is rather large, so that a more convenient approximation had to be derived. This approximation is suggested by previous investigations of one of us and of Bouckaert[5] for the case where γ_1 differs slightly from 1. Writing

$$e^{-z_0(\sigma)}=e^{-z_0}(1+u), \quad (9)$$

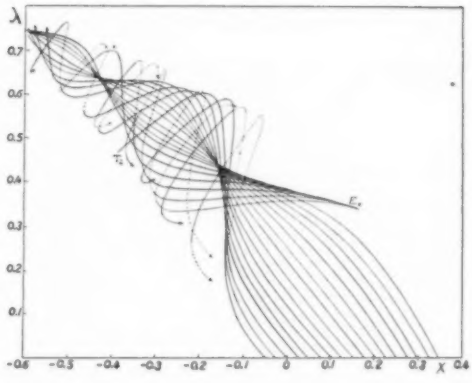

Fig. 2. A family of asymptotic trajectories. $\gamma_1=0.93$.

we have taken as approximation a solution of the equation

$$(du/\Omega d\sigma)^2=u^2(1+bu+cu^2), \quad (10)$$

where the constants b and c are determined more or less empirically. By this means it was found possible to use the expansion up to a distance 0.048 from the periodic orbit. Careful numerical checks proved it to be correct to the sixth decimal. Difference tables of the functions $y(\sigma)$, $z(\sigma)$ and the corresponding functions $\mu(\sigma)$, $\nu(\sigma)$ in the expansion for λ were then prepared for the six preceding values of σ with an interval corresponding to $\omega\Delta\sigma=15°$, i.e., $\Delta\sigma=0.293243$. While the functions y, z, etc., vary very slowly the corresponding trajectories perform many very close oscillations in the vicinity of the periodic orbit so that their calculation by the usual methods of numerical integration would be extremely difficult, in any case requiring a much smaller interval $\Delta\sigma$. For this reason instead of integrating numerically the differential equations of motion in order to find the trajectories we have preferred to integrate the differential equations of the amplitudes y, z, etc.

The differential equations satisfied by these functions can be found as follows: replacing x and λ by their series expressions and expanding in a trigonometrical series we may write

$$\tfrac{1}{2}\partial P/\partial x=\sum_k[Y_k(\sigma)\sin k(\omega\sigma+\varphi) +Z_k(\sigma)\cos k(\omega\sigma+\varphi)]. \quad (11)$$

This defines Y and Z as a function of y, z, μ

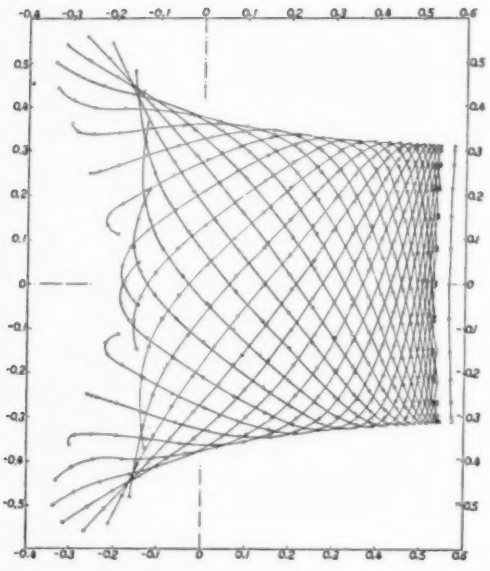

FIG. 3. Calculated family of asymptotic trajectories. $\gamma_1=0.929898$.

and ν because of the equations of motion (1). For practical use of this equation we may take advantage of the fact that with the exception of z_0, μ_1 and ν_1 all the other terms are small and powers higher than the second may be neglected. In any case ν_1 can be made to vanish by a suitable change of the phase angle. Once the phase has been shifted explicit expansion can be derived with coefficients depending on z_0 and the new μ_1', and included in a convenient computation schedule. Finally the phase must be shifted back to its original value.

The equations to be integrated are of the form

$$\begin{aligned}(d^2y_k/d\sigma^2)-2k\omega(dz_k/d\sigma)-k\omega^2y_k&=Y_k,\\(d^2z_k/d\sigma^2)+2k\omega(dy_k/d\sigma)-k\omega^2z_k&=Z_k,\end{aligned}\tag{12}$$

and similar equations for μ_k and ν_k. Ordinary methods of integration such as Adams' would have been impracticable as they would be tantamount to an attempt to calculate a sine from its second order differential equation using intervals of 15°, 30°, $\cdots$ 90° according to the value of k. Introducing the complex notation $x=y+iz$, $X=Y+iZ$ and taking the case $k=1$ as typical, the above equations may be written

$$(d^2/d\sigma^2)(xe^{i\omega})=Xe^{i\omega},\tag{13}$$

which yields upon integration and elimination of integration constants by taking second differences

$$\Delta^2xe^{i\omega\sigma}=\Delta^2\iint Xe^{i\omega\sigma}d\sigma^2.\tag{14}$$

When $\omega=0$ we fall back on Störmer's method of numerical integration. The question now is to devise a suitable method of integration for the present equation.

Writing
$$\omega\sigma=w(t_0+t),\tag{15}$$

where t is the ordinal number of the integration points and w is the interval of integration, and supposing that the values of x_n, X_n are known up to $n=-1$, the question is to compute the value of x_0 as a function of x_{-1}, x_{-2}, X_{-1}, $\delta X_{-1}=X_{-1}-x_{-2}$, $\delta^2x_{-1}=\delta x_{-1}-\delta x_{-2}$, etc. The left-hand member of the equation

$$\Delta^2xe^{\alpha t}=w^2\iint Xe^{\alpha t}dt,\tag{16}$$

where $\alpha=i\omega w$ is $x_0-2e^{-\alpha}x_{-1}+e^{-2\alpha}x_{-2}$. X may be expressed as a function of X_{-1} and its successive differences by

$$X(t)=\sum_k(1/k\,!)(t+1)(t+2)\cdots(t+k)\delta^kX_0.\tag{17}$$

If $D=\partial/\partial\alpha$ we have

$$\iint t^ne^{\alpha t}dt^2=D^n\iint e^{\alpha t}dt^2=D^n(e^{\alpha t}/\alpha^2)\tag{18}$$

and the final relation is

$$\begin{aligned}x_0&=2e^{-\alpha}x_{-1}-e^{-2\alpha}x_{-2}+\sum_k w^2(1/k\,!)(D+1)(D+2)\\&\quad\cdots(D+k)(1-2e^{-\alpha}+e^{-2\alpha}/\alpha^2)\delta^kX_{-1}\\&=2e^{-\alpha}x_{-1}-e^{-2\alpha}x_{-2}+\sum_k a_k\delta^kX_{-1}.\end{aligned}\tag{19}$$

Returning to real variables and writing $a_k=b_k+ic_k$ we have finally the working formulas

$$\begin{aligned}y_0&=2\cos\omega w\cdot y_{-1}-y_{-2}\cos 2\omega w\\&\quad+2z_{-1}\sin\omega w-z_{-2}\sin 2\omega w\\&\quad+w^2(\sum_{k=0}b_k\delta^kY_{-1}-\sum_{k=0}c_k\delta^kZ_{-1})\end{aligned}\tag{20}$$

and

$$\begin{aligned}z_0&=2z_{-1}\cos\omega w-z_{-2}\cos 2\omega w\\&\quad-2y_{-1}\sin\omega w+y_{-2}\sin 2\omega w\\&\quad+w^2(\sum_{k=0}b_k\delta^kZ_{-1}+\sum_{k=0}c_k\delta^k+Y_{-1}).\end{aligned}\tag{21}$$

The coefficients b_k, c_k have been computed up to $k=4$, i.e., up to and including the fourth difference and for $\omega\Delta\sigma=15°$, 30°, $\cdots$ 90° corresponding up to the sixth harmonic.

The integration has been actually carried out for twenty steps until the region was finally reached where the change of the integrated functions became so large that the integration could no longer be continued without splitting the interval of integration. The family of twenty-four trajectories, symmetrical in pairs, has been computed and is shown in Fig. 3. For a table of the computed points reference must be made to the complete paper. The small circles shown in the figure are calculated points for which the phase is 0°, 15°, $\cdots$ 90° and correspond with those shown on the periodic orbits (Fig. 1).

The comparison with the asymptotic trajectories found by means of the differential analyzer is shown in Fig. 4. It is seen that the agreement is excellent particularly as regards the position of the cusp C_0. One of the machine trajectories starting from $x=0.275$ and $\lambda=0°$ happens to have a value of φ_0 equal to that of the calculated trajectory and both coincide, the others have different values of φ_0 but that they all belong to the same family can be tested by analyzing their general shape and proved by the fact that they all are tangent to the same envelope. As a matter of fact the consistency between calculated and machine trajectories is as good as that found among the machine trajectories themselves. A more precise comparison may be made by calculating the value of the inclination η of three fundamental trajectories at the equator. The result is shown in Table V.

TABLE V. *Calculated values of the inclination η of three fundamental trajectories at the equator.*

x	η (mach.)	η (calc.)	Diff.
0.150	0.890	0.887	0.003
0.225	0.959	0.953	0.006
0.300	1.053	1.045	0.008

3. Determination of the Allowed Main Cone

The theory of the main cone, or region of full light, has already been outlined in our previous papers. A sketch of our method for its determination and its representation, once the families

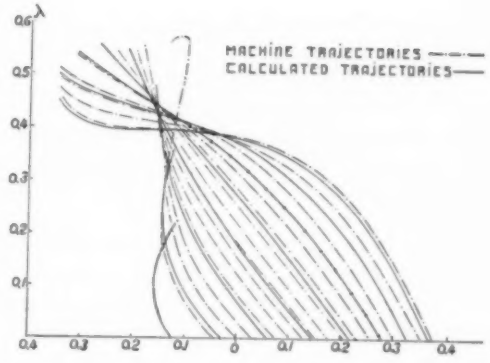

FIG. 4. Calculated asymptotic trajectories compared with trajectories obtained with differential analyzer. $\gamma_1=0.93$.

of asymptotic trajectories have been found, has also been given in our preceding paper (reference 1, p. 724). The coordinates of a representative point are $\sin\theta$ and $\cos\theta\sin\eta$; for positive particles θ and η are counted positively eastwards and northwards, respectively. Let us assume an asymptotic trajectory passing through a point of coordinates x and λ; η is then the angle with the zenith direction, i.e., with a parallel to the x axis and θ the angle between the trajectory and the meridian plane which can be immediately calculated from Störmer's formula (reference 1, Eq. (1)). The energy r in Störmer's corresponding to the given x is then given by Eq. (2).[1] We thus obtain a point of the representation of the cone for the given values of the energy and the latitude.

For the systematic utilization of the asymptotic trajectories traced by the differential analyzer two lines of attack are open. Either one may first calculate from Störmer's formula the lines $\theta=$ const. for all values of γ_1 for which asymptotic trajectories were studied and then measure the values of the angle η along these lines noting at the same time the value of x. This is equivalent to determining sections of the cones of different energies and at different latitudes by planes parallel to the meridian plane. Suppose that the lines $\theta=0°$, 5°, 10°, $\cdots$ have been computed for $\gamma_1=1.00$, 0.99, 0.98, $\cdots$ 0.78, and the angles η measured along each. Then plots may be readily constructed giving the angle η as a function λ for each value of γ_1 and, besides, the energy r as a function of x for each

value of γ_1. This is the method used for $\theta=0°$ in our preceding paper[1] where diagrams giving η as a function of λ for each value of γ_1 are given (Fig. 5, reference 1). It has not been used for other values of θ because the computation of the lines $\theta=$const. is laborious. Once these have been found, however, the calculation of the cone is immediate.

An alternative line of attack is to measure the inclination η along the lines $\lambda=$const. for each value of γ_1 which was studied, noting at the same time the value of x where the intersection between the asymptotic trajectory and the chosen line $\lambda=$const. takes place. Graphs may then be drawn showing η as a function of r for each chosen value of λ, for example $\lambda=0°$, 5°, 10° $\cdots$ and different values of γ_1.[6] An envelope is characterized on these ηr-diagrams by a point of tangency of η as a function of r with a line parallel to the η-axis, i.e., by a turning point for a maximum or minimum value of r. A cusp is characterized by the coalescence of two such points; it is a point of inflection with a tangent parallel to the η-axis. These peculiarities of the ηr-diagrams are reflected in the representation of the cone; their significance has already been taken up fully in our preceding paper.[1] If on the ηr-diagrams a value $r=$const. is picked out it is readily seen that the boundary of the cone progresses eastwards (for positive particles) as γ_1 increases.

The main cones for $\lambda=0°$, 20° and 30° are reproduced in Figs. 5, 6 and 7. The small circles are the points calculated by Bouckaert.[5] It is seen that except for high zenith angles and low energies the agreement is again quite satisfactory. The extreme northern part of the main cone where the shadow of the earth makes itself felt is given with reservations as a detailed analysis of the trajectories of the second and third kinds outside of the meridian plane still remains to be made.

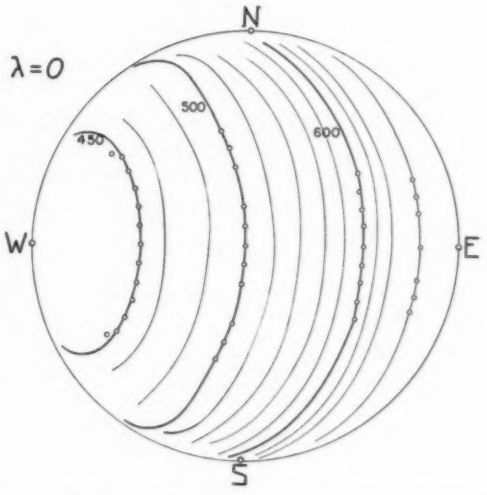

FIG. 5. The main cones. Energies in millistörmers. Positive particles, northern hemisphere.

4. THE AZIMUTHAL EFFECT

We begin by recalling that in addition to the main cones determined as described in the previous paragraph there is also the region of penumbra. While the full analysis of the latter must be left to another occasion preliminary results obtained with the differential analyzer and earlier by one of us[7] show that there are bands of light of complicated structure running alongside the boundary of the main cone alternating with bands of darkness and extending eastwards (for positive particles) clear over to Störmer's limiting cone[8] of total darkness at the value of θ corresponding to the given latitude and energy and to $\gamma_1=1$. While the chief contribution to the azimuthal effect as described later in this paragraph undoubtedly comes from the main cones the theory here presented must be improved later, particularly as regards the east-west asymmetry, so as to take the penumbra into account. Another correction must also be made to take care of the eccentricity of the earth's magnetic center. This correction at a given point on the earth affects only the energy scale and can readily be computed by methods already given in a previous paper.[9]

A consideration of the main cones drawn in Figs. 5 to 7 shows immediately that the range of

[6] This laborious piece of work was carried out by Mr. L. de Borman and forms part of his master's thesis at the University of Louvain, 1936, from which Figs. 5, 6 and 7 are taken.

[7] G. Lemaitre, Ann. de la Soc. Sci. de Bruxelles **A54**, 162 (1935).

[8] C. Störmer, University Observatory, Oslo, Publication No. 10 (1934).

[9] M. S. Vallarta, Phys. Rev. **47**, 647 (1935).

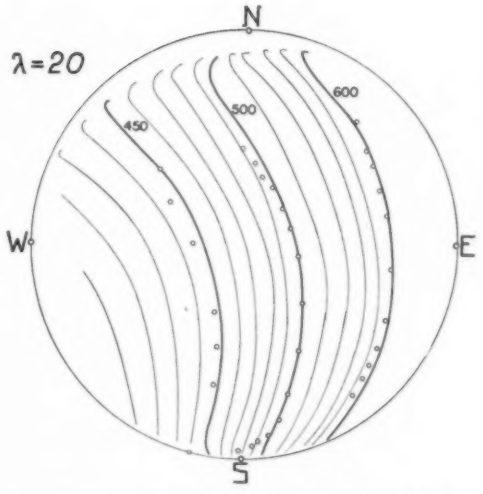

FIG. 6. The main cones. Energy in millistörmers. Positive particles, northern hemisphere.

energy which can reach a point on the earth at a given zenith angle z is not the same at all azimuths. Consequently there must be a variation of intensity at a fixed zenith angle and different azimuths (azimuthal effect). Special cases of the azimuthal effect are the north-south and east-west asymmetries. Suppose now that the circles $z=$const. are drawn on the diagrams representing the cones (Figs. 5 to 7). These intersect the boundaries of the cones of different energies at azimuths which can be read off directly on the figures. In this way the curves, Fig. 8, are obtained which give the minimum energy capable of reaching a given latitude at a zenith angle of 45° and azimuths shown by the curves. Similar curves for other zenith angles may be readily found.

Unfortunately no systematic comparison with the experimental azimuthal effect is possible at the present time because no systematic measurements covering the complete turn of the horizon have been made. The most complete data available are those of Johnson[10] who has made measurements at different azimuths and fixed zenith angles with a triple coincidence counter system covering more or less thoroughly the horizon from east to west through south. These measurements were made in Mexico ($\lambda=29°$), Panama ($\lambda=20°$) and Peru ($\lambda=0°$) at zenith angles 45° and 30° and heights of 6.8 m, 10 m and both 6.8 m and 6 m, respectively below the top of the equivalent water atmosphere. While no significant quantitative conclusions seem warranted at the present time there is good qualitative agreement between theory and experiment even without resorting to negative primaries. An important point brought out by the Peruvian experiment is that the addition of an atmospheric depth equivalent to 0.8 m of water does not change the relative order of the intensities with respect to one another. This must be expected if the azimuthal effect is essentially due to the action of the earth's magnetic field on the primaries because, since the zenith angle is constant, the length of the atmospheric path traversed by the rays is the same at all azimuths.

Besides the north-south asymmetry, already discussed extensively in our preceding paper,[1] an interesting case of the azimuthal effect is the east-west asymmetry first discussed by Rossi.[11] Historically this was the first case of the azimuthal effect to be discovered and has since been thoroughly studied experimentally; perhaps we may be permitted here to voice the regret

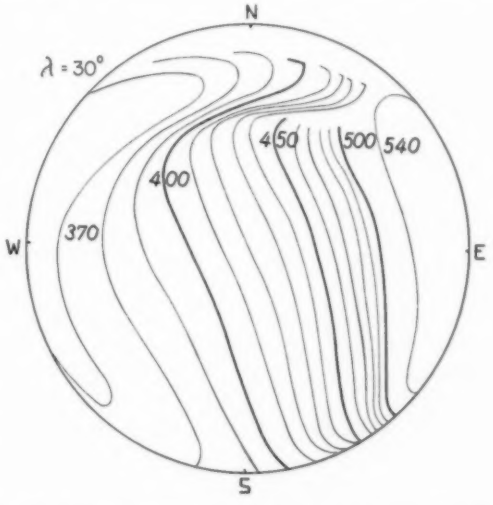

FIG. 7. The main cones. Energy in millistörmers. Positive particles, northern hemisphere.

[10] T. H. Johnson, Phys. Rev. **45**, 569 (1934).

[11] B. Rossi, Phys. Rev. **36**, 606 (1930), see also Ricerca Scientifica **1**, 561 (1934) for full references to his previous work.

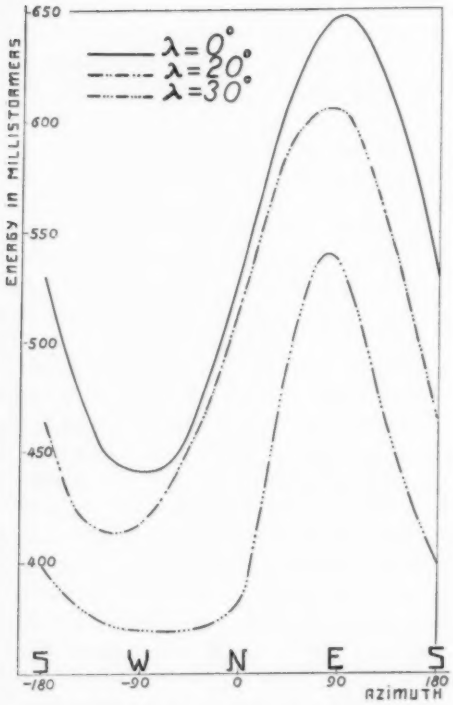

FIG. 8. The azimuthal effect for $z=45°$.

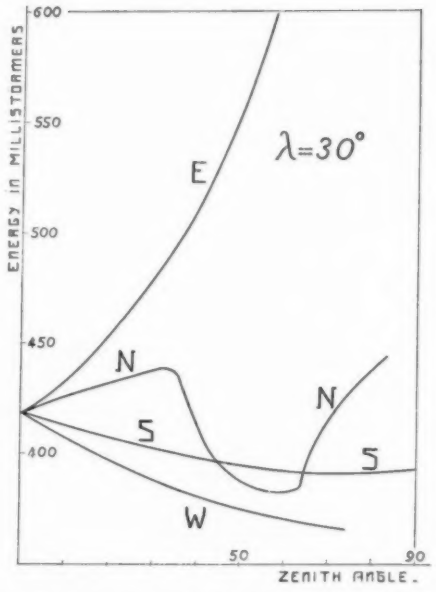

FIG. 9. The east-west and north-south asymmetries. Positive particles, northern hemisphere.

that it has been studied practically to the exclusion of all other azimuths. Fig. 9 shows a comparison of the energy ranges involved in the east-west and north-south asymmetries, where the former refers to positive particles and the latter to particles of either sign. It is immediately apparent that for purposes of gaining information as to the energy distribution of the primary radiation the study of the north-south asymmetry is superior to that of the east-west, first because the penumbra acts mainly on the east-west asymmetry but hardly on the north-south, second because the energy range is smaller and third because the north-south is independent of the particles' sign. Except that the interpretation of the east-west asymmetry is made difficult because of the penumbra, a comparison between the east-west and north-south asymmetries furnishes a means, already pointed out in a previous paper, of determining the percentage of particles of either sign. A consideration of the curves in Fig. 9 shows that if the primary cosmic radiation is made up entirely of particles of one sign the north-south asymmetry must be considerably smaller than the east-west. A mixture of positive and negatives on the other hand, decreases the east-west asymmetry but leaves the north-south unaffected, provided the energy ranges covered by positives and negatives are not the same. Thus Johnson's measurements in Mexico of the north-south and east-west asymmetries would seem to leave room for positive and negative primaries.[12]

It should also be noted that once the cones have been calculated it is quite feasible to take the finite aperture of a multiple coincidence counter system into account. Failure to consider this point may easily lead into error when interpreting experimental results.

5. The Main Cone in the Vicinity of the Zenith

A particularly interesting region from the point of view of intensity measurements is the region around the zenith to which Zanstra[13] has already called attention. We intend to devote this section to the study of this region.

[12] T. H. Johnson, Phys. Rev. **47**, 91 (1935); **48**, 290 (1935).
[13] H. Zanstra, Naturwiss. **22**, 171 (1934).

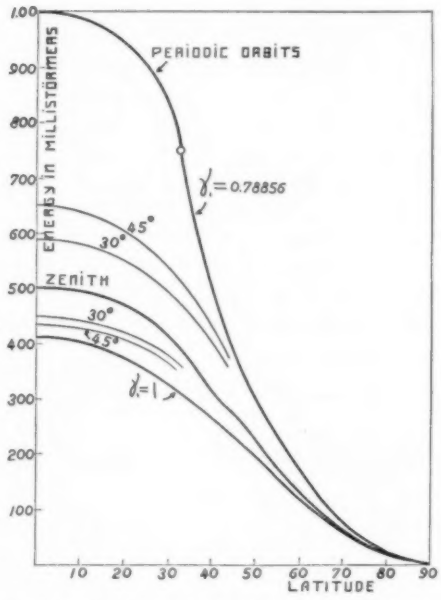

FIG. 10. Minimum energies in the region near the zenith.

In the vicinity of the zenith the boundaries of the main cones run almost parallel to one another and intersect the meridian plane at a small angle ψ which increases with latitude. The value of the energy r for which the boundary of the main cone goes through the zenith gives the minimum energy that a particle must have to reach the earth in the vertical direction at a given latitude. This can be readily found by interpolation from the data contained in Figs. 5 to 7 or from the equation of the line $\theta = 0$

$$e^z = 2\gamma_1 r = \cos^2 \lambda, \tag{22}$$

where the dependence of γ_1 on longitude in the zenith direction is given by Fig. 5 of our preceding paper.[1] This minimum energy is given in Fig. 10 together with other curves the significance of which will be taken up later. The angle ψ is plotted as a function of latitude in Fig. 11 together with the gradient dr/dz at the zenith. It is seen that the gradient varies slowly with the latitude, nevertheless it is of importance when interpreting vertical intensity measurements made with triple coincidence counter systems of large aperture. The orientation of the counter system with respect to the direction ψ is also a significant datum of the experiment.

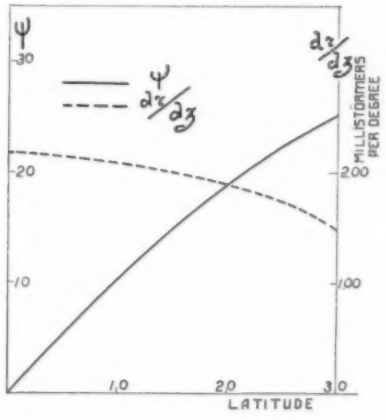

FIG. 11. The angle between the main cone and the meridian plane and the energy gradient at the zenith.

The importance of the knowledge of the least vertical energy, emphasized by Zanstra, arises from the fact that, if the spectrum of the cosmic radiation is a continuous function of the energy, then intensity measurements in the vertical direction made beginning at the equator and extending sufficiently far north or south give a ready means of estimating with fair accuracy the energy lost by a cosmic-ray particle while traversing the atmosphere. It is sufficient to find the latitude beyond which the vertical intensity remains constant. Unfortunately neither the vertical intensity measurements of Auger and Leprince-Ringuet[14] nor those of Clay[15] between $\lambda = 10°$ and $\lambda = 20°$ under 20 cm of lead extend sufficiently far north or south to make this estimate possible.

Another interesting question which can now be answered is as to the energy range which can reach a point of the earth of latitude λ coming from directions at a zenith angle z. For latitudes up to 30° the energy range involved can be read off directly from Figs. 5 to 7. The corresponding curves are plotted in Fig. 10. Their significance will be clear from the following example. Suppose we take $\lambda = 30°$ and ask what is the energy range which may arrive within the cone bounded by the directions at 45° with the zenith. The lower curve for $z = 45°$ then shows that 362 millistörmers is the minimum energy that a particle

[14] P. Auger and L. Leprince-Ringuet, Nature **133**, 138 (1934).
[15] J. Clay, Physica **2**, 308 (1935).

must have to arrive at 45° from the zenith (and in a certain azimuth) while the upper curve gives that if it has a minimum energy of 540 millistörmers it may arrive from any direction within 45° of the zenith. Similarly 408 millistörmers is the least energy a particle must have to arrive at 30° from the zenith, while 510 millistörmers is the least energy required to arrive from any direction within 30° of the zenith. In addition the limiting energies for which the main cone is completely open is given by the uppermost curve. This curve consists of two parts: first, the locus of the vertices of the periodic orbits (cf. Fig. 1) and then the limiting energy for the limit $\gamma_1=0.78856$ for which periodic orbits disappear. This curve takes into account only the trajectories of the first kind.[16] Finally the lowest curve gives the limiting energy for Störmer's limit $\gamma_1=1$ for which all directions are forbidden.

It is a pleasure to renew the expression of our gratitude to the various persons, mentioned in our preceding paper, who have helped us to carry out the research of which this paper is another fruit. One of us is indebted to the Massachusetts Institute of Technology for continued support while this investigation was being completed at Louvain, and to the University of Louvain for providing numerous facilities during the period of his residence there.

[16] For trajectories of the second kind a somewhat higher energy limit can be readily found from the relation $e^2 \leq 2 \cos \lambda$ above which the acceleration $d^2x/d\sigma^2$ is necessarily positive. For the same reason negative values of γ_1 are of no interest.

SEPTEMBER 15, 1936 PHYSICAL REVIEW VOLUME 50

Excitation-Curves for Fluorine and Lithium

L. R. HAFSTAD, N. P. HEYDENBURG AND M. A. TUVE, *Department of Terrestrial Magnetism, Carnegie Institution of Washington*

(Received July 6, 1936)

Observations on the alpha-particles emitted by lithium and the gamma-rays emitted by lithium and fluorine when bombarded with protons of energies up to 1000 kv have been improved by the use of a corona-free, 10,000-megohm voltmeter-resistor for voltage-measurements. By this means the accuracy of our measurements has been brought to two percent on an absolute scale and about one percent on a relative scale. Oscillograph-studies of voltage-fluctuations have shown that up to 1000 kv the voltage is constant to ±1.4 percent "peak-ripple." For the distribution-curve for voltage *versus* time the "half-maximum" width is about one percent at 1000 kv. Results thus far obtained for the gamma-ray resonances are as follows:

Voltage	Element	Half-width
328 kv	F	< 4 kv
440 kv	Li	11 kv
892 kv	F	<12 kv
942 kv	F	<15 kv

There is an indication of a weak multiplet structure in fluorine in the region between 500 and 700 kv with a broad but fairly prominent "resonance" at 650 to 700 kv. The existence of a resonance in lithium at 850 kv was not confirmed.

INTRODUCTION

OUR work on proton-disintegrations last year[1] demonstrated the existence of sharp resonance-effects in nuclear disintegrations which called for voltage-control considerably more refined than that given by any apparatus then in existence. Such work depends essentially on the accurate reproducibility of specified voltages, and this requirement is not sufficiently well satisfied even by rectifier and condenser installations, unless means for voltage-measurements more accurate than spark-gap or particle-range determinations are provided. Unless very special precautions are taken, sphere-gap measurements are rarely reproducible to better than five percent. Even the official calibration-curves for sphere-gaps have been changed by more than ten percent during the past two years. The absence of reliable information on the range-energy relation for protons would prevent the

[1] Hafstad and Tuve, Phys. Rev. **48**, 306 (1935); also Tuve, Hafstad and Dahl, Phys. Rev. **48**, 315 (1935).

use of this method even though apparatus which would permit both rapid and accurate determinations of ranges were devised.

In addition to the problem of specifying the mean voltage used, is that of determining quantitatively the deviations from the mean during any given interval of time. This information is essential in specifying such things as widths of resonance-levels, which have a theoretical meaning and value only when it is demonstrated that the observed widths are not produced by inhomogeneities in the incident ion-beam.

Technique

Tube

Our apparatus is essentially as previously described. A new glass tube has been installed in which provision was made for permitting accurate axial alignment of the electrodes. In this tube the baffle-plates at each electrode have been eliminated so that the pumping speed through the tube is essentially that given by the 12-inch diameter of the glass tube rather than that of the inside diameter of the electrodes. This arrangement will permit the use of much larger total ion-currents as soon as correspondingly fast pumps can be provided. At present the pumping speed at the base of the tube is approximately 30 liters per second, which is small compared to that used in most high-voltage installations.

As was expected, the new tube, with its properly aligned electrodes, practically eliminated the annoying fluctuations in position of the spot which constituted the principal difficulty encountered in the work reported last year. The effectiveness of the focusing of such a tube is attested by the fact that with the same tube a concentrated ion-beam can be obtained at any voltage from 200 to 1200 kv.

Corona-free, 10,000-megohm voltmeter-resistor

For the highest possible accuracy in voltage-measurements, a wire-wound voltmeter-resistance would be desirable. Such units are available commercially for x-ray voltages, but the cost of such units arranged for 1000 kv would be prohibitive, and a corona-free design could hardly be attained by reason of the dimensions of the unit resistors, especially if a full-scale current of 100 microamperes were required (10,000 ohms per volt). However, a close approximation can be achieved by using modern metallized "grid-leak" resistors which give voltage-current curves that are nearly ohmic in character. Any deviation from linearity can be corrected for by a calibration of such resistors against "purely ohmic" wire-wound units.

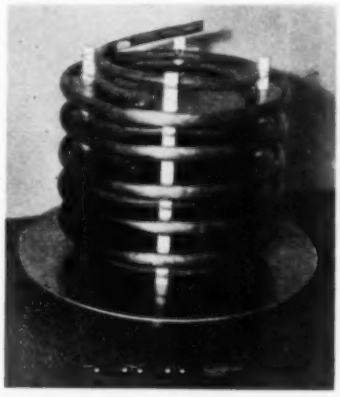

Fig. 1. Construction of corona-free voltmeter-resistor.

In the assembly of such resistors in series to be used with very high voltages, the greatest technical problem is the elimination of corona. Of several possible solutions the simplest appeared to be that indicated by Fig. 1, which has now been proved to be entirely satisfactory. The individual resistors of 10 megohms each, rated at one watt or 1000 volts maximum, are connected in series in groups of 20, slipped into a thick-walled rubber tube to insure proper spacing, and then connected between brass disks 12 inches in diameter, which are protected against edge-corona by $\frac{3}{4}$-inch copper tubing soldered to the circumference of each disk. The disks are separated by 2-inch Isolantite rods as spacers. Fifty such units make up the 10,000-megohm resistor. This construction limits the voltage-gradient to 20 kv per 2-inch section which is safely below corona-values, provided no dust or lint is permitted to collect on the surfaces. To guard against the latter the entire assembly was mounted in the "Textolite" cylinder shown in Fig. 2. This cylinder was on hand from previous work. As may be seen from Fig. 2, it is somewhat short for its purpose and

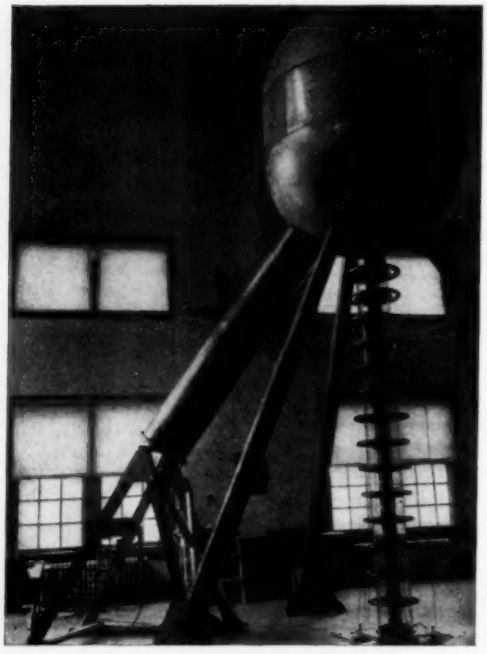

FIG. 2. 1200-kilovolt electrostatic generator showing tube and voltmeter-resistor.

at present sparks to earth over the outside of this cylinder determine the maximum voltage, 1150 kv, attained by this generator. Some difficulty was experienced when this resistance-unit was first mounted due to corona at the junction between the resistor and the sphere. This was largely eliminated when care was taken to design in such a way that the equipotential through the first corona-disk agreed roughly with the corresponding equipotential for the sphere itself.

The resistance-unit shown in Fig. 2 measures only the voltage between the outside sphere and ground. With our somewhat inconvenient arrangement of concentric spheres the voltage between the one-meter and the two-meter spheres must be measured separately. A similar resistance-unit of six 20-kv sections was accordingly installed between the two spheres, the current being indicated by a meter installed at the surface of the outside sphere and read by a telescope.

Voltmeter-calibration

Through the courtesy of Dr. L. S. Taylor of the National Bureau of Standards we were able to calibrate our resistance against his wire-wound standards in 5-section, 100-kv units. Results on separate determinations agreed to within two percent. The voltage corresponding to any given current through the entire resistor is then obtained by adding the voltages of the separate, independently calibrated units, and the total voltage is obtained by adding the separately determined inside voltage (between spheres) and outside voltage (to ground).

The possibility that part of the measured current at high voltages may be due to corona between sections of the voltmeter has been eliminated by three independent tests. First, during calibration, the units were carried to 40 percent over-voltage before corona occurred, thus allowing a safe margin above usual operation-conditions. Second, after installation the voltage-scale was tested for linearity by setting the mass-1 spot to a given deflection at the highest voltage and then reducing the voltage until the mass-2 spot was deflected to the same position. By this test the voltmeter read two percent low at the highest voltages attained. This error is therefore not only small but opposite in sign to that expected from corona. Finally, making use of an effect first reported to us by Herb but since frequently tested here, an effort was made to detect the change in current-reading which should be produced when any incipient corona was stopped by the introduction of CCl_4 vapor into the voltmeter-resistor casing. No effect was observed even at the highest voltages.

Charging current

In all work done so far our maximum target-currents have been limited by our pumping speed so that maximum charging currents have not been necessary and accordingly we have operated our belts at reduced speeds to reduce mechanical vibration. The added current-drain due to the voltmeter could be readily compensated by increased belt-speed, if desired. However, during some tests on a disk-type electrostatic generator[2] it was noted that charging currents could be greatly increased by introducing a thin dielectric between the current-

[2] O. Dahl, Rev. Sci. Inst. **7**, 254 (1936); E. H. Bramhall, Rev. Sci. Inst. **5**, 18 (1934).

carrier and the earthed inductor, and making a simultaneous increase in spray-voltage. Adoption of this technique on our belt-machine doubled our previous charging currents so that we now operate at reduced speed and with only the "ingoing" belts charged, thus reducing the unsteadiness arising from incipient sparking at the belt-openings when operating at the higher voltages.

Voltage-fluctuations

As before, variation of voltage was accomplished by moving a set of corona-points toward or away from the sphere. At all except the highest voltages, where sparking occurred, it was immediately obvious from the steadiness of the voltmeter-needle that no erratic voltage-fluctuations were occurring. It is important to note that this steadiness is a property which is apparently inherent in a corona-limited, constant-current machine, and is attained without recourse to smoothing condensers or compensating devices of any kind.

Since the period of a portable microammeter is usually of the order of one second, there was of course a possibility of relatively fast fluctuations which were smoothed out by the period of the meter. To eliminate this possibility observations were made with a cathode-ray oscillograph connected across a one-megohm resistance in series with the voltmeter-multiplier resistance. When due allowance was made for the low impedance of the resistor-unit to high frequency pulses (capacitative impedance equals resistive impedance at 100 cycles), it was immediately clear that no deviations from the mean of greater than one or two percent were occurring. To obtain a quantitative measure of the fluctuations, however, a photographic record was necessary. For this purpose the 10,000-megohm resistor was connected to a single-stage, vacuum-tube amplifier operating a high-sensitivity Dudell oscillograph (700 cycles) which recorded on a moving film. The results for the voltage on the outside sphere are shown in Fig. 3. From these records the distribution-curves for 250 equally spaced ordinates measured from each of these curves were obtained. Similar records were taken for the voltage-fluctuations on the inside sphere. The voltage between the spheres showed a noticeable 60-cycle ripple which was absent on the outside sphere; from this and other evidence the voltage-fluctuations may be considered inde-

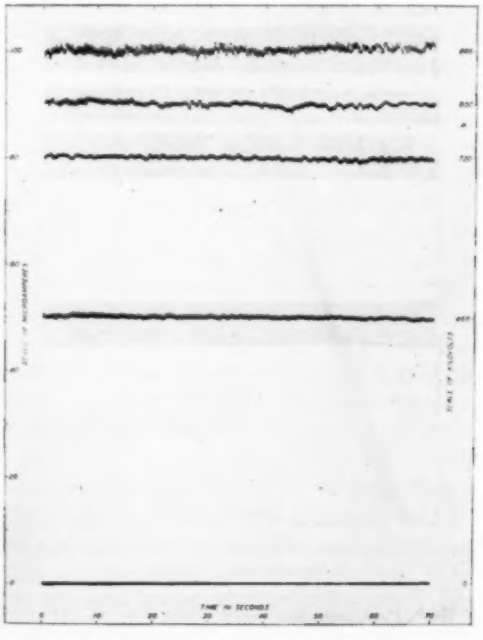

FIG. 3. Voltage-fluctuations, 2-meter electrostatic generator.

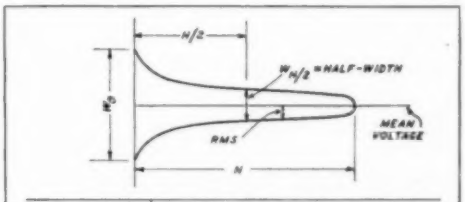

VOLTAGE IN KV	FLUCTUATION IN KV OR PER CENT		
	RMS	$W_{H/2}$	W_0
488 (OUTSIDE)	1.20	3.70	5.60
105 (INSIDE)	1.20	1.20	1.90
573 (TOTAL)	1.70	3.90	5.90
FLUCTUATION %	0.29	0.68	1.03
720 (OUTSIDE)	1.9	5.5	11.1
105 (INSIDE)	1.2	1.2	1.9
825 (TOTAL)	2.24	5.7	11.2
FLUCTUATION %	0.26	0.69	1.35
900 (OUTSIDE)	3.3	8.0	18.0
105 (INSIDE)	1.2	1.2	1.9
905 (TOTAL)	3.5	9.2	18.2
FLUCTUATION %	0.39	0.89	1.8
996 (OUTSIDE)	4.6	9.7	27.7
105 (INSIDE)	1.2	1.2	1.9
991 (TOTAL)	4.7	9.8	27.8
FLUCTUATION %	0.48	0.98	2.8

ORDINATES: INSTANTANEOUS VOLTAGE FROM OSCILLOGRAPH-TRACE
ABSCISSAE: TOTAL TIME SPENT AT CORRESPONDING VOLTAGE

FIG. 4. Analysis of voltage-fluctuations on 2-meter electrostatic generator.

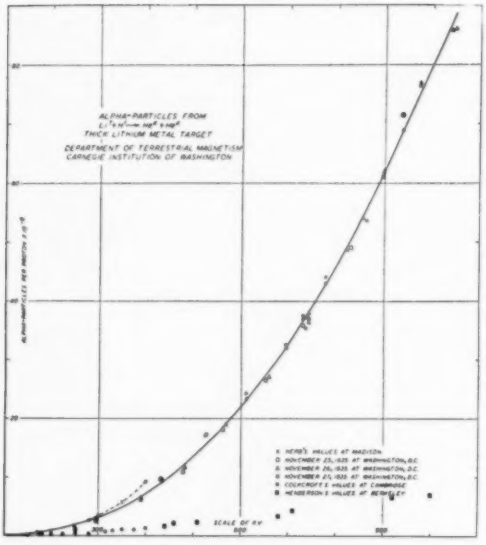

FIG. 5.

pendent. In this case the widths of the two distribution-curves for the fluctuations should be added in the same way as the probable errors for independent error-curves, namely, $W_{1+2}=(W_1^2+W_2^2)^{\frac{1}{2}}$. The data for the separate distribution-curves as well as for the total voltage are given in Fig. 4. This study shows that even at 990 kv the maximum "spread" of the fluctuations is only 28 kv or ± 1.4 percent "peak-ripple."

YIELD-CURVES

Accurate yield-curves for either particles or gamma rays can give much information of value in the development of a theory of the nucleus, as has been demonstrated especially by the work of Breit.[3] While yield-curves are desirable for all possible elements, we have thus far concentrated on lithium, on which much work has already been done,[4] and on fluorine[5] in order to establish an absolute voltage-scale by means of its many resonances. Observations will be extended to other elements as time permits.

[3] Breit and Yost, Phys. Rev. **48**, 203 (1935).
[4] Cockcroft and Walton, Proc. Roy. Soc. **A137**, 229 (1932); Henderson, Phys. Rev. **43**, 98 (1933); and Oliphant and Rutherford, Proc. Roy. Soc. **A141**, 259 (1933).
[5] McMillan, Phys. Rev. **46**, 868 (1934).

ALPHA-PARTICLES FROM Li^7+H^1

This problem has long been studied under gradually improving experimental conditions. The recent precision work[6] on this problem and consequent calculations of theoretical expectations[7] emphasized the need for more observations at the higher voltages.

Our most recent results for a thick target are given in Fig. 5, with results of other observers included for comparison. In order to obtain reproducible results it was necessary to adopt a target-technique in which a freshly prepared target of lithium metal, evaporated onto a copper plate in vacuum, could be moved across the ion-beam so as to present a fresh surface as often as desired. This technique has not yet been extended to thin targets because of the obvious difficulty of insuring uniformity. Un-

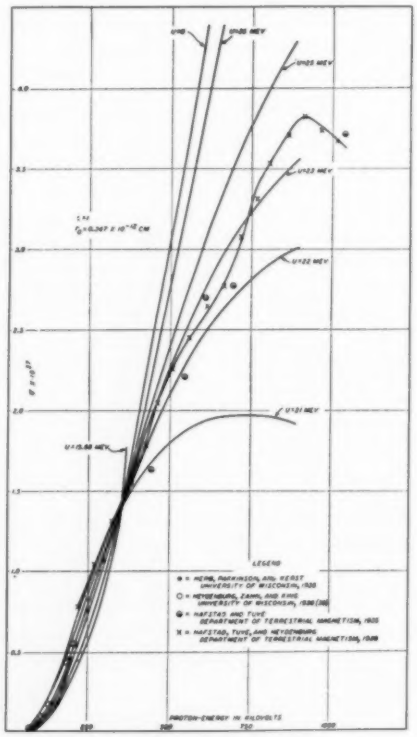

FIG. 6. Comparison theoretical and observed excitation-functions for lithium.

[6] Herb, Parkinson, and Kerst, Phys. Rev. **48**, 118 (1935); Heydenburg, Zahn, and King, Phys. Rev. **49**, 100 (1936).
[7] Ostrofsky, Breit, and Johnson, Phys. Rev. **49**, 22 (1936).

fortunately thick target data can be compared with theory only by assuming a law for the range-energy relation for the protons in lithium. This has been done following Herb[6] and the results compared with theoretical values[7] in Fig. 6. It may be seen that our recent results deduced from thick-target data agree well with preliminary values obtained from thin-target observations last year. Plotted in this way the data exhibit irregularities not present in the original data and lead one to suspect that the range-energy relation for protons in lithium may be something other than the V^1 law assumed. However, it is clear from these data that the cross section is not constant above 400 kv as reported by Henderson.

Still more detailed observations on lithium will be needed before the thin-target yield-curve or, more explicitly, the true "excitation-function" for this process can be definitely established.

Gamma-Rays from Li^7+H^1

Our work on the gamma-rays from lithium reported last year has been repeated (1) in order to establish the resonances on an absolute voltage-scale and (2) in order to determine, if possible, the widths of the resonance-levels. Observations were made, as before, using the Lauritsen type of electroscope. Representative results, the last of a series of curves, are given in Fig. 7. By comparison with our previous work it will be noted that the lower resonance occurs at practically the same position on this voltage-scale (440 kv) as on the rather arbitrary scale used last year (450 kv), again disagreeing markedly with the resonance-position of 650 kv reported by the Pasadena observers.[8] In Fig. 7 it may also be noted that there is no confirming evidence for the resonance at 850 kv reported in our paper last year. It is probable that the gamma-rays observed were due to a contamination by fluorine which has an extremely strong resonance-line at approximately this voltage. This possibility is favored by the fact that in order to obtain a sufficiently thin lithium target (less than 20 kv stopping power) the amount of Li present was reduced dangerously close to the contamination-levels of any materials giving

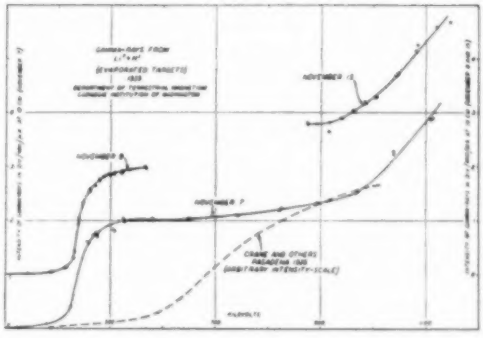

Fig. 7.

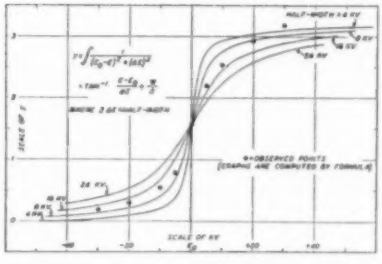

Fig. 8. Determination of half-width of 440-kv lithium gamma-ray resonance.

large yields. In the present instance fluorine is especially to be suspected since CaF_2 had been used as a target in experiments just preceding the observations on lithium.

The importance of obtaining estimates of absolute yields for curves such as the above is recognized, but the problem is too difficult to permit dependable values to be given at the present time. Comparisons with radium are misleading, for the gamma-rays involved in the present reaction are of extremely high energy as has been shown by the work of Lauritsen and his collaborators.[8] It appears at present that both energies and intensities of gamma-rays will have to be determined by the laborious cloud-chamber methods.

In addition to the location of a level, the question of the width of the resonance-level is of theoretical importance. A special effort was made to set limits on the 440-kv resonance in lithium. In Fig. 8 are shown integrated curves for resonances of various "half-widths"[9] with the ob-

[8] Crane, Delsasso, Fowler and Lauritsen, Phys. Rev. **48**, 125 (1935).

[9] It is customary to use the width at half-maximum or "half-width" as a measure of the sharpness of a resonance-

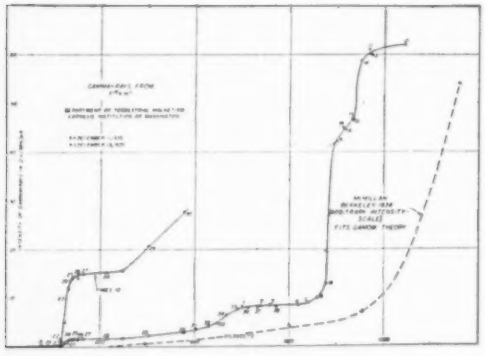

FIG. 9.

served points for the lithium-curve superimposed. From this comparison one can conclude that the "half-width" of the observed lithium-resonance curve is about 12 kv. However, part of this width must be ascribed to voltage-fluctuations, which produce a spread in the energies of the ions in the incident beam. Referring to Fig. 4 one estimates this width to be about 4 kv, leaving a width of about 11 kv $=(12^2-4^2)^{\frac{1}{2}}$ for the true resonance-width for this 440-kv process in lithium. This conclusion is open to the possible objection that the measurements of the voltage-fluctuations were not made at the same time as the gamma-ray measurements. However, the consistent behavior of the generator as indicated by the resistance-voltmeter and in our oscillographic tests seems to preclude the possibility that the voltage-fluctuation was abnormal by a factor of three during the taking of the observations on lithium. Further evidence that the above width is not due to the apparatus is given by the fact that a much smaller width was observed in fluorine as will be discussed below.

GAMMA-RAYS FROM F+H^1

Our results for this process are given in Fig. 9. The observations were primarily made to establish the several fluorine resonances on an absolute voltage-scale and to test the "resolving power" of our apparatus in the higher voltage-regions. The points shown in Fig. 9 are numbered in the order in which they were taken, each point requiring from three to ten minutes for a complete observation. The agreement between points 1, 2, 3 and points 36, 37, 38 taken several hours later is particularly satisfying. The existence of the close doublet with components at 894 and 942 kv has been checked by several indedently observed curves and appears to be real. The fact that these two lines are close probably accounts for the broad resonance-peak observed in this region in the observations made last year, when with less precise voltage-measurements our apparatus effectively had less "resolving power."

In the region from 400 to 700 kv the rapid rise in the curve suggests the possibility of several minor resonances. An effort was made to test this possibility, but no conclusive results were obtained due to difficulties in devising a suitable target. Crystals of CaF_2 were shattered by the localized heat of bombardment, and CaF_2 powder was blown about by electrostatic forces; hence, to obtain more precise data, experimentation with other compounds of fluorine will probably be required.

Estimates of the "half-widths" of the 328-kv, 892-kv, and 942-kv resonances made in the same way as for lithium give "observed" values of about 4 kv, 10 kv, and 15 kv, respectively. Since from the table in Fig. 4 these values appear to be practically equal to the "half-widths" of the voltage-distribution curves, the only permissible conclusion is that the "true" widths are probably smaller than these "observed" values.

DISCUSSION

Process of gamma-ray emission[10]

Any explanation of the observed resonance for the emission of gamma-rays when Li^7 is bombarded with protons has to make use of a temporary semistable state (virtual level) of Be^8. The mean life of this level is determined by the half-value breadth of the level and is thus $(1/4\pi)(510/11)(h/mc^2)=3.7h/mc^2=3\times10^{-20}$ sec. The width of the level must be due to its damping by all possible modes of decay.[11]

curve; see, for example, Slater and Frank, *Introduction to Theoretical Physics*, p. 37.

[10] We are indebted to Dr. Placzek and Professor Teller for valuable discussions of the problem of gamma-ray emission. We understand that these ideas will be published in a paper in the Physical Review which will appear shortly. The theoretical treatment given here in connection with the Li gamma-ray problem is due to Professor Breit.

[11] See, for example, Breit and Wigner, Phys. Rev. **49**, 519 (1936).

The virtual level of Be^8 may either radiate directly into a lower level of Be^8 or it may decay by disintegration into two alpha-particles at least one of which will then have to be excited. It is hard to account for a number of gamma-ray wave-lengths using only quantum jumps between different levels of Be^8 because such levels are more likely to disintegrate into two normal alpha-particles than to radiate gamma-rays. For this reason Crane and Lauritsen have assumed that the Be^8 nucleus first of all disintegrates into a normal and an excited alpha-particle; later the excited alpha-particle is supposed to radiate the complex gamma-ray spectrum. According to a recent report[12] the spectrum consists of a single line having an energy of 17 MEV and the main support for this picture of the process appears to be withdrawn.

Some preliminary observations made in Washington indicate that there may be also present a gamma-ray of 8-MEV energy. These observations were made on the magnetic curvature of Compton electrons expelled from a thin sheet of glass (about 500 kv thick) in a Wilson cloud-chamber by the $Li+H^1$ gamma-radiation. It was found that of 31 tracks with energies above 2 MEV which definitely originated in the thin glass sheet 22 fell in the region between 7.5 to 9.5 MEV. The only higher-energy Compton electrons were in the vicinity of 11 MEV, where three tracks were found.

According to the above it is still somewhat uncertain whether the gamma-ray spectrum consists of a single line or not. If it does, the simplest explanation is to suppose that the virtual state radiates directly into the normal level of Be^8. Afterwards the Be^8 nucleus may or may not dissociate depending on its still somewhat uncertain mass. We failed to observe any irregularity in the excitation function for the ordinary 8-cm alpha-particles in the vicinity of 440 kv either with thick or with thin targets. In the thick-target observations alpha-particles having a range greater than 7.6 cm would have been counted. The thin-target experiments were concerned with particles having greater penetrating power than 1.2-cm alpha-particles. This indicates that the resonance to gamma-rays has to do with states of excitation of the Be^8 nucleus which do not dissociate into normal alpha-particles. Quantitative measurements of gamma-ray intensities are at present still too uncertain to be sure of their number. Since, however, the probability of mechanical disruption is, under ordinary circumstances, many times greater than the probability of radiation it is probable that the virtual level of Be^8 is *barred* from disintegration into alpha-particles through the operation of some rather rigid selection-rule. This conclusion appears to be very probable for any mechanism involving radiative transitions within the Be^8 nucleus. It does not follow on the hypothesis of disintegration into a normal and an excited alpha-particle because such a disintegration could conceivably be so much more probable than disintegration into normal alpha-particles that no change in the yield of the 8-cm alpha-particles would be expected.

According to our present admittedly crude measurements of the yield of gamma-rays the collision cross section at resonance is roughly 10^{-27} cm^2. Substituting this into formula (14) given by Breit and Wigner and using $h\Gamma=5$ kv one finds that either $h\Gamma_\gamma\sim 1$ volt and $h\Gamma_\alpha\sim 5$ kv or else $h\Gamma_\alpha\sim 1$ volt and $h\Gamma_\gamma\sim 5$ kv. This means that there are essentially two possibilities for accounting for the order of magnitude of the yield: (1) The damping of the virtual level is due practically entirely to the possibility of break-up by dissociation into Li^7+H^1, the order of magnitude of $h\Gamma_\gamma$ is then so small that it is most reasonable to explain the process as being due to the emission of gamma-rays to a lower level of Be^8. (2) The damping due to disintegration into Li^7+H^1 could be supposed to be small ($h\Gamma_\alpha\sim 1$ volt) and all of the width of the level would be attributed so some other mode of disintegration. The high value of $h\Gamma_\gamma$ would not fit in with the expected probability of gamma-radiation within the nucleus. This mode would then involve some such process as the disintegration into excited and normal alpha-particles. The very small value of $h\Gamma_\alpha\sim 1$ is however somewhat improbable because it indicates that transitions from Li^7+H^1 to the virtual level are much less likely than ordinary calculations indicate. [It would be possible similarly to interpret $h\Gamma_\alpha$ as due to protons and $h\Gamma_\gamma$ as due

[12] Delsasso, Fowler, and Lauritsen, Seattle Meeting, Am. Phys. Soc. (1936).

to alpha-particle disintegrations using a large Γ_α and a small Γ_γ arising from some selection rule.] A process with a small Γ_α and a large Γ_γ cannot, however, be completely excluded, particularly since the gamma-ray spectrum is not yet certain. It would mean that the virtual level happens to be practically decoupled from Li^7+H^1 and at the same time it would have to dissociate more readily into a normal and an excited alpha-particle than into two normal alpha-particles. Thus even though a small Γ_α and a large Γ_γ are not logically excluded the number of conditions to be satisfied is greater and the radiative capture of Be^8 hypothesis fits in more naturally with present evidence. Experiments on the anomalous scattering of protons by lithium at the resonance voltage should differentiate between the two alternatives. On the hypothesis of the radiative transitions within Be^8 a scattering cross section of the order of 5×10^{-24} cm^2 would be expected while alpha-particle disintegration would be associated with a much smaller scattering cross section.

According to quantum mechanics energy-levels can be classified into even and odd and for closed systems there are no transitions between levels of these two classes; on the other hand electric dipole radiation jumps occur only between levels of one class and those of another[13] (Laporte's rule). It has been mentioned that if radiation takes place between levels of Be^8 a selection rule is needed to prevent the disintegration of the resonance level into two normal alpha-particles. Since two normal alpha-particles obey Einstein-Bose statistics and have no spin, the resonance level could be assumed to be odd and disintegrations into normal alpha-particles would be then prohibited. At the same time it would be necessary to arrange for stability against decay into a normal and an excited alpha-particle. Such stability can be automatically provided by supposing that the first odd excited level of the alpha-particle lies more than 17 MEV above the normal level. This is not in contradiction with Feenberg's calculations on the position of the lowest ^1P level in the alpha-particle and the ^3P level is probably above the ^1P level on account of the presence of exchange forces in the nucleus. On the above picture an

[13] E. Wigner, *Gruppentheorie.*

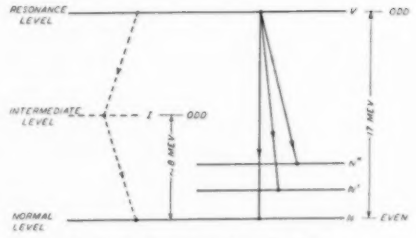

FIG. 10. Level system for Be^8.

electric dipole radiation can take place from the virtual to the normal level of Be^8. If the gamma-ray is actually quite monochromatic then one has to suppose that there is no other level between the resonance level and the normal state to which a transition with radiation can take place. It is very difficult, however, to be sure that even the 17-MEV component of the gamma-ray is monochromatic and so far as we are able to tell at present there is just as much evidence for a gamma-ray multiplet having components between 13 MEV and 17 MEV as for an entirely monochromatic gamma-ray. Confining ourselves for the present to the possibility of the first radiative transition occuring in Be^8 the following type of energy-level diagram of Fig. 10 can be considered as possible. The resonance level V is is responsible for the capture of the protons. It is supposed to be "odd" so as not to disintegrate into normal alpha-particles. No irregularity in the excitation-curve for the 8-cm particles will be then expected because odd and even levels do not interact. The normal level of Be^8 is designated by N and is supposed to be even. The 17-MEV ray may arise through electric-dipole radiation in the jump VN. In addition there may be either odd or even levels N', N'' within say 3 MEV of N. If these levels are even, there may be electric dipole-transitions VN', VN'' accompanied by subsequent disintegration into short range alpha-particles. If the levels N', N'' are odd no disintegration into alpha-particles would be likely to occur from them and instead soft gamma-rays would be emitted, in such jumps as $N'N$. It is more probable that the levels N', N'' are even and a search for short range alpha-particles appears to be worthwhile. In addition to the group of levels N', N'' there appears to be no reason against admitting an odd level I approximately

between V and N. Magnetic dipole or quadripole radiation would then account for 8-MEV gamma-rays, an indication of which has been obtained. Since, it was supposed that the first odd level of the alpha-particle is more than 17 MEV above normal in order to account for the stability of V, the level I would also be stable towards mechanical disruption and the absence of 4-MEV alpha-particles would follow. It is as yet not completely certain experimentally that such particles are not present in small amounts and the "odd" character of the level I is, therefore, not an absolute necessity. It should be noted that in thick targets with protons well above the resonance voltage the 4-MEV alpha-particles would be produced somewhat inside the target and would consequently be harder to detect.

In the above discussion and diagram levels are designated as odd and even in accordance with what appears to be likely from present conjectures about the normal state of Be^8. Clearly the only essential part of the argument is concerned with using selection rules. Thus the level V could be supposed to be even with odd spin and would still be stable towards disintegration into normal alpha-particles. It appears to be premature to list all possible arrangements of levels which might be consistent with present experimental facts. A certain degree of probability can be attached however to the particular assignment of levels given above making use of some recent and as yet unpublished calculations of Wigner and Feenberg. According to these one expects an even ^1D level to lie about 3 MEV above N which should be a ^1S level. The next even level (^1G) would lie about 8 MEV above N and would be thus approximately in the position of I. In order to have an electric dipole transition to N one may suppose V to be an odd P level which would then be also likely to give radiation to $N'=^1D$. On this view there should be short-range (1.5-MEV) alpha-particles emitted from N'. Transitions to the ^1G level would not occur except through the possible influence of higher multiple radiations. If transitions to the ^1G level should occur some 4-MEV alpha-particles will be emitted because its mean life is short when estimated by means of formulas for barrier-penetration.

If the virtual level V disintegrates by gamma-ray emission all of its width must be attributed to the probability of dissociation into Li^7+H^1. A theoretical estimate of the width can be made easily by regarding the proton as subjected to a central field due to the lithium nucleus. Using the formula[14]

$$\Delta T/T=1/\int_0^{r_0}\bar{G}^2 d\rho;\quad \bar{G}(r_0)=G(r_0)=D_L\rho^{-L}\Theta_L$$

where r_0 = nuclear radius, L = angular momentum of proton with respect to Li^7, the graphs for Θ_0, Θ_1, given by Yost, Wheeler, Breit,[15] and the WKB approximation for $L=2$, we obtain for the half-width $2\Delta T=400$ kv for $L=0$, 20 kv for $L=1$ and $\frac{1}{2}$ kv for $L=2$. In this calculation the integral in the denominator was approximated by $G^2\rho$. The above estimates are likely to give too high values for the width because the disintegration of V into Li^7+H^1 depends not only on the probability of the proton escaping but also on the chance of an internal nuclear rearrangement. There is thus no difficulty in accounting for the width using head-on collisions ($L=0$) and even those for $L=1$, but it is probable that $L=2$ plays little part in the process. The normal configuration of Li^7 is very probably *odd*. Since V must also be *odd* it is probable that the capture and dissociation occurs through the partial wave $L=0$. If, contrary to present views, the normal configuration of Li^7 should be even then $L=1$ will have to be held responsible. This is less likely also since little leeway is left for the probability of internal rearrangement.

Observations recently taken in this laboratory jointly with Dr. Rumbaugh of the Bartol Foundation indicate that there is stationary level in Li^7 about 400 kv above the normal state. Presumably this level corresponds to an angular momentum of $\frac{1}{2}$ and constitutes together with the normal state of Li^7 a doublet p term. It is conceivable that the small cross section for the production of gamma-rays is partly due to the disintegration of the virtual level V into a slow proton with an excitation of Li^7 to "p_1" level. The probability of this happening at 440 kv incident proton-energy should be small, because the barrier-penetration factor for the 440 − 400

[14] Breit and Yost, Phys. Rev. **48**, 203 (1935).
[15] Yost, Wheeler and Breit, Phys. Rev. **49**, 174 (1936) (the notation of this reference is used in the text above).

=40-kv protons decreases the probability of their interaction with the virtual level. It is possible, however, that at higher energies of incident protons evidence of inelastic collisions due to the excitation of the 400-kv level may be found.

Considerations such as the above cannot at present be effectively applied to the fluorine resonances, which have been shown to be significantly sharp, since even the reaction or reactions involved are at present uncertain.[5, 16]

Voltage-Scale for Inter-Laboratory Comparison

It has long been customary to measure voltages of ion-accelerators by giving the range in air of the ion-beam produced. However, the accurate specification of such ranges is by no means a simple matter, for such factors as straggling, ion-distribution, and current-density must be taken into account. The most readily determined specification of an ion-beam is probably a quantity which we might call the "visual range," this being merely the range of the particles in air as observed by the fluorescence produced when the beam is passed through a thin window into a darkened room. This quantity will be found to vary with current-density, room light, and different observers, and bears no definable relation to the "mean" range which is usually the quantity desired. In spite of these difficulties, however, it is repeatable to about ± 1 mm, and hence gives an accuracy of about ± 10 percent in voltage-measurements in the range in which this indicator can be conveniently used. For such purposes the relation $R = 2.5V^{\frac{3}{2}}$, where V is in megavolts, describes our results for the region between 500 and 1000 kv.[17] The "visual" range will in general be longer than the "mean" range due to thin spots in windows, voltage-fluctuations (since the peaks will be measured), variations in current-density, and other such causes.

For nonhomogeneous beams the visual range will of course give only the upper limit of energies. The effective voltage for disintegrations may then be any lower value, depending on the form of the ion-energy distribution-curve. Since in such cases sharp resonance-curves such as those described in this paper will no doubt be useful in calibrating ion-beams for both energy- and ion-distribution, we have endeavored to make our determinations as accurately as was immediately practicable. The original calibration against wire-wound standards insures that the measured voltages agree with the international scale to within two percent. This includes such errors as temperature-variation, which in the present design is relatively unimportant for the resistors are operated at only one-tenth of their rated capacity. While the location of a resonance is easily determined, the accurate specification of "half-widths," on which conclusions as to ion-distribution must be based, is difficult for two reasons. First, for sharp resonances, observations must be made at intervals of about 5 kv, which at voltages over 500 kv requires that the mean energy be measured to less than one percent; second, any asymmetry in the observed resonance-curves causes an ambiguity in the specification of "half-widths" when plotted as in Fig. 8. This problem becomes even more difficult when the observed width approaches the "fluctuation-width" for in this case any slight asymmetry in the ion-energy distribution would also have to be taken into account. With these qualifications in mind the points at present available for the calibration of ion-beams of unknown energy or distribution are as follows:

Voltage	Element	Half-width
328 kv	F	< 4 kv
440 kv	Li	11 kv
892 kv	F	<12 kv
942 kv	F	<15 kv

Acknowledgment

The authors take pleasure in expressing their indebtedness to Professor G. Breit for his continued interest and advice, to O. Dahl for invaluable aid in the design and construction of apparatus, and to Dr. R. G. Herb for his enthusiastic assistance in the construction and testing of the voltmeter-resistor while a guest at our Laboratory. Our thanks are especially due to our Director, Dr. J. A. Fleming, for his constant encouragement and unfailing support.

[16] Feather, "Reports on progress in physics," Proc. Phys. Soc., Vol. II.

[17] The voltage-scale used in this laboratory last year was based on a visual range of 2.85 cm at 1000 kv, 1.00 cm at 500 kv.

The Precise Measurement of Three Radium B Beta-Particle Energies

F. T. ROGERS, JR., *The Rice Institute*

(Received July 1, 1936)

The $H\rho$ of the three most intense Ra B β-particle lines have been measured by a precise magnetic spectrograph method and found to be 1406.0, 1671.1, and 1931.5 gauss cm. An explicit analysis has been made of the Cotton balance equations for H in this experiment and on the basis of this a complete analysis was made of the maximum relative error to be expected in the accepted values of $H\rho$. It is shown that the maximum relative error to be expected in the least $H\rho$ is 1 part in 3000 and that within this possible error the greatest $H\rho$ agrees with the value obtained by Scott. It is suggested that the accuracy of 1 part in 10,000 hoped for by Scott is rather too optimistic. The energies of these three β-particles are 1.512, 2.044, and 2.610 in units of 10^5 electron volts. It is shown that the least of these cannot be expected to be any more accurate than 1 part in 1000. The conclusion is that except for systematic errors which might have been present and undetected throughout this experiment and that of Scott, these experiments have established the values of these $H\rho$'s to within 1 part in 3000.

INTRODUCTION

IN 1924 Ellis and Skinner[1] measured $H\rho$ (H is the magnetic field necessary to produce a radius ρ of curvature in the path of a β-particle) for many of the β-particle energies of Ra B; for the three most intense lines of Ra B they got, correctly to within what they thought was 1 part in 500,

$$H\rho = 1410,\ 1677,\ 1938 \text{ gauss cm.}$$

In 1934 Ellis[2] repeated this work with more precision and got

$$H\rho = 1400.4,\ 1665.9,\ 1925.5 \text{ gauss cm}$$

(in which the last figures are not entirely significant) for these same lines. In 1934 also, Scott[3] performed a precise experiment on the most intense of these lines using the Cotton balance method of measuring the magnetic field rather than an inductive method; he got for this most intense line

$$H\rho = 1931.8 \text{ gauss cm}$$

and hoped it to be correct to 1 part in 10,000.

The present experiment was undertaken to check Scott's work and method and to extend the measurements to other lines in the Ra B β-particle spectrum. The values of

$$H\rho = 1406.0,\ 1671.1,\ 1931.5 \text{ gauss cm}$$

were obtained, the last of which is in good agreement with Scott's value for the most intense line. The $H\rho$'s for the other two lines as found by this experiment yield slightly different relative values of $H\rho$ from those previously obtained.

A more thorough investigation of the theory of the Cotton balance method of measuring H was carried out for this experiment. On the basis of it an analysis was made of the errors which might be present in the finally accepted values of $H\rho$. The conclusion was reached that in this experiment an accuracy of 1 part in 3000 is attainable if the value of H used in the finally accepted $H\rho$'s is determined from the mean of at least forty separate, equally weighted determinations of the mass used with the Cotton balance and if the values of ρ used finally are the means of seven separate, equally weighted determinations.

The good agreement (within 1 part in 6400 in $H\rho$) of the present experiment with that of Scott would seem to indicate that this type of measurement has at last established the absolute values of the $H\rho$'s for the three most intense lines in the Ra B β-particle spectrum to within 1 part in 3000 except for possible systematic errors which may have been present and undetected in both experiments.

The energies corresponding to the three $H\rho$'s we have determined are found to be

$$V = 1.512\times10^5,\ 2.044\times10^5,\ 2.610\times10^5 \text{ electron volts}$$

and can be considered as accurate to not better than 1 part in 1000.

APPARATUS

The apparatus used in this experiment was, except for a few small changes, that used by

[1] Ellis and Skinner, Proc. Roy. Soc. **A105**, 165 (1924).
[2] Ellis, Proc. Roy. Soc. **A143**, 352 (1934).
[3] Scott, Phys. Rev. **46**, 633 (1934).

Scott in his work and described by him in his paper.[3] It consists of a large permanent magnet with cobalt steel poles and with a 1.52 cm air gap faced on each side by soft iron disks 15 cm in diameter and 7.5 cm thick; the faces are quite nearly parallel and vertical. The flux density in the air gap can easily be adjusted to the desired value to within 1.5 gauss by means of a controlled current in two solenoids around the pole pieces. An investigation of the direction of the field in the gap showed that it deviates from the normal to the pole faces by less than 0° 05′. Computation by the series for cos 0° 05′ shows that the horizontal component of H differs from H by less than 1 part in 500,000. Thus the force which the Cotton balance measures, i.e., the horizontal component of H, is sensibly H.

The field in the air gap could be explored with search coils and galvanometers calibrated as fluxmeters. H as a function of the distance from the center of the field was determined with a coil and galvanometer designed to give an accuracy of one percent. Small variations of H near the center of the field were obtained with a 1000 turn coil of diameter 0.9 cm and an 18 ohm, high sensitivity galvanometer, the combination having a sensitivity of 0.0241 gauss per cm.

Supported above the air gap was a new Becker precision balance of which one pan had been removed. In place of the pan was hung a Pyrex glass plate about 30 cm long and 3 cm wide with its longer edges optically worked to be parallel to within 1/500 mm for 15 cm from one end. This plate hung from the lower ends of two parallel aluminum strips which hung in turn from a support-assembly attached to a knife edge of the balance. The plate-assembly was free to swing in two dimensions and was protected from external air currents by a surrounding brass case. Two straight silver strips about 1/10 mm thick were cemented with very dilute white shellac around the lower end and the two long edges of the plate; they were joined by a flat fold at the middle of the lower edge and formed the conductor of current in the magnetic field. This lower edge was placed along the x axis of Fig. 1 while measurements of H were in progress; the center line of the plate was along the y axis.

Measurements of plate and strips could be made with a Brown and Sharpe gauge which was

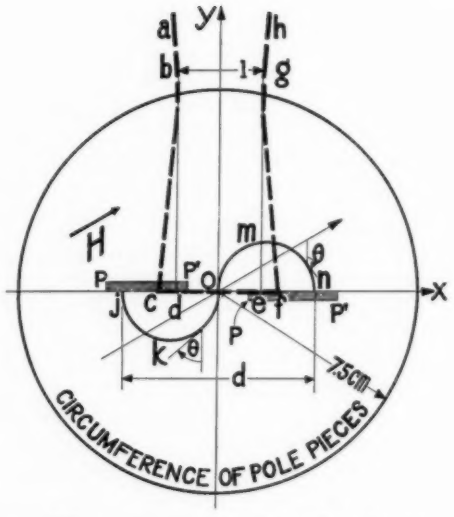

FIG. 1. PP' are photographic plates; O is the source of β-particles.

graduated in 10^{-4}'s of an inch and which could be reliably estimated to a 10^{-5} of an inch, with a Gaertner comparator and invar steel standard scale 10 cm long, and with a new Brown and Sharpe 31 mm standard disk. The invar scale was stated by the Bureau of Standards to be accurate to 1 part in 10^6. All measurements of the plate, strips, and photographic plates are expressed in terms of this standard scale when used as absolute lengths.

When the current in the strips was reversed, the change in force on them was measured by balancing it with a mass m on the balance. m was nearly 400 mg and was obtained in the main by combining the 200, 100 and 100 mg weights of a new and previously unused set of platinum, assayers' weights by Becker; each of these weights is quoted by the manufacturer as being accurate to within 0.005 mg. To get m really accurately, small balance deflections (occurring when the current in the strips was reversed) could be measured by the motion of a spot of light reflected from a small mirror on the balance beam to a scale about two meters from the balance. The location of the spot of light could be read to within 1/5 mm with a magnifying glass. When fully loaded in the experiment, the balance had a sensitivity of 0.409 mg/cm, which was entirely sufficient to get m accurately.

Current was supplied to the strips around the plate by two 160 ampere-hour lead storage batteries connected in parallel. The current was sent through two standard resistors of 4.0001 international ohms at 25°C and having negligible temperature corrections near 25°C. These resistors were connected in parallel by heavy copper bars and the current through them adjusted until a galvanometer in series with a standard cell (the two being connected across the resistors) showed no deflection. A measurement of H using one resistor balanced by two standard cells yielded the same value of H as this arrangement, so the resistance between the resistors and the copper bars was entirely negligible. The resistors were calibrated to 0.005 percent by the Bureau of Standards in February, 1934, and, except for Scott's work then, have not been used until the present experiment. The standard cell along with two others was calibrated to 0.01 percent by the Bureau of Standards at the same time and was found to have an e.m.f. of 1.01884 international volts at 25°C; at the time of this experiment these cells had not changed their relative e.m.f.'s by more than $\frac{1}{2}\times10^{-5}$ volts, so it was assumed that their absolute values had not altered appreciably. The galvanometer used to indicate the existence of the correct current was of sensitivity 1.84×10^{-8} amp./cm, readable to 1/5 mm easily. The current I could be adjusted by means of a variable resistance network to within $\frac{1}{2}\times$mm scale deflection, or to within 10^{-6} amp.

The Ra B β-particles (from the active deposit from the radon of 23 mg of radium) were emitted from the surface of a platinum wire placed at 0 (Fig. 1); they traveled in opposite directions as allowed by slits in the camera and fell on photographic plates PP'. The distances between the outer edges of the three sets of clearly defined "images" on the plates could be measured with the Gaertner comparator and standard scale. The camera and its enclosing box are of brass tested previously for magnetic effects and found to have none; Scott fully describes them in his paper.[3] The vacuum in the box was got by a Cenco Hyvac pump running continuously during the three and one-half hour exposures.

All observations and measurements were made in two rooms which were maintained at temperatures between 23° and 25°C.

Theory

Preliminary measurements have shown that when the glass plate is in position for field measurements, the center of the silver strip around the glass plate lies, in the large, along a curve C of the form (exaggerated in the diagram) of *abcdefgh* in Fig. 1; this curve is sufficiently nearly symmetric to be treated for our purposes as symmetric. In Fig. 1 the magnetic field H is perpendicular to the plane of the paper and directed into the paper; x and y axes perpendicular to H are chosen with their origin in line with the centers of the pole faces and half way between them, the x axis horizontally; ds with x component dx is an element of length along C. The width l of the current loop is measured at some convenient location (as bg) along the glass plate.

To get the field H_0 at the origin by the Cotton balance method, note that the force acting on the current I (e.m.u.) in the strip is, besides gravity, $I\int_c Hdx$; when I is reversed, the change in force on the strip is measured by the weight of the mass m which will just counterbalance it; then

$$mg=2I\int_c Hdx.$$

Since H and C are necessarily continuous, we can write

$$\int_c=\int_a^c+\int_c^d+\int_d^e+\int_e^f+\int_f^h;$$

and since subsequent experiment shows that

$$\int_a^c,\ \int_c^d,\ \int_e^f,\ \int_f^h<10^{-3}\int_d^e,$$

approximate evaluation of these integrals is satisfactory. Let

$$H=H_0+h(x) \text{ along } de,$$
$$H=H_0F(y) \text{ along } ac \text{ and } fh,$$
$$H=H_0 \text{ along } cd \text{ and } ef;$$

then

$$mg=2I\Big\{H_0\int_a^c F(y)dx+H_0\int_c^d dx$$
$$+\int_d^e[H_0+h(x)]dx+H_0\int_e^f dx+H_0\int_f^h F(y)dx\Big\}.$$

Also let C be represented from a to c by $x=f(y)$, and let

$$\int_c^d dx=\tfrac{1}{2}\Delta l;$$

then in view of the symmetry of C with respect to the y axis,

$$mg=2I\left[2H_0\int_a^c F(y)f'(y)dy+H_0\Delta l+H_0 l+\int_{-l/2}^{l/2}h(x)dx\right].$$

By solving for the coefficient of l,

$$H_0=\frac{1}{l}\left[\frac{mg}{2I}-2H_0\int_a^c F(y)f'(y)dy-H_0\Delta l-\int_{-l/2}^{l/2}h(x)dx\right];$$

here m, g, l and I are measurable with high accuracy; the last three terms in the right member are of the nature of corrections to the first and (as previously stated) are fairly small, so in them only the approximate value of H_0 need be used.

To this Cotton balance equation for H_0 must be added for this experiment the Hartree correction for non-uniformity of H along the β-particle paths. In Fig. 1 two semi-circular paths for the same β-particle energy are Okj and Omn; measuring θ along them as shown in the figure, let

$$H=H_0+h_1(\theta) \text{ along } Okj,$$
$$H=H_0+h_2(\theta) \text{ along } Omn.$$

Then according to Hartree,[4] the first order correction to be applied to H_0 to give the constant value of H which, if it were acting all along the β-particle path Okj, would produce the observed deviation Oj is

$$\tfrac{1}{2}\int_0^\pi h_1(\theta)\sin\theta d\theta.$$

Applying to the above equation for H_0 the mean of the two Hartree corrections for the two paths of the same energy of β-particle, we get

$$H_0=\frac{1}{l}\left[\frac{mg}{2I}-2H_0\int_a^c F(y)f'(y)dy-H_0\Delta l-\int_{-l/2}^{l/2}h(x)dx\right]+\frac{1}{4}\left(\int_0^\pi h_1(\theta)\sin\theta d\theta+\int_0^\pi h_2(\theta)\sin\theta d\theta\right), \quad (1)$$

which is the expression adopted for H_0 to be used in $H\rho$.

To get ρ, the distance d between the outer, clearly defined edges of corresponding images on the photographic plates is measured; from it is subtracted the diameter D of the platinum wire supporting the source at O. Then

$$\rho=(d-D)/4. \quad (2)$$

$H\rho$ for a β-particle energy is the product of the appropriate value of expressions (1) and (2).

The relative error to be expected in a single determination of H_0 follows from two principles concerning errors:[5] the relative error in a product of quantities having known relative errors is the sum of the relative errors of the multiplicands, and the absolute error of a sum of quantities having known absolute errors is the sum of the absolute errors of the summands. Let ϵ_i, $i=1$ through 10, be the absolute errors which might possibly be present in single determinations of d, D, l, m, g, I, $H_0\int Ff'dy$, $H_0\Delta l$, $\int h(x)dx$, and $\int h(\theta)\sin\theta d\theta$ respectively; these must be estimated from the precisions of the observations on the several quantities entering into expressions (1) and (2). Then since (by the definition of relative error) there corresponds to the relative error in a quantity an absolute error whose magnitude is equal to the product of the magnitude of the quantity into the relative error,

$$(mg/2I)(\epsilon_4/m+\epsilon_5/g+\epsilon_6/I)+2\epsilon_7+\epsilon_8+\epsilon_9$$

is the absolute error to be expected in the bracketed part of expression (1); to it corresponds quite nearly the relative error

$$\epsilon_4/m+\epsilon_5/g+\epsilon_6/I+(2\epsilon_7+\epsilon_8+\epsilon_9)/(mg/2I).$$

Hence the absolute error in the first term of the

[4] Hartree, Proc. Camb. Phil. Soc. **21**, 746 (1923).
[5] Gibbs, *Adjustment of Errors in Practical Science* (Oxford Press, 1929), pp. 76–78.

right member of (1) is approximately

$$H_0\left(\frac{\epsilon_3}{l}+\frac{\epsilon_4}{m}+\frac{\epsilon_5}{g}+\frac{\epsilon_6}{I}+\frac{2\epsilon_7+\epsilon_8+\epsilon_9}{mg/2I}\right);$$

added to the absolute error

$$\tfrac{1}{2}(\tfrac{1}{2}\epsilon_{10}+\tfrac{1}{2}\epsilon_{10})=\epsilon_{10}/2,$$

in the second term and divided by H_0, we have as the relative error to be expected in a single determination of H_0:

$$e_1=\frac{\epsilon_3}{l}+\frac{\epsilon_4}{m}+\frac{\epsilon_5}{g}+\frac{\epsilon_6}{I}+\frac{2\epsilon_7+\epsilon_8+\epsilon_9}{mg/2I}+\frac{\epsilon_{10}}{2H_0}. \quad (3)$$

The relative error to be expected in a single determination of ρ is obviously

$$e_2=(\epsilon_1+\epsilon_2)/(d-D). \quad (4)$$

If ϵ_i, $i=1$ through 10, are estimated conservatively as the maximum absolute errors to be expected in their parent magnitudes, the corresponding maximum relative error to be expected in an accepted $H\rho$ is

$$e_3=e_1+e_2. \quad (5)$$

To get the energy E of a β-particle of known $H\rho$, combine with the relativistic expression

$$E=m_0c^2[1/(1-v^2/c^2)^{\frac{1}{2}}-1]$$

for E the relativistic force equation

$$Hev=mv^2/\rho=m_0v^2/\rho(1-v^2/c^2)^{\frac{1}{2}}$$

so as to eliminate v. Here v is the velocity of the β-particles, m_0 their rest mass, e their charge, and c the velocity of light. The resulting expression

$$E=m_0c^2[(A+1)^{\frac{1}{2}}-1],\ A=(H\rho e/m_0)^2(1/c)^2,$$

is the one commonly used. If e/m_0 is in e.m.u. and if e is in e.s.u., then $m=(m_0/e)(e/c)$; also if E is expressed (as V) in electron volts, its value in ergs must be multiplied by $10^{-8}\ c/e$; thus if $H\rho$ is in gauss cm, the energy in electron volts is

$$v=(m_0/e)c^2[(A+1)^{\frac{1}{2}}-1]\times10^{-8}. \quad (6)$$

This can be put more conveniently for computation if we define ϕ by

$$\phi=\tan^{-1}A^{\frac{1}{2}}=\tan^{-1}(H\rho e/m_0)(1/c),$$

then

$$v=(m_0/e)c^2(\sec\phi-1)\times10^{-8}. \quad (7)$$

If ϵ_{11} and ϵ_{12} are the absolute errors to be expected in e/m_0 and c respectively, the relative error to be expected in $(A+1)$ (see Eq. (6)) is

$$\frac{A}{A+1}\left(2e_3+\frac{2\epsilon_{11}}{e/m_0}+\frac{2\epsilon_{12}}{c}\right).$$

Since the extraction of the square root of a quantity with a known relative error yields roots with relative errors only half that of their square,[6] the absolute error in $(A+1)^{\frac{1}{2}}$ is

$$\frac{A}{(A+1)^{\frac{1}{2}}}\left(e_3+\frac{\epsilon_{11}}{e/m_0}+\frac{\epsilon_{12}}{c}\right),$$

which is also to be expected in $[(A+1)^{\frac{1}{2}}-1]$. Hence by addition of the relative errors in m_0/e, c^2, and $[(A+1)^{\frac{1}{2}}-1]$, the relative error to be expected in V is

$$e_4=\frac{\epsilon_{11}}{e/m_0}+\frac{2\epsilon_{12}}{c}+\frac{A}{(A+1)-(A+1)^{\frac{1}{2}}}\left(e_3+\frac{\epsilon_{11}}{e/m_0}+\frac{\epsilon_{12}}{c}\right). \quad (8)$$

The values of ϵ_{11} and ϵ_{12} are preferably the maximum errors judged to be possible in the accepted values of their parent magnitudes; if they are not, but are the probable errors quoted with the accepted values, e_4 is of the nature of an hybrid which is only a lower bound of the maximum relative error to be expected in V.

It should be remembered that expressions (3), (4), (5) and (8) do not take into account any systematic errors which might have been present and undetected in the determinations of the quantities appearing in expressions (1), (2) and (7).

Measurements

The experiment consisted in measuring the quantities appearing in expressions (1) and (2) so as to determine, respectively, H and the ρ's

[6] For if a is a quantity with a small known absolute error Δa, then

$$(a+\Delta a)^{\frac{1}{2}}=a^{\frac{1}{2}}+\Delta a/2a^{\frac{1}{2}}+\cdots\leqq a^{\frac{1}{2}}+\Delta a/2a^{\frac{1}{2}}.$$

Thus the relative error in $a^{\frac{1}{2}}$ is

$$(1/a^{\frac{1}{2}})\times(\Delta a/2a^{\frac{1}{2}})=1/2(\Delta a/a),$$

or is one-half the relative error in a.

for the three lines. H_0 was determined from forty determinations of m and each ρ was determined seven times in order to reduce the maximum possible relative error to be expected in $H\rho$ as far as is reasonably possible. The accepted $H\rho$ for an energy is the product of the H_0 value (from the forty determinations of m) as corrected for the proper path by the Hartree correction, into the appropriate radius of curvature of the path. The correction quantities were in general determined first. The error quantities ϵ_i were estimated as each quantity was measured. All measurements were repeated at least once, usually more than once. Data are usually recorded with more figures than are strictly significant, in order to prevent the entrance of errors in computation.

The functions $h(x)$ and $h(\theta)$ were determined from changes in H revealed by the 1000 turn coil and the sensitive galvanometer. Table I is the data obtained for $\int h(x)dx$ at $H_0=1250$ gauss. Integration was effected numerically by assuming that $h(x)$ is linear between adjacent experimentally determined points; the result is that

$$\int_{-l/2}^{l/2} h(x)dx = -0.319 \text{ gauss cm.}$$

It is estimated that $\epsilon_9=0.01$. Table II is the data used in calculating $\int h(\theta)\sin\theta d\theta$ for $H_0=1250$ gauss and $\rho=1.54$ cm; $h(\theta)$ are given in gauss. Integration is exactly as before and the results for this radius and for the two other radii used are tabulated in Table III; the Hartree correction as tabulated is the mean of the two corrections for the two paths from 0. It is estimated from experience with these that $\epsilon_{10}=0.01$.

The value of l was measured at the location bg (Fig. 1), which is between $y=8.0$ and $y=9.0$. It was measured first with the comparator and standard scale and found to be 3.07918 cm. After the experiment was terminated, l was measured again, but with the 31 mm disk and the Brown and Sharpe gauge. The value of 3.07891 cm was obtained in this way. The finally accepted value of l is the mean of these two: $l=3.07905$ cm. These values of l are got by subtracting from the overall width of the glass plate and silver strips at bg, half the thicknesses of the silver strips at that location. To accompany l we assign $\epsilon_8=0.00015$.

TABLE I. *Data for* $\int h(x)dx$.

x (cm)	$h(x)$ (gauss)
−1.5	−0.018
−1.0	−0.106
−0.5	−0.076
0.0	−0.000
0.5	−0.113
1.0	−0.187
1.5	−0.263

TABLE II. *Data for* $\int h(\theta)\sin\theta d\theta$, $\rho=1.54$ *cm.*

	$\rho=1.54$ cm	
θ	$h_1(\theta)$	$h_2(\theta)$
0°	0.000	0.000
30°	−0.027	−0.263
60°	−0.115	−0.566
90°	−0.110	−0.667
120°	−0.234	−0.501
150°	−0.130	−0.314
180°	−0.189	−0.150

TABLE III. *Hartree corrections.*

ρ (cm)	$\frac{1}{2}\int h_1 \sin\theta d\theta$ (gauss)	$\frac{1}{2}\int h_2 \sin\theta d\theta$ (gauss)	Correction (gauss)
1.12	−0.098	−0.352	−0.225
1.34	−0.128	−0.418	−0.273
1.54	−0.122	−0.471	−0.296

To evaluate $f'dy$ and Δl, the total width of the glass plate and of the silver strips in place was measured at many locations along the plate with the 10^{-4} inch gauge; as above, from these widths were subtracted half the thicknesses at the same locations of the silver strips. In Table IV are representative data from the large amount actually obtained by these measurements. As before it is assumed that $f(y)$ is linear between points determined experimentally. Since l was chosen as the width of the current loop between $y=8.0$ and $y=9.0$, Δl is obtained by subtracting the width of the current loop at $y=8.5$ from the width at $y=0.0$; from Table IV we have $\Delta l=3.08251-3.07905=0.00346$ cm.

The function $F(y)$ was obtained with the less sensitive fluxmeter arrangement; its values are given in Table V. For purposes of integration, $F(y)$ was also assumed to be linear between observed points. It is found that $2\int Ff'dy=$

TABLE IV. *Width of current loop.*

y (cm)	Width of strips and plate (cm)	½ sum of strip thicknesses (cm)	$2f(y)$ = width of current loop (cm)
0.0	3.09195	0.00944	3.08251
0.5	3.08914	0.00945	3.07969
1.0	3.08901	0.00945	3.07956
2.0	3.08853	0.00947	3.07906
2.3	3.08835	0.00948	3.07887
2.4	3.08876	0.00949	3.07927
2.8	3.08905	0.00950	3.07955
2.9	3.08862	0.00951	3.07911
3.0	3.08849	0.00952	3.07897
4.3	3.08966	0.00952	3.08014
4.5	3.08953	0.00953	3.08000
5.5	3.08878	0.00952	3.07926
6.0	3.08877	0.00951	3.07926
6.7	3.08903	0.00949	3.07954
7.0	3.08911	0.00950	3.07961
8.5	3.08853	0.00948	3.07905
9.5	3.08837	0.00946	3.07891
11.5	3.08861	0.00950	3.07911
12.0	3.08873	0.00949	3.07924
12.4	3.08854	0.00948	3.07906
12.6	3.08876	0.00946	3.07932
13.2	3.08905	0.00944	3.07963
13.5	3.08861	0.00944	3.07917
15.0	3.08861	0.00945	3.07916
17.0	3.08869	0.00945	3.07924
17.5	3.08903	0.00943	3.07960
18.0	3.08854	0.00943	3.07911
20.0	3.08847	0.00942	3.07905
25.0	3.08872	0.00944	3.07928

-0.00354 using the entire set of data of which Table IV is a representative portion; the Table IV data give a slightly lower value than this.

The actual values of the corrections $H_0\Delta l$ and $2H_0\int Ff'dy$ are obtained directly as

$$H_0\Delta l = 1250\times 0.00346 = 4.33 \text{ gauss cm},$$
$$2H_0\int Ff'dy = 1250\times(-0.00354) = -4.43 \text{ gauss cm}.$$

It is estimated that $\epsilon_7=\epsilon_8=0.05$.

Since the resistors used in getting I are calibrated to only 0.005 percent and since the standard cells, to only 0.01 percent, the maximum error to be expected in I is at least 0.015 percent. The error inherent in adjusting for I with the resistance network is at most 10^{-7} e.m.u. By Ohm's law I is 0.509403 international ampere; the conversion[7] to e.m.u. gives $I=0.0509433$ e.m.u. Thus $\epsilon_6=0.0000076+0.0000025=0.00001$; the second term is added because of the uncertainty in the factor of conversion from international to electromagnetic units.

[7] *The Smithsonian Physical Tables*, eighth edition (1933), p. 81, gives one international ampere equal to (0.99995 ±0.00005) absolute ampere.

Because three weights are required to produce the 400 mg of m, ϵ_4 must contain 0.015 mg. Because of errors possible in locating the ends of the balance deflections when I is reversed, which come to $2\times0.02\times0.41=0.0164$ mg, ϵ_4 is larger than 0.015. Since m was measured nine times in each of the forty determinations of it, we take[8] $\epsilon_4=(0.015+0.0164/9^{\frac{1}{2}})/40^{\frac{1}{2}}=0.0032$ mg.

The value of g in the locality of the experiment is 979.28 cm/sec.^{2} and $\epsilon_5=0.005$ cm/sec.^{2}.

By observing the balance deflections when I was reversed and when the 400 mg were placed on the balance, the correction to be applied to the 400 mg to give m accurately could be found. These deflections were observed nine times for each determination of m. The forty mean observations of the balance deflection are recorded with their mean in Table VI. The evaluation of H_0 by taking for m the mean of a large number

TABLE V. *Function $F(y)$.*

y (cm)	$F(y)$
0.0	1.00
5.6	1.00
7.5	0.91
8.5	0.50
9.5	0.26
10.5	0.17
11.5	0.13
12.5	0.11
15.0	0.07
17.5	0.04
22.5	0.02

TABLE VI. *Observations of balance deflections for m.*

Trial	Defl. (cm)	Trial	Defl. (cm)	Trial	Defl. (cm)	Trial	Defl. (cm)
1	1.53	11	1.52	21	1.52	31	1.52
2	1.52	12	1.54	22	1.50	32	1.52
3	1.52	13	1.53	23	1.52	33	1.52
4	1.53	14	1.54	24	1.51	34	1.52
5	1.52	15	1.54	25	1.51	35	1.51
6	1.53	16	1.50	26	1.51	36	1.51
7	1.51	17	1.51	27	1.52	37	1.54
8	1.52	18	1.51	28	1.53	38	1.51
9	1.53	19	1.52	29	1.52	39	1.52
10	1.54	20	1.52	30	1.52	40	1.50

Mean = 1.520

[8] Analogously to the customary procedure used in the operation of classical error computations, we assume that the relative error of the mean of n determinations of a quantity varies inversely as $n^{\frac{1}{2}}$. See, e.g., Bartlett, *The Method of Least Squares*, third edition (1915), p. 44, Eq. (46).

of observations which extended over several days is valid because Scott[3] showed in his experiment that over a period of weeks the value of H_0 remained sensibly constant. The value of m to be used is thus $0.4000000+1.52\times0.000409=0.400622$ gm. By use of Eq. (1) and the previously evaluated correction quantities it is seen that, except for the Hartree corrections,

$$H_0=\frac{1}{3.07905}\left(\frac{0.400622\times979.28}{2\times0.0509433}+4.43-4.33+0.32\right)=1250.70 \text{ gauss.}$$

Values of d were read from the photographic plates with the Gaertner comparator corrected by the standard scale; they could be repeated to within 0.0001 cm usually. Since each was done seven separate times, $\epsilon_1=0.0001/7^{\frac{1}{2}}=0.000038$. The value of D was found with a direct-reading 10^{-4}-inch Brown and Sharpe micrometer caliper and is 0.02405 cm to within $\epsilon_2=0.0001$ cm. In Table VII are presented the seven values of each ρ got by Eq. (2) and their three means. Since H_0 is constant, these should be constant within the proper groups in the table.

Knowledge of the H_0 from Table VI, of the mean ρ's of Table VII, of the Hartree corrections of Table III, of the various correction terms, and of the estimates of the possible errors is sufficient to provide the desired values of $H\rho$ and of the possible errors present.

Results

Tables VIII, IX, X, and XI contain the results of the experiment. The accepted $H\rho$'s of Table VIII are from the value of H_0 from Table VI and corrected by Table III and from the ρ's of Table VII. In view of the good agreement (1 part in 6400) of the present value of $H\rho$ for the most intense β-particles and that of Scott, it seems safe to consider the $H\rho$'s listed in Table VIII as sufficiently adequately determined in absolute value (within the possible limits of relative error given below) to serve as rather reliable standards of β-particle $H\rho$'s.

In Table IX are the possible relative errors necessary to the computations based on Eqs. (3), (4) and (5) for the least $H\rho$; they are collected from the section on Measurements. Thus the values of $H\rho$ in Table VIII cannot be considered as any more accurate than 1 part in 3000, even though each measurement used in getting $H\rho$ is more accurate than 1 part in 3000. Evidently some 60 percent of the uncertainty is accounted for by the uncertainty in the calibrations of the standard cells and standard resistors and in the uncertainty in the conversion factor for international and electromagnetic units of current. Within this limit of 1 part in 3000 the present experiment yields the same value of $H\rho$ for the most intense Ra B β-particles as Scott's experiment, though it is seen that Scott's hopes for an accuracy of 1 part in 10,000 are rather too optimistic.

The energies corresponding to the $H\rho$'s we have established are obtained from Eq. (7) using[9]

Table VII.

Trial	ρ (cm)	Mean ρ (cm)
1	1.12442	
2	1.12446	
3	1.12442	
4	1.12440	1.12440
5	1.12442	
6	1.12440	
7	1.12426	
1	1.33642	
2	1.33642	
3	1.33650	
4	1.33645	1.33644
5	1.33657	
6	1.33635	
7	1.33642	
1	1.54471	
2	1.54476	
3	1.54468	
4	1.54462	1.54472
5	1.54478	
6	1.54470	
7	1.54471	

Table VIII. *$H\rho$'s of three intense Ra B β-ray lines.*

Line	$H\rho$ (gauss cm)
Least intense	1406.0
Of medium intensity	1671.1
Most intense	1931.5

[9] The value of e/m_0 is that given by Birge, Phys. Rev. **49**, 204 (1936). c is taken from *The Smithsonian Physical Tables*, eighth edition (1933), p. 74.

TABLE IX. *Maximum relative errors to be expected in least $H\rho$.*

Error	Magnitude	Magnitude (parts per 10,000)
ϵ_2/l	0.00015/3.079	0.49
ϵ_4/m	0.00002/.4007	0.08
ϵ_5/g	0.005/979.3	0.05
ϵ_6/I	.00001/.05094	1.97
$2I(2\epsilon_7+\epsilon_8+\epsilon_9)/mg$	0.16/3850	0.41
$\epsilon_{10}/2H_0$	0.01/2500	0.04
$\epsilon_1/(d-D)$	.000038/4.496	0.08
$\epsilon_2/(d-D)$	.0001/4.496	0.22
Sum $=e_3$		3.34

$$e/m_0 = 1.7562\times10^7 \text{ e.m.u./g},$$
$$c = 2.99796\times10^{10} \text{ cm/sec.}$$

with $\epsilon_{11}=0.00027\times10^7$ and $\epsilon_{12}=0.00004\times10^{10}$. They are in Table X.

In Table XI are the numbers necessary for the calculation of the lower bound e_4 of the relative error to be expected in the least V according to Eq. (8). They follow from the preceding two paragraphs. Eq. (8) becomes by substitution of these numbers

$$e_4=\frac{1.54}{10{,}000}+\frac{0.24}{10{,}000}+\frac{0.678}{0.383}\left(\frac{3.34}{10{,}000}+\frac{1.54}{10{,}000}+\frac{0.24}{10{,}000}\right)=\frac{1.1}{1000}.$$

Thus the energies V cannot be considered as more accurate than 1 part in 1000. In fact, since ϵ_{11} and ϵ_{12} are only classical probable errors, e_4 may be even larger than 1 part in 1000, the increase depending only upon how much larger than the probable errors the corresponding absolute errors possible in e/m_0 and c are.

TABLE X. *Energies of three intense Ra B β-rays.*

$H\rho$ (gauss cm)	V (electron volts)
1406.0	1.512×10^5
1671.1	2.044×10^5
1931.5	2.610×10^5

TABLE XI. *Quantities for calculation of e_4 for least V.*

Quantity	Magnitude	Magnitude (parts per 10,000)
$\epsilon_{11}/(e/m_0)$	0.00027/1.7562	1.54
ϵ_{12}/c	0.00004/2.998	0.12
e_3	3.34/10,000	3.34
A	$\left(\frac{1.406\times1.756}{2.998}\right)^2=0.679$	

It is also noteworthy that even though $H\rho$ is accurate to within 1 part in 3000, the major part of the 1 part in 1000 accuracy allowed for V is accounted by possible errors in $H\rho$.

Finally, it should be noted that the improvements of this experiment over that of Scott lie in the facts that: a new balance of higher sensitivity, a new set of weights for m, straight silver strips, the standard scale, and a new gauge graduated in 10^{-4}'s of an inch were available; twice as large a current, determined by a far simpler potentiometer, was used in the Cotton balance; it includes measurements for the three most intense Ra B lines rather than for only one; and it provides a conservative, explicit estimate of the precision of which it is capable, 1 part in 3000 in $H\rho$, 1 in 1000 in V.

The writer also wishes in conclusion to record his appreciation both for the suggesting of this experiment and for the valuable aid given him during the experiment, by Dr. H. A. Wilson.

Tests of the Validity of X-Ray Crystal Methods of Determining e

JESSE W. M. DUMOND AND VERNON L. BOLLMAN, *California Institute of Technology, Pasadena*

(Received June 15, 1936)

The procedure in determining the electronic charge, e, from measurements of x-ray diffraction angles and the density of crystals has been criticized on the ground that while the density measurements are averages of a large volume, say 10 cc of crystal, the x-rays are diffracted from a surface layer as determined by "extinction" only about 4×10^{-4} cm thick, a very small fraction of the total volume in an entirely specialized location. Partial answers to this criticism by Y. C. Tu and by Allison and Armstrong have rendered its validity much less probable. The present work with extremely fine powdered calcite samples whose density was determined with a pycnometer closes the question completely, we believe, leaving no ground whatever for the criticism and placing the x-ray determinations of e on a very solid experimental foundation. Our work yields a value for e of 4.799 ± 0.007 abs. e.s.u. based on the scale of ruled grating wave-lengths in which Cu $K\alpha_1$ has a wave-length (Bearden's value) of 1.5406×10^{-8} cm. Efforts to remove the above objection by studies on macroscopic calcite samples which failed to withstand our own criticisms are described since they emphasize the pitfalls that a conclusive test must avoid. Several new unexplained crystal diffraction effects discovered in this search for a conclusive test are also described. Agreement to one part in six thousand between Bragg and Laue diffraction angles was established for two different sets of Miller indices in macroscopic calcite.

I. CRITICISMS OF THE X-RAY METHOD OF DETERMINING e

IT now seems highly probable that the excellent and concordant ruled grating measurements[1] of the wave-lengths of a number of characteristic x-ray lines establish in absolute centimeter units a reliable scale of wave-length values which combined with the very precise relative scale of x-ray wave-lengths in terms of Siegbahn's conventional unit fixes the absolute values of all of the carefully measured x-ray lines to a precision of say one part in two thousand. The usual procedure in determining the electronic charge e then involves a measurement of the diffraction angle θ in Bragg reflection from a crystal surface and a computation of the interplanar spacing d of the crystal lattice in absolute units by means of the familiar formula (with refractive index correction of Siegbahn)

$$n\lambda = 2d \sin\theta(1-\delta/\sin^2\theta). \qquad (1)$$

By such methods the absolute dimensions of the crystal lattice may be determined. If, as in the case of calcite, the lattice is not cubic the absolute volume of the unit cell may be determined either (1) by combining the value of d with x-ray or optical goniometric measurements on a macroscopic crystal to establish the characteristic angle β of the rhombohedron or (2) x-ray determinations of the interplanar spacing may be made for several Miller indices, two being theoretically sufficient to establish the necessary angular relationships. The first mentioned procedure is by far the more common. The absolute volume of the unit cell for calcite generally expressed as $8d^3\Phi(\beta)$ is then combined with a measurement of the macroscopic density ρ of the crystal employed and by means of the formula

$$d=(Me)^{\frac{1}{3}}[2Q\rho\Phi(\beta)]^{-\frac{1}{3}} \text{ or } e=2d^3Q\rho\Phi(\beta)M^{-1} \qquad (2)$$

the value of e is computed. M is the molecular weight of $CaCO_3$; and Q the Faraday constant.

Three criticisms enumerated

(1) Criticisms have been raised from time to time that the macroscopic density which is an average value for a crystal volume of, say, 10 cc may not apply to the extremely thin superficial layer (5×10^{-5} cm thick in the first order) involved in Bragg reflection. Allison and Armstrong[2] have endeavored to answer this criticism by measuring the reflection angles in different orders up to the fifth where the penetration, they

[1] The following is far from an exhaustive list of such work: Compton and Doan, Proc. Nat. Acad. Sci. **11**, 598 (1926); J. Thibaud, J. de phys. et rad. **8**, 13 (1927); E. Bäcklin, Inaugural dissertation (Uppsala, 1928), Zeits. f. Physik **93**, 450 (1933); J. M. Cork, Phys. Rev. **35**, 1456 (1930); J. H. Bearden, Phys. Rev. **37**, 1210 (1931).

[2] Allison and Armstrong, Phys. Rev. **26**, 701 (1925). See also Allison's excellent discussion in Compton and Allison, *X-Rays in Theory and Experiment*, page 698. For experimental support of the shallow penetration depths given by extinction formulae see recent work by W. Kossel and H. Voges, Ann. d. Physik **23**, 677 (1935).

compute, should be of the order of 1.2×10^{-3} or 40,000 planes. Y. C. Tu[3] finds that calcite, rock-salt, KCl and diamond agree very well in giving the same value of e. Criticisms of the x-ray method of determining e nevertheless have continued on the above grounds and it must be admitted that the superficial layers of a crystal constitute such a specialized part of its volume that every effort should be made to extend the x-ray measurements so as to make the latter as representative as possible of the entire volume whose density has been measured. Unless this is done there is certainly a logical hiatus in the above reasoning by which we arrive at the value of e and it is the closing of this gap by a solid experimental procedure which we here chiefly wish to report.

(2) It is not out of place to mention that the methods we have employed also conclusively answer the criticism sometimes raised that the crystal may contain minute cracks, gaps or crevices in its structure.

(3) Another type of criticism which we have never heard raised but which we believe might have occurred to the truly critical minded is a question as to the precise validity of the Eq. (1) relating θ, λ and d, when the variables are regarded as having an absolute significance. A really critical defense of this equation requires an appeal to the dynamical theory of x-ray diffraction. Darwin, Ewald, Prins, and Laue have all contributed brilliantly to this subject. Nevertheless the dynamical theory for the space grating, taking account of mutual to and fro interaction between all of its parts, becomes so complicated that none of the treatments can quite be regarded as straightforward rigorous solutions of the wave equation for the case of a medium with a threefold periodic distribution of refractive index with the same beautiful generality and finality of the corresponding treatment by Eckart[4] on diffraction from ruled plane gratings. The effect of extinction about which there is yet very little good experimental information probably operates to produce very rapidly changing intensities and amplitudes of the electromagnetic radiation from point to point within the crystal. Such an assumption as the immediate reorganization of secondary dipole wavelets to form plane waves inside the crystal, so essential to Ewald's theory, or the assumption of constancy of phase displacement for all atoms might not be quite correct for instance. The precision measurements in the third order here described using calcite powdered to the order of 10^{-4} cm and smaller seems to us to answer completely any objections founded on doubts as to the rigor of the dynamical theory since the simple elementary theory of Laue or Bragg must certainly apply to crystals so small that the radiation is negligibly extinguished in passing through them.

II. Search for the Most Conclusive Method

The idea of the powdered calcite method of answering the above objections only came to us as an evolution from two other methods which after much research we felt did not meet critical objections which we ourselves could raise. It is probably valuable therefore to describe as briefly as possible the pitfalls discovered in this way the better to emphasize what must be avoided if a truly conclusive conclusion is to be drawn. Furthermore we ran across certain interesting new and as yet unexplained phenomena, well worth reporting for themselves, in this search for a conclusive method.

Two crystal spectrometer studies

Our first attempt consisted in a comparison, by means of the two crystal spectrometer, of the calcite reflection angles for the two cases which we called briefly Bragg reflection and Laue reflection. We reasoned that in the Laue case with the incident beam entering one face and the reflected beam emerging from an opposite face after reflections by internal planes parallel to neither of these faces *the whole interior structure* of the crystal must have served for reflection of the radiation and the reflection angle should therefore be representative of the entire crystal just as was the mean density measurement. This method of course fails to meet criticisms (2) and (3) above however.

On account of the construction of the only two crystal spectrometer then available,[5] not the entire Bragg or Laue angle θ was measured but

[3] Y. C. Tu, Phys. Rev. **40**, 662 (1932).
[4] C. Eckart, Phys. Rev. **44**, 12 (1933).
[5] J. W. M. DuMond and A. Hoyt, Phys. Rev. **36**, 1702 (1930).

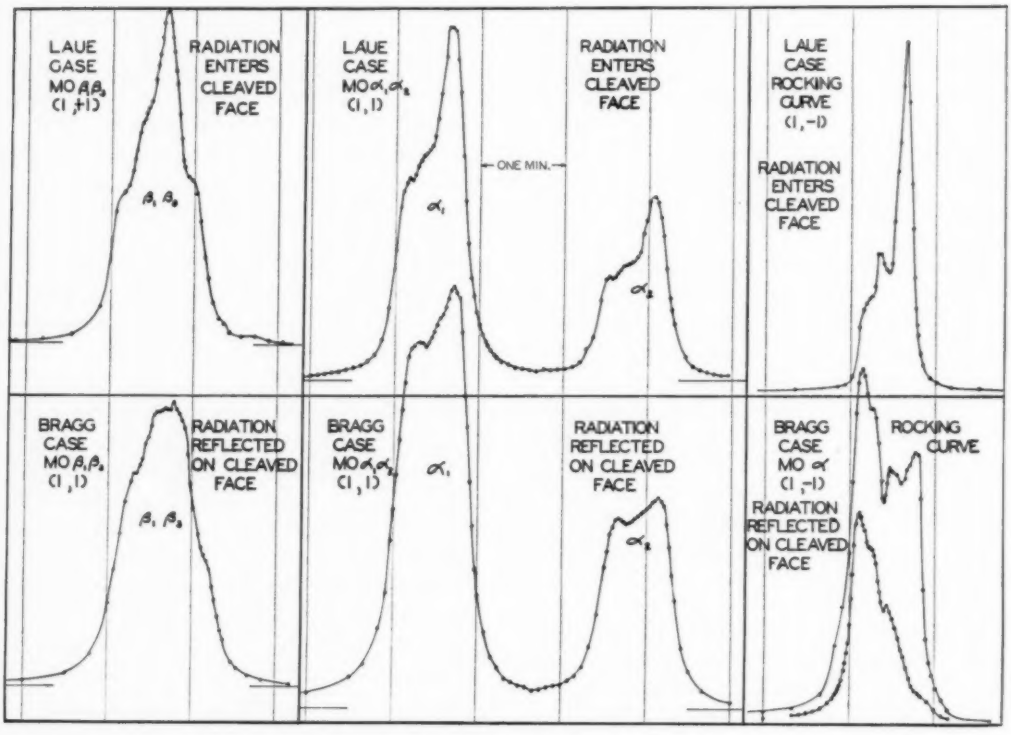

FIG. 1. Line structures obtained with etched calcite.

only the angular interval between two widely separated lines of the molybdenum K spectrum. Crystal No. 1 of this spectrometer, a large and very perfect specimen of split calcite obtained from Steeg and Reuter in Hamburg was regarded as the collimator. Crystal No. 2 was very thin and could be oriented so as to reflect the collimated beam from No. 1 either in Bragg reflection from its large flat surface or in Laue reflection with the beam traversing its thin dimension reflected from internal planes parallel to a cleavage surface, in this case the thin edge of the flake. All appropriate alignments of the crystals by optical reflections from the faces and from the thin edge were carefully attended to. Gliding of the reflecting region across the crystal faces in the exploration of a spectrum was prevented by the mechanism of the spectrometer and x-ray table support. The effort was to see whether the angular interval between two given lines would be identically the same for the Bragg case as for the Laue. One of the first calcite samples used for test was rendered thin by etching down a rectangular portion in the center of a thicker (5 mm) slab with dilute HCl squirted through a fine nozzle. The etching did not proceed very uniformly and had to be controlled by stopping off various regions from time to time with wax. The thin window so formed varied in thickness from 0.5 to 0.2 mm. The unetched cleavage face on the reverse side could be used for Bragg reflection.

The etched crystal yielded the surprising line structures of Fig. 1. Prominent facts and inferences about these curves are: (1) The "lines" are about 3 times as broad as those usually observed with good calcite though the specimen was initially of the highest quality. (2) The curious rugged profile of each line, suggesting the presence of several simple component lines partially resolved, is reproduced for quite different wavelengths (Mo $K\alpha_1$ Mo $K\beta_{1,3}$). (3) The invariability of pattern for *different* wave-lengths indicates that these component peaks are caused by a variety of orientations in the crystal rather than

by a variety of grating constants. (4) A composite structure appears even in Bragg reflection for the unetched and apparently quite undamaged cleavage face on the opposite side to the etched surface. This may be caused either by released strains and disorientations of parts of the crystal where etching occurred extending themselves elastically through the thin dimension of the crystal to the unetched face or by the penetration of radiation from the unetched face through to the disturbed etched region sufficiently to permit considerable reflection there. (5) The rocking curves in the (1–1) order both in Bragg and Laue reflection also exhibit a composite broad structure but the structures in Laue and in Bragg reflection for (1,1) and (1–1) orders, four cases in all, have each a different characteristic profile.

These results which we cannot explain are the more surprising since it has recently been shown that the rocking and reflection curves can actually be markedly narrowed for calcite by appropriate light etching. This etched sample was obviously useless for our primary purpose. These results made us perhaps overcautious in regard to the possible existence of internal stresses in calcite which may have been released and thus rendered observable by the nonuniform etching process.

The work with the two crystal spectrometer was continued with thin cleaved plates of calcite for the crystal No. 2. Several good thin samples a millimeter or less in thickness were obtained. A great deal of experimentation was required to work out the best mounting for such thin and easily deformed flakes and much trouble was encountered with slight angular shiftings of the flake in its mount. In order to get reliable results which would average out any slight effect of curvature of the flake it was eventually found essential to take measurements of the angular interval between lines from both sides of the crystals both for the Bragg and Laue cases. Slight differences of temperature in different parts of the spectrometer, caused by a lamp used to read the angle scale, were found to cause some of the anomalies. Some mysterious erratic shiftings of the line positions with time were never completely explained but fortunately disappeared in our later and more careful work. Our first observation before all of these difficulties had been found and corrected happened to show by pure accident a difference between the angular intervals for Laue as compared to Bragg reflection indicating a difference in grating constant for these two cases of 0.2 percent and of the right direction to explain the, at that time, current magnitude of the discrepancy between x-ray and oil drop values of e. The possible importance of such a result made it imperative to check the two crystal spectrometer work by an independent method which would permit of measuring with precision the *entire* diffraction angle in Laue reflection. We therefore constructed an especial precision photographic spectrometer, to be described below, which yielded Laue diffraction angles with identically the same thin calcite crystal that had been used on the two crystal spectrometer in complete agreement with the most reliable determinations of Bragg diffraction angles to well within the estimated error of the method (one part in six thousand).

To eliminate all uncertainties we continued the two crystal spectrometer comparisons and found that with a sufficient number of precautions and especially that above mentioned of taking an average of the angular interval measurements from both faces of the crystal to eliminate minute curvature effects we could obtain complete and satisfactory agreement between the Bragg and Laue angular intervals. The slight shifting effect of differential absorption across the width of a line in Laue reflection was established as negligible. Lines α_2 and β_2 of molybdenum were used. An aluminum filter was introduced in the case of the α_2 line as a convenience to make the intensity comparable to that of the β_2 line

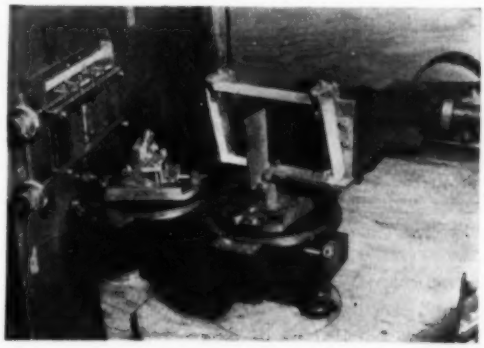

FIG. 2. Two crystal spectrometer arrangement for comparing Laue and Bragg diffraction angles.

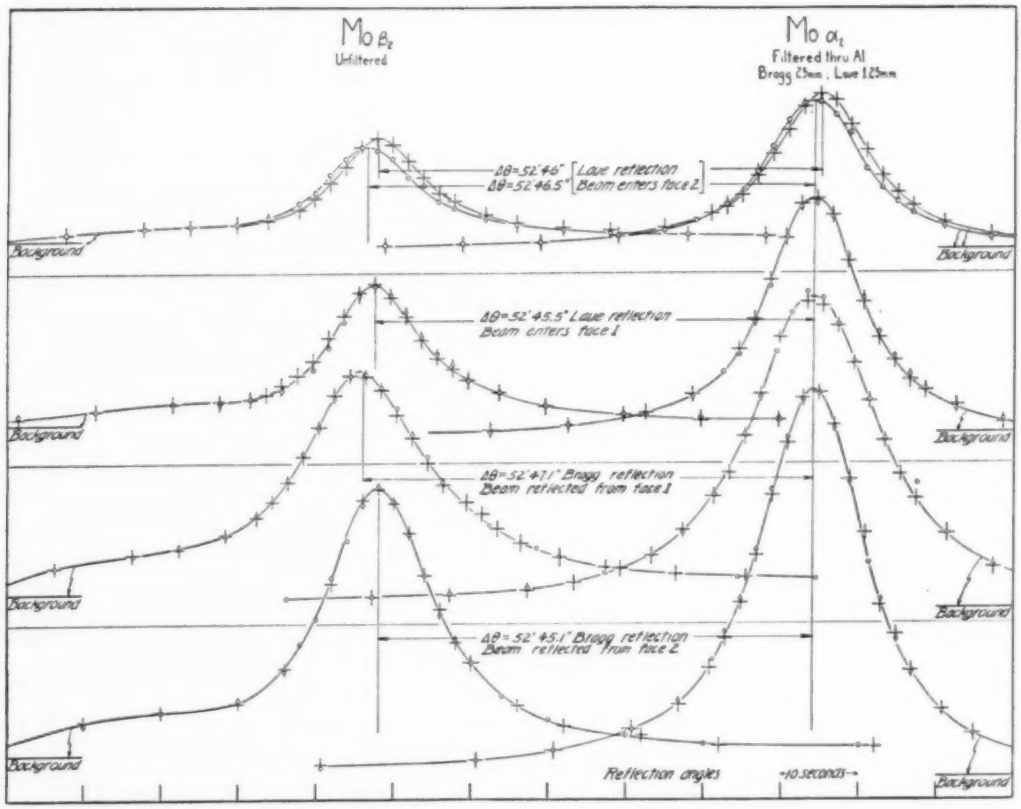

FIG. 3. Angular intervals between Mo $K\alpha_2$ and Mo $K\beta_2$ lines obtained on two crystal spectrometer comparing Laue and Bragg cases.

without changing the electrometer sensitivity. A thinner filter was appropriate for the Laue case than for the Bragg since the crystal itself is a strong filter. Fig. 2 shows the two crystals in place in the two crystal spectrometer while Fig. 3 shows the final results of the angular interval comparisons with this method.

In the Laue reflection work with the two crystal spectrometer it was found that the symmetry and width of the lines depended greatly on the region of the crystal used for reflection in the case of all samples. Regions too near the point of support were always "bad" but other regions with no such easily explained cause also showed distortions of line shape. Such distortions often seemed present at, as nearly as we could estimate, the same general regions in Bragg reflection. A suspicion could have appeared at this point that our Laue measurements were not as representative of the interior portions of the crystal as we at first thought. At this point however we merely felt the strong need for some statistical method which would free the x-ray measurements of the individual peculiarities of different crystals and of different regions in the same crystal.

Study of Laue reflection with precision photographic transmission spectrometer

Fig. 4 is a photograph of the precision photographic transmission spectrometer. Its chief novelty is the crystal and slit mounting. The crystal and slit are held on small independently movable carriages sliding in ways on the top of a brass disk which turns on a well made conical pivot whose axis is accurately normal to the plane bed plate surface of the instrument. The plate holder is carefully made so as to maintain the photographic emulsion also accurately normal to

the bed plate surface. By means of appropriate slides and leveling screws the slit was placed accurately parallel to and in coincidence with the axis of rotation of the pivot by reversals under a microscope with cross hairs and the thin crystal flake by means of other slides and leveling screws had its vertical thin edge and its flat face both made parallel to the pivot axis by optical reflections. One of the slides permitted moving the crystal flake so that one face stood very close indeed to the jaws of the slit. By further optical adjustments the pivoted disk was so oriented that a plane through the slit parallel to the reflecting planes to be used in the crystal flake would strike the photographic plate accurately normally and a small lead shield with a fine slit was placed at this point on the plateholder opening, just where the foot of this perpendicular fell on the plate, to serve as a fiducial mark. The pivot was firmly clamped during x-ray exposure. Initially, spectral line photographs were taken with the crystal on the x-ray tube side of the slit. By swinging the spectrograph with respect to the x-ray tube, $K\alpha$ lines of the Mo spectrum could be formed on the plate by Laue reflection both from the right and from the left side of the lattice planes inside the crystal flake, the transmitted beam being shielded in each case from fogging the plate by a movable lead slide. The fiducial center mark was also recorded on the plate by a short auxiliary exposure through the slit and crystal with direct radiation. In all cases the foot of the perpendicular from slit to plate proved to be so accurately centered between the right-hand and left-hand spectra that no correction for geometrical asymmetry would have been significant. The distance from slit to plate was carefully measured with a cathetometer and found to be 606.5 ± 0.1 mm. The cathetometer scale was checked on the same comparator used for measuring line separations on the plate. Fig. 5 shows the geometry of the set-up.

Very beautiful and finely resolved lines of the α doublet were obtained on several plates. Compton's precise measurements[6] of the Bragg reflection angle in calcite with a precision Société Génevoise two crystal spectrometer yielded an angle of 6° 42′ 36″ for the α_1 line of molybdenum. If this same angle holds for Laue reflection the separation δ of the right- and left-hand lines on our plate should be 142.710 mm. On two photographic exposures we obtained

$$\delta_1 = 142.725$$
$$\delta_2 = 142.712$$
$$\delta_m = 142.719 \text{ mm}.$$

These Laue reflection data are in better agreement with Compton's Bragg data then the precision of our cathetometer measurement warranted. These cathetometer measurements, good to 1 part in 6000, constitute the determining element in the accuracy of this method and the agreement between Bragg and Laue reflection angles was thus established to that relative precision.

This was identically the same crystal flake used on the two crystal spectrometer and it was the above result that completely proved the unreality of the preliminary apparent discrepancy between Laue and Bragg angles obtained at first with the two crystal method.

As a further check we also made a measurement with the photographic transmission spectrometer using $(1\bar{1}0)$ planes (these indices are referred to cleavage axes). These planes are shown in Fig. 6 which is a projection of a unit cleavage cell looking along one of its edges. It is evident that

$$d_{100}/d_{1\bar{1}0} = 2 \cos \tfrac{1}{2}\alpha.$$

Bearden gives $\alpha = 105°\ 3'\ 29''$. The wider separation of the right- and left-hand spectra in this case required moving the plateholder to a new position closer to the slit. The new slit to plate distance (482.55 mm $\pm$ 0.03) was determined

FIG. 4. Photograph of precision photographic transmission spectrometer. Slit and crystal are here in position of Fig. 7 or Fig. 9a.

[6] A. H. Compton, Rev. Sci. Inst. 2, 365 (1931).

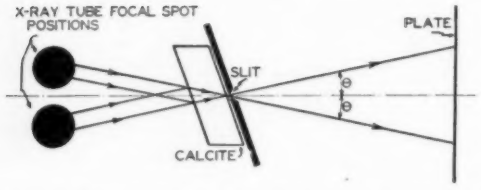

FIG. 5. Geometry of precision photographic transmission spectrometer as normally used for determining diffraction angles with slit on plate side of crystal. The radiation left the nearly horizontal target surface in the x-ray tube at a small glancing angle of about 5°. The diameter of the round focal spot furnished a sufficiently extended source just to permit the simultaneous reflection of the α and β doublets with careful adjustment.

as before and the computed separation of the lines reflected from $(1\bar{1}0)$ based on Compton's Bragg (100) reflection data was $\delta = 138.613$ mm. On two plates we obtained

$$\delta_1 = 138.621$$
$$\delta_2 = 138.614$$
$$\delta_m = 138.617 \text{ mm.}$$

This would furnish a complete check for this piece of calcite not only of the lattice parameter but of the angles characteristic of the calcite rhomb for reflection from internal planes were it not for the results of the next experiment.

Laue reflection probably not a valid test of the interior of a crystal

As a last precaution we thought it would be safer to make quite sure that, in the above work with the two crystal spectrometer and the photographic spectrometer, the reflection was indeed coming from the interior of the crystal. To our astonishment and chagrin the contrary proved true.

We turned the crystal and slit mounting of the precision photographic transmission spectrometer round through 180° so that now the crystal was between the slit and the photographic plate. The geometry of the new arrangement appears in Fig. 7. Now instead of a fine line on the plate for each wave-length we expected to get a broad band of width d_1 and d_2 for the right- and left-hand spectra, respectively. The triangular region OAB in the crystal we thought would be a field in which multiple to and fro selective reflection would take place so as to fill out the spaces between lines A_1B_1 and A_2B_2 with more or less uniform distributions of widths d_1 and d_2. Instead of this lines only appeared at A_1, B_1, A_2 and B_2 with negligible intensity between them. Fig. 8 shows an enlargment of a very short section of these doubled lines. For simplicity of discussion we will here describe the phenomenon entirely in terms of the appearance of a single monochromatic line, say α_1.[7]

Entry and exit surface Laue reflections not quite parallel

From the thickness of the crystal and the angle ψ Fig. 7 we computed the separations d_1 and d_2 to be expected as 0.0232 cm and 0.0217 cm, respectively. The observed separations of the line pairs A_1B_1 and A_2B_2 turned out to be not quite equal to these expectations at all distances but to approach these values the closer the plate came to the crystal. The beams $A_1B_1A_2B_2$ which one would have expected to be propagated in parallel pairs turned out to have the members of each pair apparently very slightly convergent. This *might* have been an effect on the plate of the slightly increased overlapping of the members of a pair at greater distances as the breadths of the members increased slightly with increasing

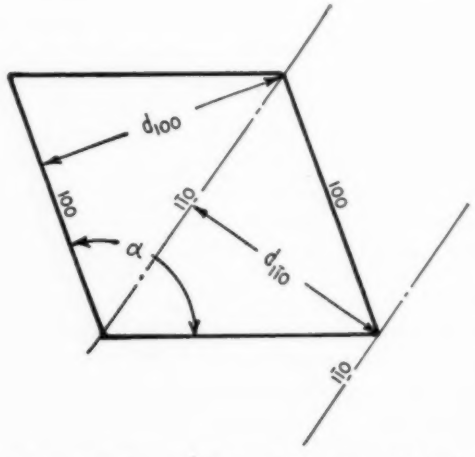

FIG. 6. Projection of unit cleavage cell of calcite looking along a direction parallel to one edge to illustrate the $(1\bar{1}0)$ planes in relation to the cleavage planes.

[7] The effect of enhanced Laue reflection at a ground or otherwise disturbed crystal face is of course well known and understood. The crystals here used however had excellent cleavage surfaces with narrow rocking curves and we were quite unprepared for the almost complete absence of reflected intensity between A and B.

distance. The tendency for doublet separations to appear smaller than they should as the members overlap more and more is a well-known illusion. We tend to doubt this explanation and to think the convergence real.

Fluctuations of intensity along the lengths of the spectral lines

An even more surprising peculiarity of the spectral lines taken with the crystal in this position and one which we believe has never before been reported, is a more or less periodic fluctuation of the intensity vertically along the *length* of the line. Both these phenomena were observed in varying degrees in all the thin flake samples of calcite we examined, some of which had very marked fluctuations of intensity amounting to complete extinction of the line at roughly uniformly spaced intervals. A careful study of these fluctuations at different slit-plate distances with the x-ray tube at different vertical elevations with respect to the slit and plate convinced us that each of these fluctuations is definitely associated with some local condition permanently assignable to different localities in the crystal and is not as we thought at first some sort of Fresnel interference effect. It seems strange however that the extinguished points on the two lines forming a pair such as A_1B_1 seemed to occur at about the same vertical heights with more than accidental agreement. If, as appears probable, the two members of each pair are merely strongly enhanced reflections from the disturbed front and back surfaces of the crystal it is hard to see why these disturbances should be localized at corresponding points on the two sides of the thin flake. No such fluctuation of intensity along the length of the lines was observed with the slit between crystal and photographic plate.

Faint radiation between the exit and entry Laue reflections

We had to settle the question as to whether the radiation was absent between the members of a pair such as A_1B_1 because of some sort of destructive Fresnel interference or whether its absence there was simply because the interior of the crystal failed to reflect. This we did by introducing auxiliary slit jaws J_1, J_2 with micrometer

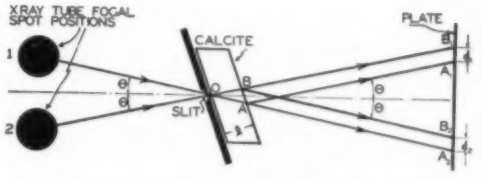

FIG. 7. Geometry of precision photographic transmission spectrometer as used to study entrance and exit surface Laue reflections. The slit is now on the opposite side of the crystal from the plate.

screw movements close behind the crystal as shown in Figs. 9a and 9b, so as to cut off at will either line A_1 or B_1 or both. It was found that with either member of the pair cut off the remaining member was unchanged. With both members cut off so as to have a slit that would only permit radiation C_1C_1' or C_2C_2' reflected from the interior of the crystal to reach the plate, some fifteen times as much exposure was necessary to obtain lines, and these lines were hazy, ill defined and unsuitable for precise measurement.

More work should certainly be done in the study of these strange effects for themselves but for the point at issue the methods so far described of studying Laue reflection in macroscopic calcite may be criticized (I) as really failing to measure the interior grating constant of the crystal which is involved in the density determinations, (II) as being too highly dependent on peculiarities of individual crystals or individual regions in one crystal.

III. The Powder Method a Conclusive Answer to All These Criticisms

Since one is apparently restricted to investigations of a very superficial layer when using macroscopic calcite either in Laue or Bragg reflection *a conclusive answer to all these criticisms should come from a study of finely powdered calcite of grain size smaller than the extinction layer.* If one investigates the diffraction angles and density of crystals of size 10^{-4} cm on a side, so small that extinction is negligible in them, it is obvious that a statistical result truly representative of the entire sample is obtained both for density and diffraction. If it be a valid criticism that unbalanced forces near the surface of a macroscopic crystal render the density there somewhat dif-

FIG. 8. Photographic reproduction of Laue reflections from exit and entry surfaces of a thin calcite crystal.

ferent from the mean then one might expect the density of the finely powdered calcite to be different from the mean density of macroscopic calcite. *It is important therefore to measure the density of the identical calcite powder used in the diffraction experiment.* This was done with a pycnometer with included thermometer.

Pycnometric density determination on powdered calcite

The density of the pycnometer water was checked by weighing a known volume which had been measured out with a standardized "ausguss" pipette. The laboratory distilled water was 0.08 percent lower density than that given by the handbooks and it was necessary to redistill it in an all glass still and boil it to remove occluded gas. With these precautions the average deviation from the standard table values of six determinations of the density of this water was only three parts in one hundred thousand. The density of both macroscopic and microscopic calcite crystals was determined in the same pycnometer bottle as a check, the macroscopic samples being slivers as large as would go in the neck of the bottle. The macroscopic samples weighed 12 grams while the powdered samples ranged from 21 grams to 10 grams in amount. The powder was made by grinding in an agate mortar and rejecting the coarser grains by precipitation in water. The impalpable powder thus obtained had some visible grains under an immersion microscope of a size which we estimated as 2×10^{-4} cm. The method of precipitation of course would give grain sizes ranging down below this upper limit into the submicroscopic. In measuring the diffraction rings from the powder the few isolated specks caused by reflection from the fortuitously oriented larger grains were ignored and the measurements were taken to the centers of the smoothly filled out parts of the rings only. It seems likely therefore that the grains actually involved in the measurements were very considerably smaller than these few largest ones seen in the microscope and that they constituted the bulk of the samples.

The results of our density determinations on macroscopic and powdered calcite are compared in Table I with the excellent data obtained by Bearden[8] on macroscopic calcite by weighing in fluids. The probable errors of our data are computed from internal consistency of the observations. The reproducibility of the measurements of the fine powder is indeed remarkable. In filling the pycnometer bottle containing the calcite powder with water it was found that preevacuation of air by means of a vacuum pump decreased the tendency for small air bubbles to be trapped by the powder. Stirring by rotation of the bottle during filling also helped.

It is easy to show that the solubility of calcite in water introduces an error of only one part in forty thousand in the density determination.

The powder diffraction measurements

To obtain the maximum possible precision in the absolute determination of the size and shape of the lattice a Seeman-Bohlin spectrograph was used and reflections were chosen for such primary wave-length and Miller indices that the reflected beam would return almost directly backward to a region *FF'* (see Fig. 10) not far from the pinhole

TABLE I. *Density of calcite.*

STATE	METHOD	OBSERVER	DENSITY	PROBABLE ERROR	NO. OF OBSERVATIONS
Powdered	Pycnometer	Bollman	2.71022	+0.00035	6
Macroscopic	Pycnometer	Bollman	2.71085	+0.00019	3
Macroscopic	Immersion	Bearden	2.71030	+0.00003	

[8] Bearden, Phys. Rev. **38**, 1389 (1931).

at S through which the primary rays had entered. This means that θ in the equation $n\lambda = 2d \sin \theta$ is nearly 90°. Considering λ as a known constant from grating wave-length determinations if we differentiate this equation and replace θ by $\alpha = \frac{1}{2}\pi - \theta$ (since the measurements of the diameters of diffraction rings centered around the entrance pinhole are nearly proportional to α) we obtain

$$\alpha \tan \alpha(\Delta\alpha/\alpha) = \Delta d/d \qquad (3)$$

or for small α $\quad \Delta d/d = \alpha^2(\Delta\alpha/\alpha).$ (4)

Thus if in radian measure α is of order 0.1 the relative error in determining the lattice constant d is only one one-hundredth as great as the relative error committed in measuring on the film.

Nickel K radiation was chosen for the work. A rather long wave-length is necessary in order to have reasonably intense reflections in calcite at angles θ near 90°. On the other hand too long a wave-length limits the depth of penetration by extinction whereas the whole point of the experiment is to have the penetration into the small particles as great as possible. In fact the two requirements, low extinction and strong reflection, are more or less mutually contradictory. The obvious solution is to tolerate the *weakest possible diffraction ring intensities that will yield acceptable precision in measuring their locations in order to get as little extinction as possible in the passage of radiation through the particles.* The reason for choosing nickel for the target was because we computed that the Ni $K\alpha$ lines would be just reflected in the third order from the $(1\bar{1}0)$ planes (cleavage system) of Fig. 6 at an angle θ slightly less than 90°. Measurements eventually were discarded on this reflection as it was found to be too faint and diffuse on account of the enormous dispersion at this large angle but three planes with other Miller indices were found to yield all the information needed from the nickel radiation. The target of the tube was made by nickel plating an old water-cooled copper target. A cylindrical Nonex glass envelope about $1\frac{1}{2}$ inches in diameter provided with a thin concave glass window in the end of a short side tube was blown around the cathode and target and a thoroughly outgassed charcoal trap in a side tube was kept in liquid air during operation.

The spectrograph had a lead alloy lining to reduce the general scattering. Diffraction exposures taken without the calcite powder but with the x-rays simply incident on the lead showed strong diffraction rings inconveniently located close to the calculated positions of diffraction rings from calcite. These were completely eliminated by covering the lead in the radiated area with several sheets of gold foil which in a test exposure showed no rings whatever in the region where our calcite rings appeared. The spectrograph had a tight cover provided with a gasket and could be evacuated with a fore pump. This precaution we found necessary to reduce the fogging and general background of the film. Even so the calcite diffraction rings were very faint and are unfortunately unsuitable for reproduction by half-tone process.

Fig. 11 shows the x-ray tube and the spectrograph with cover removed. The calcite powder which was made to adhere to the cylindrical

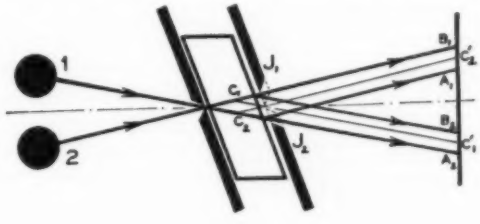

a

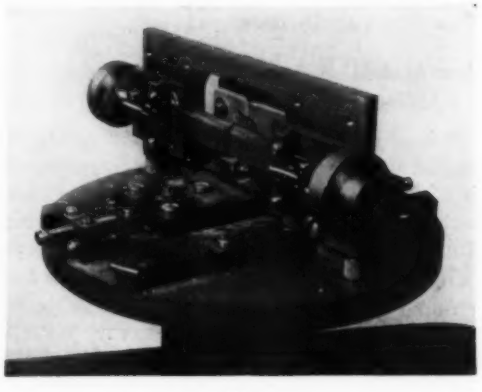

b

FIG. 9a. Auxiliary slit jaws used in study of entrance and exit surface Laue reflections. 9b. Photograph of transmission spectrometer slit and crystal mounting with auxiliary jaws.

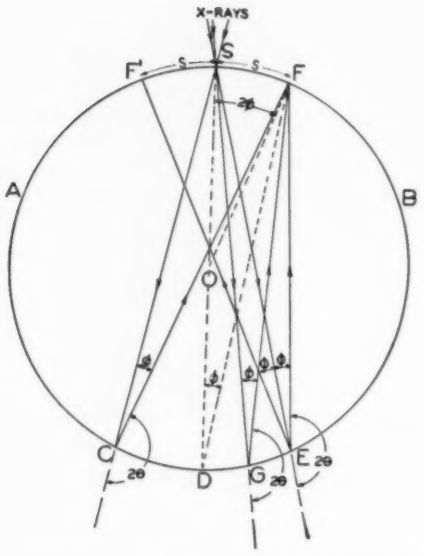

FIG. 10. Geometry of Seeman-Bohlin spectrograph.

surface with a tiny quantity of collodion can be seen as a white patch on the inner wall of the spectrograph. Part of the film holder and the slit both on the opposite side of the spectrograph can also be seen. The calcite powder sample had a thickness of 0.25 mm to correspond with the thickness of the double-coated x-ray film. The diameter of the spectrograph $D=6.905$ inches was carefully calipered inside at a number of points. The greatest deviation from uniformity of D was one part in 7000.

Identification of powder diffraction rings with Miller indices

It is of course absolutely essential to identify beyond all doubt the Miller indices corresponding to all powder rings measured. If a reciprocal lattice for calcite is constructed the coordinates of each point of which correspond to the Miller indices of a set of planes and a sphere is struck out centered at the origin with radius $R=(2\sin\theta)/\lambda$

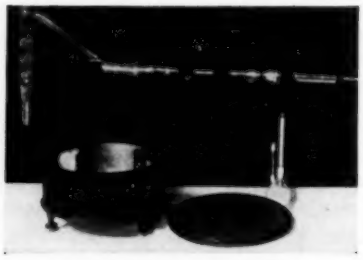

FIG. 11. Nickel target x-ray tube, Seeman-Bohlin spectrograph and pycnometer bottle.

Ewald has shown that any points of the reciprocal lattice lying on this sphere will correspond to the Miller indices of planes which can reflect radiation λ under angle θ. Two such reciprocal lattices were graphically constructed. The points lie in planes equally spaced in a vertical direction. In each plane the points lie at the corners of lozenge shaped cells having angles of 60° and 120°. Fig. 12 shows a projection of the reciprocal lattices looking along the vertical axis. A sphere of radius $R=(2\sin\theta)/\lambda$ was struck out in one of these for $\theta=75°\ 24'$ and in the other for $\theta=83°\ 39'$. This sphere intersects the equally spaced horizontal planes in circles as shown in the figure. Thus if a circle passes through a lattice point in the projection that point *may* correspond to a possible reflection. The method of constructing the reciprocal lattice by starting for convenience with the calcite lattice *in the hexagonal system* gives *all* possible calcite Miller indices and some which are *not* a part of the calcite system. These can be easily discarded since they do not yield integers for the Miller indices in the rhombohedral system. This method is thus a *completely exhaustive one* for enumerating the Miller indices of all calcite planes which can be responsible for reflections of λ at the angle θ. The following formula[9] gives the grating space $d_{h_1h_2h_3}$ for any set of Miller indices expressed in the rhombohedral crystallographic (not cleavage) system

$$d_{h_1h_2h_3}=\frac{a(1+2\cos^2\gamma-3\cos^3\gamma)^{\frac{1}{2}}}{[(h_1^2+h_2^2+h_3^2)\sin^2\gamma+2(h_1h_2+h_1h_3+h_2h_3)(\cos^2\gamma-\cos\gamma)]^{\frac{1}{2}}}, \tag{5}$$

[9] For the structure of calcite and its representation in different systems of reference see Ewald-Hermann, *Strukturbericht*, p. 292.

TABLE II. *Designation of all possible planes that have values of d appropriate to the regions in which powder rings were observed.*

Hex. Indices, $(H_1H_2H_3)$	Rhomb. Indices, $(h_1h_2h_3)$	Grating Space, $d_{h_1h_2h_3}$	Weight Factor, P	Structure Factor, F	Intensity	Depth of Penetration to ½ Intensity (cm)
1,2,17	476	0.8532	12	3.66	161	
3,1,14	374	.8528	12	4.38	230	
3,2,10	163	.8557	12	8.04	774	0.585×10^{-2}
0,5,4	$\bar{2}33$	.8458	6	11.3	762	0.416×10^{-2}
5,0,2	$\bar{1}41$	.8586	6	4.38	115	
5,0,1	$\bar{2}32$	.8619	6	1.83	20	
0,1,20	677	.8349	6	11.3	762	0.416×10^{-2}
2,4,15	357	.8389	12	0	0	
0,4,13	733	.8326	6	0	0	
2,5,11	146	.8338	12	3.66	161	
5,5,5	005	.8366	6	0	0	
3,3,0	$\bar{3}30$	.8304	6	7.58	343	0.62×10^{-2}

in which to an accuracy sufficient for the identification of diffraction rings the constants can be assumed to have the value $a=6.361$A, $\gamma=46°\ 7'$.

A knowledge of the relative intensities to be expected from the various planes served as a final identification test. These were computed from the formula

$$I=KPF^2, \tag{6}$$

in which K is simply a proportionality constant, P is the permutation factor entering because some planes admit of reflection with the crystalline particle in more orientations than do other planes, and F is the crystal structure factor. In computing the crystal structure factor, values of the atomic structure factors for Ca, C, and O were obtained from the work of Pauling and Sherman.[10] Table II gives all of the possible planes expressed both in hexagonal and rhombohedral crystallographic indices that have values of d appropriate to the regions in which powder rings were observed. Referring to the rhombohedral indices the computed intensities immediately identify (163) and ($\bar{2}33$) as the planes giving the two observed reflections in the region 75° 24′ while in a similar way (677) was identified with the reflection in the 83° 39′ region. As before stated the reflection ($\bar{3}30$) which we have referred to in Fig. 6 did not present sufficient intensity and contrast to be used with certainty.

Depths of penetration into the crystal particles

The depths of penetration to ½ intensity in Table II were computed from the formula for the extinction coefficient μ_e

$$\mu_e=4\pi F\delta/Z\lambda\sin\theta_0, \tag{7}$$

in which Z is the number of electrons in the calcite unit cell, $\delta=10^{-5}$ is the difference between the refractive index and unity for the wavelength $\lambda=1.658$A, $\theta_0=90°$ approximately. Note that the largest crystals observed with the microscope in our powder sample have dimensions only half the shallowest half penetration depth computed above. Thus in the worst cases the beam only lost about a quarter of its original intensity in passing through a single crystalline particle.

Measurements of diffraction angles

Five different exposures were taken but since not all of these showed the same degree of contrast some of the lines could not be measured with certainty on certain of the exposures. Table III giving the observed distances $2s$ (Fig. 10) measured on the film indicates the

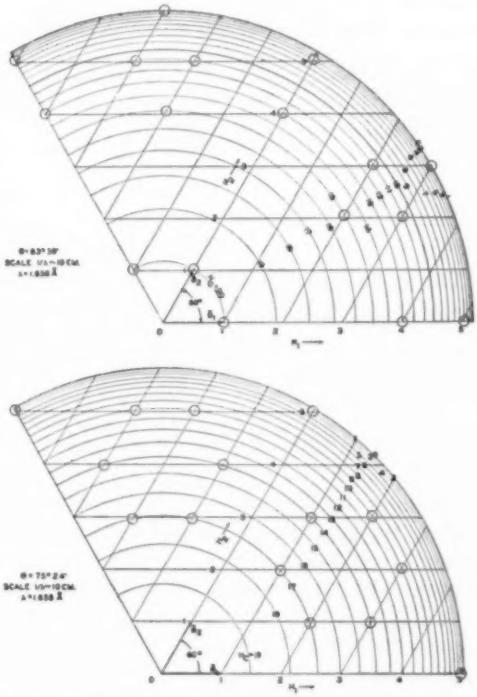

FIG. 12. Projection of calcite reciprocal lattice and circular intersections of propagation sphere with the lattice planes for two radii.

[10] Pauling and Sherman, Zeits. f. Krist. **81**, 1 (1932).

TABLE III. *Observed values of the distance 2s measured on the film.*

Miller Index	Spectral line	Film No. 1	2	3	4	5	Mean
		Distances 2s (inches)					
$h_1h_2h_3$ (1 6 3)	α_1	7.05	7.07	7.06	7.05	7.05	7.056
	α_2	6.79	6.75	6.75	6.80	6.75	6.768
($\bar{2}$ 3 3)	α_1		5.70			5.67	5.685
	α_2		5.39			5.30	5.345
(6 7 7)	α_1	3.78	3.79	3.80	3.75	3.76	3.776
	α_2	3.30	3.30	3.26	3.29	3.30	3.290

TABLE IV. *Lattice constants of planes in terms of Siegbahn conventional scale.*

Indices Crystallograph Rhomb. $h_1h_2h_3$	Angstroms d From α_1	d From α_2	d average	Indices Cleavage Cell $c_1c_2c_3$
1 6 3	0.85500	0.85472	0.85486	$\bar{6}$,14,2
2 3 3	.84510	.84494	.84502	$\bar{1}$2,8,8
6 7 7	.83504	.83510	.83507	4,8,8

inner consistency here. The resulting probable relative error in d is of course far smaller.

Now by means of the formula

$$d=\lambda/(2\cos 2s/4D), \tag{8}$$

which can be easily shown to follow from the geometry of the spectrograph and assuming the wave-length values for Ni $K\alpha_1$ and $K\alpha_2$ as measured by Eriksson[11] based on Siegbahn's conventional value of the calcite lattice constant

$$d_{100}=3.02904\text{A at } 18^\circ\text{C for calcite,}$$

$$\lambda_{\alpha_1}=1.65450, \quad \lambda_{\alpha_2}=1.65835,$$

we can compute the lattice constants of our planes in terms of the Siegbahn conventional scale. These are given in Table IV.

Cohen[12] has analyzed the sources of error in precision work with the Seeman-Bohlin spectrograph. Using his formula and also taking into account the inner consistency of the measurements on $2s$ we estimate *very conservatively* that the total error from both systematic and random causes cannot exceed 0.05 of one percent in the above results of Table IV. The agreement between the results on α_1 and α_2 is in accord with this estimate.

Determinations of the angle β of the calcite cleavage cell

The above data are all that we need to determine the angle β characteristic of the calcite cleavage cell. This is the angle which enters into the function $\Phi(\beta)$ in the formula (2) by which e is computed. If c_1c_2 and c_3 are the Miller indices in terms of the cleavage cell we have

$$d_{c_1c_2c_3}=\frac{c(1+2\cos^3\beta-3\cos^2\beta)^{\frac{1}{2}}}{[(c_1^2+c_2^2+c_3^2)\sin^2\beta+2(c_1c_2+c_2c_3+c_1c_3)(\cos^2\beta-\cos\beta)]^{\frac{1}{2}}}. \tag{9}$$

The ratio of the d's for any two different sets of planes is then sufficient to calculate β. If the subscripts i and k refer for brevity to two such different sets of planes we have

$$\cos\beta=\frac{\{n_k-n_ib_{ik}^2\}\mp\{[n_k-n_ib_{ik}^2]^2+4[a_ib_{ik}^2-a_k][m_k-m_ib_{ik}^2]\}^{\frac{1}{2}}}{2[a_k-a_ib_{ik}^2]}, \tag{10}$$

where $b_{ik}=d_i/d_k$, $m=c_1^2+c_2^2+c_3^2$, $n=2(c_1c_2+c_1c_3+c_2c_3)$, $a_k=n_k-m_k$, $n_i-m_i=a_i$.

The three sets of planes observed in our powder camera thus permitted three ratios b_{ik} to be formed from which three independent determinations of β were computed as follows

Pairs of Cleavage cell indices	Values of β	Mean value of β
(4,8,8)/($\bar{1}$2,8,8)	101° 53′ 40″	
(4,8,8)/($\bar{6}$,14,2)	101° 52′ 51″	101° 54′ 18″±48″
($\bar{1}$2,8,8)/($\bar{6}$,14,2)	101° 56′ 24″	(Probable error from inner consistency)

This should be compared with Bearden's value of β for macroscopic calcite[13]

$$\beta=101^\circ\ 54'\ 4''\pm 10''.$$

Determination of d for the cleavage planes in microscopic calcite

We are now in a position to compute the value of d for the cleavage planes in our microscopic

[11] Eriksson, Zeits. f. Physik **48**, 360 (1928).

[12] M. U. Cohen, Rev. Sci. Inst. **6**, 68 (1935).

[13] Bearden, Phys. Rev. **38**, 2089 (1931).

calcite for comparison with macroscopic values. We proceed by first computing the lattice parameter C of the cleavage cell by means of the formula

$$C_i = d_i \frac{(m_i \sin^2\beta + n_i(\cos^2\beta - \cos\beta))^{\frac{1}{2}}}{(1+2\cos^3\beta - 3\cos^2\beta)^{\frac{1}{2}}}; \qquad \begin{matrix} i=2,\ 3,\ 4 \\ \beta = 101°\ 54'\ 18'' \end{matrix} \tag{11}$$

Three different values distinguished by subscript i were obtained from the data for the three different sets of planes observed with the result

$$C_2 = 12.8238\text{A}, \quad C_3 = 12.8194\text{A}, \quad C_4 = 12.8159\text{A},$$

all of course on the Siegbahn scale. The mean value is

$$C = 12.8197 \pm 0.0016\text{A (Siegbahn scale)}$$
$$\beta = 101°\ 54'\ 18'' \pm 48''.$$

Remembering that the cleavage d_{100} is really d_{400} in the 32 molecule cell we have

$$d_{400} = \frac{12.8197(1+2\cos^3\beta - 3\cos^2\beta)^{\frac{1}{2}}}{(16\sin^2\beta)^{\frac{1}{2}}} = 3.02823\text{A on the Siegbahn scale.} \tag{12}$$

The corresponding value for macroscopic calcite *on the same scale is* $d_{400} = 3.02904$A.

Value of electronic charge from grating wave-length data

Transformation from the Siegbahn scale to the absolute scale of lengths as determined by ruled gratings was effected by a comparison of the crystal results of Wennerlöf[14] on Cu $K\alpha_1$ radiation $\lambda_{\alpha 1} = 1.537395$ (Siegbahn scale) with Bearden's measurement of the same wave-length with a ruled grating $\lambda_g = 1.5406 \times 10^{-8}$ cm. Using then the value of d on the absolute scale together with $M = 100.078 \pm 0.005$, $Q = 2.89270 \pm 0.00021 \times 10^{14}$ abs. e.s.u., $\rho = 2.71022 \pm 0.00035$ g/cc, $\Phi(\beta) = 1.09602 \pm 0.00048$ one obtains by formula 2

$$e = 4.799 \pm 0.007.$$

IV. Conclusions

The results of this investigation we believe conclusively and permanently answer all three of the objections raised to the x-ray crystal method of determining e. The angles of diffraction are representative of the entire powder sample since the half depth of penetration computed from the extinction coefficient is double the dimensions of the largest crystals used in the sample. The density determination therefore applies to identically the same calcite as has been used to diffract the x-rays.

The agreement between the densities of microscopic calcite and macroscopic calcite as well as the agreement of absolute size and shape of the lattice cell for these two is surprising evidence of the permanence of the lattice structure against mechanical maltreatment by powdering.

The elementary diffraction theory of Laue or Bragg must apply to the case of diffraction by crystals so small that the radiation is negligibly extinguished in passing through them and hence any critical objection to the crystal determination of e based on doubts as to the absolute rigor of the dynamical theory of x-ray reflection are invalidated by our results.

V. Acknowledgments

Dr. V. A. Brown (University of Arizona) did a part of the work falling under the heading of "Search for a Conclusive Test" as his Thesis for the Doctor's degree and we wish here to express our sincere appreciation for his assistance. Our sincerest gratitude also goes to Dr. J. H. Sturdivant of this Institute for his helpful discussions and suggestions regarding the analysis of the powder diffraction data.

The funds for this investigation are derived from the gift of Dr. Leon L. Watters of New York City for research work in x-rays and atomic structure known as the Watters Memorial Research Fund given by Dr. Watters as a memorial to his wife, Frances Hayes Watters. We are grateful for this opportunity to express our deep appreciation of his gift.

[14] Wennerlöf, Ark. Met. Astr. O. Fys. (A) **22**, No. 8 (1930).

Deep Terms in the Spectra of Pb V and Bi VI

G. K. SCHOEPFLE, *Department of Physics, A. and M. College of Texas*

(Received March 7, 1936)

In earlier investigations the Pt I-like isoelectronic sequence was extended to Pb V and Bi VI, establishing terms due to the $5d^9 6s$, $5d^9 6p$, and, later, $5d^9 7s$ and $5d^{10}$ configurations. This paper extends further the previous results by Mack and by the author to include terms assigned as arising from $5d^9 8s$, $5d^9 9s$, $5d^9 7p$ and $5d^9 8p$ configurations. A total of 69 term values involving 205 lines are listed for Pb V, and 40 terms involving 94 lines for Bi VI. The wave-length measurements for the lines involved are those made by Arvidsson and range from 1400A to 200A, and in more than half the cases the discrepancies are not more than ± 1 cm^{-1}. The absolute values of the $5d^9{}_{5/2}6p_{3/2}$ $J=3$ terms are computed by a Ritz formula.

INDEPENDENT extensions of the Pt I-like isoelectronic sequence to Pb V and Bi VI were made and announced almost simultaneously by Mack[1] and by the author.[2] As the results were not in complete agreement, a more detailed study has been made by Mack[3] and also by the author,[4] including a study of the spectra of Pb IV and Bi V.[5] The results are now almost in agreement, differences being discussed in the comments to Tables I and III. The wave-length region concerned is from 1400A to 200A, the measurements used being those made on a grazing incidence spectrograph at Upsala by Arvidsson.[6]

In Table I the 69 term values assigned to Pb V are given, which involve a total of 205 lines for over half of which the discrepancy is not more than ± 1 cm^{-1}. The wave-lengths of newly assigned lines are given in Table II. Similarly the 40 terms assigned to Bi VI, which involve a total of 94 lines for over three-quarters of which the discrepancy is not more than ± 1 cm^{-1}, are given in Table III. The wave-lengths of newly assigned lines are given in Table IV. The terms assigned as arising from $5d^{10}$, $5d^9 6s$, $5d^9 7s$, and $5d^9 6p$ configurations are as assigned by Mack. By a Ritz formula, the absolute value of the $5d^9{}_{5/2}6p_{3/2}J=3$

[1] A. T. Goble and J. E. Mack, Phys. Rev. **42**, 909 (1932).
[2] G. K. Schoepfle, Phys. Rev. **43**, 374 (1933).
[3] J. E. Mack and M. Fromer, Phys. Rev. **48**, 357 (1935).
[4] G. K. Schoepfle, Phys. Rev. **45**, 747 (1934).
[5] G. K. Schoepfle, Phys. Rev. **47**, 232 (1935).
[6] Gustaf Arvidsson, Ann. d. Physik **12**, 1 (1932).

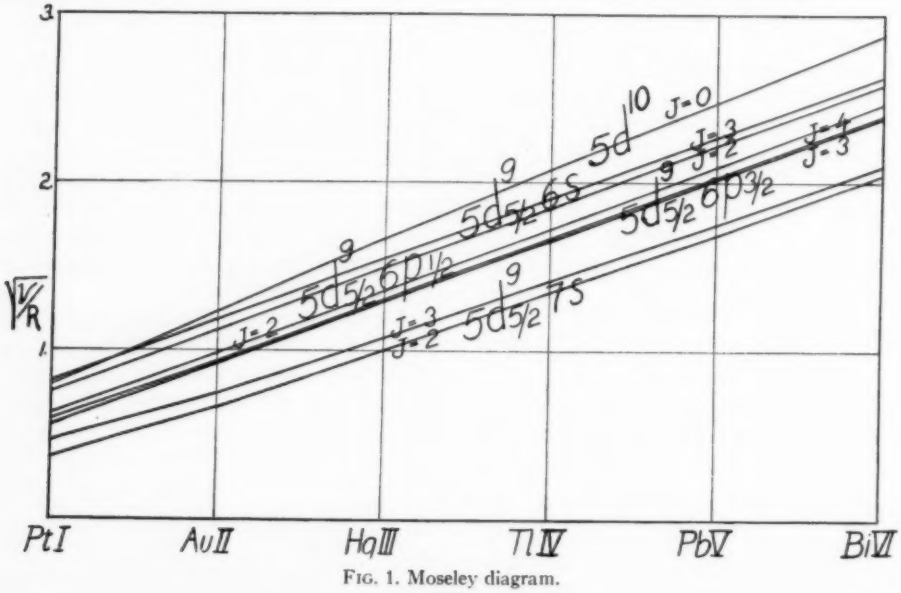

FIG. 1. Moseley diagram.

TABLE I. *Energy levels and transitions in* Pb V.

M indicates lines listed by Mack;[3] a number locates the line in Table II. Terms 327433, 329572, 329935 ($J=4$), 332358, and 332501 are listed by Mack with question marks and assigned as arising from $5d^9_{3/2}6s$. Two of these terms, 329572 and 332501, were independently announced by the author.[4]

| Term designation | J | Term value | $5d^{10}$ | $5d^9_{\frac{3}{2}}6s$ | | $5d^9_{\frac{1}{2}}6s$ | | |

TABLE II. *Newly classified lines of* Pb V.

z indicates the classification according to the state of ionization by Arvidsson.[6] The number in the column labeled "Designation" refers to Table I. b = broad, d = diffuse, a = found in arc.

z	Intensity	λ(vac.)	ν(vac.)	Designation	Discrepancy	z	Intensity	λ(vac.)	ν(vac.)	Designation	Discrepancy
V	2	284.329	351705	129	0	V	2	979.38	102105	3	+1
VI	5	358.636	278834	120	−5	V	1	982.18	101814	115	+2
VI	4	387.870	257818	111	−3	VI	2	983.06	101723	67	0
VI	5	389.745	256578	121	+5	VI	0	988.94	101118	18	−1
	0	390.882	255832	117	−4	V	4	989.15	101097	12	−2
V	1	395.280	252985	126	0	V	0	996.23	100378	62	+1
V	3	395.770	252672	124	−1	V	1	996.73	100328	51	0
V	2	403.217	248005	6	+2	VI	2	997.03	100298	44	0
VI	3	404.644	247131	122	0	VI	2	998.62	101138	63	0
V	1	409.728	244064	103	0	VI	1	1002.55	99745.6	2	−.4
V	3	410.705	243484	106	−3	V	2	1003.01	99699.9	56	+5.1
V	2	416.950	239837	118	+1	III	6	1005.56	99447.1	74	+.1
	0	418.264	239083	93	−3	VI	1b	1006.75	99329.5	17	+.5
V	1	419.650	238294	95	+2	VI	3	1008.82	99125.7	70	−.3
V	2	423.906	235901	14	+1	VI	0	1012.23	98791.8	69	−.2
V	1	428.99	233106	107	+2	VI	0	1015.53	98470.7	57	+.7
V	2	429.51	232823	92	−4	V	1	1015.97	98428.1	11	+2.1
V	2	431.86	231557	112	+2	VI	2	1018.70	98164.3	10	−2.7
V	3	433.487	230687	108	+2	VI	3	1019.74	98064.2	40	+.2
	0	436.10	229305	127	+6		0	1021.26	97918.3	81	−.7
	1	440.11	227216	22	−1		0	1021.51	97894.3	72	−.7
	0	446.56	223934	30	+3	V	4	1022.14	97834.0	27	+1
V	0	462.97	215997	91	−3	VI	1	1022.57	97792.8	71	+4.8
V	1	464.20	215424	102	+1	V	0b	1023.47	97706.8	50	+4.8
IV	7	465.450	214846	105	0	V	3	1024.33	97624.8	123	−.2
	3	647.71	154390	110	+3	VI	3	1026.38	97429.8	33	−.2
	0	670.70	149098	130	0	V	0	1033.23	96783.9	9	+1.9
	0	671.08	149014	99	+5	VI	1	1041.21	96042.1	26	−.9
	4	675.94	147942	104	0	VI	2	1043.04	95873.6	78	+.6
	1	678.58	147367	100	+2	VI	3	1043.70	95813.0	8	+4
	0	695.02	143881	13	−2	IV	4	1052.25	95034.4	16	−.6
V	5	749.46	133429	65	−2	V	0	1059.22	94409.1	68	+5.1
VI	2	762.76	131103	66	0	VI	1	1065.44	93857.9	113	+4.9
VI	1	778.50	128452	101	−4	VI	2	1069.67	93486.8	52	−1.2
VI	2	781.48	127962	21	−1		0	1078.74	92600.7	114	+4.7
VI	3	782.79	127748	94	+1	VI	0	1083.10	92327.6	82	−3.4
	1	793.79	125978	125	+1	VI	4	1089.93	91749.0	25	0
	2	794.41	125880	20	+3		0	1100.25	90888.4	53	+2.4
	5	795.58	124679	29	+2	VI	4	1103.32	90635.5	90	−.5
III	4	812.60	123062	5	0	VI	3d	1132.76	88280.0	1	0
V	1	814.45	122782	87	0	V	3	1148.29	87086.0	{83	−2
V	0	815.70	122594	28	+3					{M2	+5
VI	4	826.35	121014	85	0	VI	1	1151.63	86883.4	47	−2.6
IV	0	832.57	120110	88	+1		0	1154.71	86601.8	41	+3.8
	1	835.89	119633	86	+4	VI	0	1159.95	86210.6	75	+.6
	0	842.57	118685	35	−1	V	0	1170.56	85429.2	98	−1.8
VI	1	842.86	118644	116	+1	VI	0	1183.18	84518.0	32	−5
VI	1	855.31	116917	64	−2	V	0	1184.34	84435.2	36	+.2
V	7	857.65	116598	34	−2		0?	1185.63	84343.3	7	+.3
	0	877.06	114017	58	+1	V	0	1188.30	84153.8	84	−.2
V	1	879.08	113755	59	−2	IV	0	1191.83	83904.6	48	+.6
V	1	879.45	113707	79	+1	V	0	1192.08	83887.0	76	−5
	0	918.74	108845	60	0	IVa?	6	1203.47	83093.1	15	+.1
IV	2	924.51	108165	89	−2	V	0	1210.07	82639.8	49	+.8
IV	10	932.18	107275	4	0		0	1235.77	80921.2	97	+.2
V	5	936.96	106728	54	0	VI	0	1249.28	80046.1	42	+3.1
V	3	937.16	106705	19	−2		0	1252.99	79809.1	24	+2.1
V	0	953.30	104899	45	−6		0	1258.12	79483.7	128	−.3
V	3	959.08	104267	109	0		0d	1264.72	79068.9	43	−.1
VI	2	960.98	104006	80	+3	V	0	1290.32	77500.2	31	+.2
V	0	971.07	102979	61	0	V	3	1296.43	77134.9	23	+.9
V	0	974.91	102574	46	−3	IVa	6	1308.10	76446.8	39	+3.8
V?	5?	976.93	102362	{119	0	V	0	1328.21	75289.3	38	+1.3
				{M1	−2	III	6	1371.75	72899.6	77	+.6
V	2	977.46	102306	55	−1	IV	5	1388.97	71995.8	37	−.2
V	1	978.69	102177	96	0		0	1401.56	71349.1	73	+2.1

TABLE III. *Energy levels and transitions in* Bi VI.

M indicates lines listed by Mack;[3] a number locates the line in Table IV. Mack's choice of 298862, $J=0$, is strengthened by the expected transition $5d^9_{5/2}6p_{3/2}-5d^9_{3/2}7s$ designated as 26, apparently overlooked by him.

Term designation		Term value	$5d^{10}$	$5d^9_{\frac{5}{2}}6s$	$5d^9_{\frac{3}{2}}6s$		$5d^9_{\frac{3}{2}}6s$			$5d^9_{\frac{5}{2}}7s$		$5d^9_{\frac{3}{2}}7s$				$5d^9_{\frac{5}{2}}8s$		$5d^9_{\frac{3}{2}}8s$		$5d^9_{\frac{5}{2}}9s$	$5d^9_{\frac{5}{2}}10s$
	J		0	3	2	1	2	2	2	2	3	2	1	2	1	2	3	2	2	2	3	3
			0	149495	153737	175017	176585	176479	373679	401592	426587	427483	452280	452914	539649	580252	606519	606754	631304	644278	771313	773055?
	2	237881		1	3											30						
$5d^9_{\frac{5}{2}}6p_{\frac{1}{2}}$	2	244721		M	M				13		M	M					34				43	46
	3	247165		M	M				14		M					31		37				
	2	250191		2		5		11	15	17					27							
$5d^9_{\frac{3}{2}}6p_{\frac{1}{2}}$	2	270603			M	M		M				M	M	M								
	1	274158	M		M	M		M	16					M	28	32						
$5d^9_{\frac{5}{2}}6p_{\frac{3}{2}}$	4	277866		M							M						35				44	
	2	280930		M	M			M				M										
	1	284036	M		M		8	M		18		M			29	33				40		
	3	284058		M1	M						M	M										
$5d^9_{\frac{3}{2}}6p_{\frac{3}{2}}$	0	298862				M							26									
	3	305272			M		9	M						M					39			
	1	305903	M		M	M		M		19			M							41		
	2	308613		M?	M	M		M2						M?								
	1	315254			4	6																
	2	319159				7	10	12														
$5d^9\,7p?$	3	556721									20	23								42		
	3	562057									21	24									45	
$5d^9\,8p?$	3	744960										25						38				
	3	749193									22					36						

TABLE IV. *Newly classified lines of* Bi VI.

σ indicates the classification according to the state of ionization by Arvidsson.[6] The number in the column labeled "Designation" refers to Table III. b = broad, d = diffuse, a = found in arc.

σ	Intensity	λ(vac.)	ν(vac.)	Designation	Discrepancy	σ	Intensity	λ(vac.)	ν(vac.)	Designation	Discrepancy
	2	189.274	528334	46	0	VI	4	710.32	140782	12	+2
VI	2	214.318	466596	45	+4	VI	5	713.08	140237	6	0
	1	230.710	433445	44	−2	VI	2	723.56	138206	38	−1
VII	2	276.397	361798	34	0	V	10	738.17	135470	21	0
VI	1	277.591	360242	40	0	VI	10b	743.13	134566	24	−8
VI	1	278.095	359589	39	0					M1	+3
VI	1	292.080	342372	30	+1	VI	4	768.44	130134	20	0
VI	3	295.530	338375	41	0					M2	0
VII	0	300.225	333084	31	+3		1	773.76	129239	23	+1
VI	4	304.278	328647	35	+6	V	3	775.43	128961	13	−3
VI	6	306.718	326032	39	0	V	1	777.65	128692	9	−5
VI	5	309.976	322606	22	0	IV	2	790.425	126514	14	−2
VI	2	314.982	317478	25	+1		1	809.82	123484	15	+1
VI	3	326.695	306096	32	−2	V	3	850.66	117556	18	0
VI	3	337.590	296217	33	−1	IV	4	930.65	107452	8	−1
	1	345.479	289453	27	+5		1	993.10	100695	2	−1
IV	8	376.660	265491	28	0	VI	7b	1004.75	99527.2	16	−6.2
IV	8	391.215	255614	29	−1	VI	4	1045.066	95687.7	19	+1.3
V	4	619.13	161517	4	0	IV	2	1131.39	88386.9	1	+.9
	1	651.82	153417	26	−1		0b	1142.11	87557.2	42	−1.2
V	3	660.52	151396	17	−5	IV	4	1188.45	84143.2	3	−.8
	2bd	669.99	149256	45	0	IV	0	1330.19	75177.2	5	+3.2
V	4	693.29	144240	7	−2	V	0	1394.46	71712.3	11	+.3
VI	5	700.90	142674	10	0						
				36	0						

term is computed as 562,600 cm^{-1} for Pb V and as 761,800 cm^{-1} for Bi VI. The ionization potentials are 69.40 volts and 93.97 volts respectively, which values are 1.3 percent and 6.6 percent higher than those obtained by the extrapolation method by Mack. In Fig. 1 a Moseley diagram is given.

The author wishes to express his appreciation to Chairman R. C. Gibbs of the Physics Department of Cornell University, where most of this work was done, and particularly to thank Professor J. E. Mack and his associates of the University of Wisconsin for their friendly and helpful correspondence.

SEPTEMBER 15, 1936 PHYSICAL REVIEW VOLUME 50

The Pressure Effect on the *C* Band of Strontium Hydride

R. F. HUMPHREYS AND W. R. FREDRICKSON, *Syracuse University, Syracuse, N. Y.*

(Received June 6, 1936)

At low hydrogen pressures the emission spectrum of the 3808A band of SrH shows a sharp break-off at $R(18)$, while at high pressures the lines extend to $R(49)$. The presence of lines with high K values allows an accurate determination of the constants of the upper state. Analysis shows the presence of an uncoupling term $-0.1415\ (K-1)$ in the upper state. Perturbations due to resonance and predissociation are present. The electronic configurations and probable dissociation energies are considered.

OF the known five band systems which the spectrum of SrH exhibits the *C* system at 3808A is particularly interesting, because its main band, the (0,0), has a line structure that is intense and well defined to a certain point and then abruptly breaks off, leaving no further trace of lines to be found. An analysis of this band has shown it to be a $C^2\Sigma \rightarrow N^2\Sigma$ transition.[1] The only other band observed in the system is a weak (0,1) band, which permitted a sufficiently complete analysis to show the same kind of abrupt breaking-off in rotational structure. This phenomenon has been attributed[1] to predissociation of the upper ("*C*") state due to the influence of a neighboring electronic state (probably the *D* state).

An analogous situation had long been known to exist in the *C* system of CaH.[2] Later Grundström and Hulthén[3] obtained its spectrum with the pressure of the hydrogen surrounding the calcium greatly increased. The bands were no longer predissociated, but were more or less normal in appearance. Bearing in mind the close analogy between the spectrum of CaH and SrH it was thought worth while to investigate the effect of pressure on the SrH *C* band.

[1] W. R. Fredrickson, M. E. Hogan, Jr., and W. W. Watson, Phys. Rev. **48**, 602 (1935).
[2] Mulliken, Phys. Rev. **25**, 509 (1925).
[3] Grundström and Hulthén, Nature **125**, 634 (1930).

Experimental Procedure

The spectrum was obtained from an arc between a copper cathode and a copper cup containing metallic strontium as an anode. The arc burned in an atmosphere of hydrogen at pressures varying from a few mm of Hg to 700 mm of Hg. The cathode was water cooled, and a continuous stream of water was directed on the glass walls of the tube containing the arc. With this arrangement it was possible to operate the arc continuously for two or three hours.

A 120-cm concave grating with a dispersion of 5A/mm in the second order was used in a Rowland mounting. Exposure times were of the order of four hours for second-order plates.

Analysis

When the *C* band is photographed with a hydrogen pressure of a few mm of Hg its rotational structure breaks off at $K'=19$. When the pressure is increased to 400 mm or more the band no longer exhibits this predissociation but displays a fairly normal structure. In addition to the (0,0) very weak traces of the (1,1) and (2,2) bands appear. The assignment of the K values is given in Table I. Combination differences permit these assignments up to $K=28$, beyond which the P branch becomes too weak to observe. For $K>28$ the R lines were fitted to a Fortrat para-

TABLE I. *Assignment of frequencies in the $C^2\Sigma \rightarrow N^2\Sigma$ (0,0) band of SrH (cm^{-1} units). Two lines blocked together indicate the boundary of a wide line.*

Intensity	ν (obs.)	$P(K)$	$R(K)$	Intensity	ν (obs.)	$P(K)$	$R(K)$
2	26,245.01	9, 13		4	494.01 497.59		15
9	251.35 254.45	8, 9, 10, 11, 12, 13, 14, 15, 16		4	510.73		16
9	257.42 259.62	7, 9 11, 17		1	531.13 538.95		17
8	262.45	6, 18		4	547.38		18
3	268.18	5, 19		2	569.16		19
7	271.98	4, 20		2	586.09		20
3	278.13	3		1	605.97		21
3	279.85	21		1	626.09		22
3	284.62	2, 22		1	647.17		23
2	291.26	1, 23		1	668.15		24
2	298.24	24		1	689.44		25
1	306.85	25	0	0	711.54		26
2	314.79	26	1	1	734.40		27
4	323.58	27	2	2	757.22		28
2	333.36	28	3	1	781.66		29
3	343.08		4	0	800.19		30
3	353.21		5	0	816.72		31
1	357.66*			0	846.97		32
1	362.24		6	0	868.61		33
0	368.16		7	0	888.85		34
1	374.48		7	0	909.68		35
4	378.73 382.49		7	0	934.56		36
				arc line	963.32		37
4	391.82		8	arc line	990.18		38
4	403.95		9	0	27,017.39		39
2	407.65		9	0	030.17		40
0	413.23*			0	049.48		41
5	417.77		10	0	076.44		42
0	425.17		11	0	105.00		43
6	432.01		11	0	140.19		44
9	445.93		12	0	165.16		45
0	454.19*			0	201.09		46
5	461.26		13	0	231.69		47
3	474.27		14	0	262.44		48
				0	293.47		49

* Unassigned lines.

bola and thus given their K values. The resolving power of the grating was not sufficient to distinguish the spin doubling nor to resolve the abnormally broad lines in the head of the P branch and in several other places throughout the R branch.

A study of the photographic plate and of the assignments given in Table I reveals the presence of several perturbations in the band, evidenced by anomalous displacements, irregular intensity distribution and abnormal doubling of certain lines. In order to obtain information about these perturbations an attempt was made to write a theoretical equation for the lines of the R branch. A deviation of the observed position of a line from its theoretical would thus indicate a perturbation. To write such an equation necessitates the determination of the coefficients of the energy level equation

$$T(K)=T_0+B_0K(K+1)+D_0K^2(K+1)^2 \quad (1)$$

for the two states in question, and thus determining the coefficients of the line equation. For the lower state B_0'' and D_0'' have been calculated[4] (Table II). The levels of the upper state were found with the aid of combination differences and were observed to be somewhat irregular. In view of this, the procedure used by Grundström[5] for CaH bands was followed. An additional function $f(K)$ was assumed to exist, so that

$$T'(K)=T_0'+B_0'K(K+1)+D_0'K^2(K+1)^2+f(K).$$

TABLE II. *Constants for the N and C states of SrH.*

Normal state	C state
$B_0''=3.6344$	$B_0'=3.9416$
$D_0''=-1.287\times10^{-4}$	$D_0'=-1.3986\times10^{-4}$
$\omega_e=1206$ (experimental)	$\omega_e=1349$ (experimetal)
$x_e\omega_e=17$ (experimental)	$x_e\omega_e=24$ (experimental)
	$r_0=2.067$Å
α(uncoupling) $=-0.1415$	

[4] Watson, Fredrickson and Hogan, Phys. Rev. **49**, 150 (1936).

[5] Grundström, Zeits. f. Physik **95**, 574 (1935).

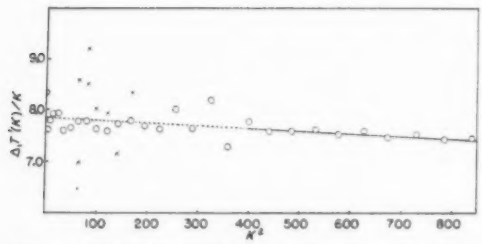

FIG. 1. $\Delta_1 T'(K)/K$ *vs.* K^2. The circles are obtained from upper state levels; the crosses represent additional levels giving rise to the anomalous doubling. The y intercept of the straight line equals $2B_0'$ and the slope equals $4D_0'$.

From this we may obtain

$$\Delta_1 T'(K)/K = [T'(K) - T'(K-1)]/K = 2B_0' + 4D_0' K^2 + [f(K) - f(K-1)]/K.$$

If $\Delta_1 T'(K)/K$ is plotted against K^2 we should expect to get a straight line only when $[f(K) - f(K-1)]/K$ is zero or negligible. Such a plot is given in Fig. 1. The straight line occurs from $K^2 = 400$ on. Therefore, by substituting the term values for levels from $K = 20$ to $K = 30$ into Eq. (1), the values of B_0' and D_0' were obtained (Table II). For points at small K^2 values in Fig. 1 there seems to be a general sinking below the straight line (except, of course, for points marked with x's, which represent anomalous doublets and thus cannot be considered). This sinking of the points suggests the possibility of an additional term, α/K, where α is a constant. Thus $[f(K) - f(K-1)]/K = \alpha/K$ or $f(K) = \alpha(K \pm n) +$ const. where n is any integer. The assumptions are made that $n = 1$, the sign is negative and the const. $= 0$. These assumptions are quitè arbitrary and are chosen to produce the best agreement between the observed and theoretical wave numbers of the levels. The upper state, therefore, may be represented by

$$T'(K) = T_0' + B_0' K(K+1) + D_0' K^2 (K+1)^2 + \alpha(K-1).$$

If we combine the values of B and D for the two states we get the following equation:

$$R(K) = 26{,}298.53 + 7.5760(K+1) + 0.3072(K+1)^2 - 2.6856 \times 10^{-4}(K+1)^3 - 11.16 \times 10^{-6}(K+1)^4 + \alpha K.$$

By substitution in several presumably unperturbed lines the average α is found (Table II). It is a measure of "uncoupling" of the orbital angular momentum in the C state. The wave numbers of the line of the R branch were calculated from the above equation and then subtracted from those of the observed lines. Perturbations were thus found to occur in four regions: $R(7)$ to $R(11)$, $R(17)$ to $R(18)$, $R(30)$ to $R(40)$ and $R(40)$ to $R(49)$. For high K values the differences between calculated and observed positions become large due to a lack of powers above the fourth in the theoretical equation, but these differences are readily distinguishable from perturbations by their uniformity in trend.

In the region $K = 7$ to $K = 11$, the perturbations are of the resonance type, but those in the regions following $K = 17$, 30 and 40 must be due to the overlapping of levels which are above the dissociation limit of their own state and consequently would cause predissociation of the C state if the hydrogen atmosphere were not under pressure. Unfortunately, the D state has not been sufficiently analyzed to permit a quantitative investigation of these perturbations.

TABLE III. *Probable configurations and dissociation products.*

State	Probable Configuration	Dissociation Products	Dissociation Energy
$N-{}^2\Sigma$	$5s\sigma^2 4d\sigma$	Sr, ^1S+H, ^2S	12,000 cm^{-1}
$A-{}^2\Pi$	$5s\sigma^2 5p\pi$	Sr, ^3P+H, ^2S	13,300
$B-{}^2\Sigma$	$5s\sigma^2 5p\sigma$	Sr, ^3P+H, ^2S	12,300
$D-{}^2\Sigma$	$5s\sigma 5p\sigma^2$	Sr, ^3P+H, ^2S	10,000 (?)
$F-{}^2\Pi$	$5s\sigma 5p\sigma 5p\pi$	Sr, ^3P+H, ^2S	7,800
$C-{}^2\Sigma$	$5s\sigma^2 6s\sigma$	Sr, ^2S+H, ^2S	15,000

DISSOCIATION PRODUCTS

In a recent paper[6] Grundström has called attention to the analogous spectra of the hydrides of the alkaline-earths. If one makes the assumption —logical by comparison with MgH and CaH— that the C state of SrH predissociates into the ^3P Sr atom (the dissociation product of the disturbing D state) and a normal ^2S H atom, then the relative positions of the levels of the SrH molecule and the Sr atom can be obtained. Again, by analogy, one would assume the product of dissociation of the C state to be a ^3S Sr atom, which would give a value of the energy of dissociation of approximately 15,000 cm^{-1}. To check this the ordinary extrapolation methods of Birge and Rydberg[7] were used. To obtain ω_e and $x_e\omega_e$

[6] Grundström, Zeits. f. Physik **99**, 595 (1936).
[7] Jevons, *Report on Band Spectra of Diatomic Molecules*, p. 193.

for the normal state the C (0,0), (0,1) and D (v',2), (v',3), (v',4) bands[8] were used. With these and the C (1,1), (2,2) bands, with heads at 26,380 cm^{-1} and 26,495 cm^{-1}, respectively, the vibration constants of the C state were calculated (Table II). These gave for the dissociation value: by Rydberg's method, $D=10{,}000$ cm^{-1}; linear extrapolation, $D=18{,}200$ cm^{-1}. Since neither of these agrees with the position of an atomic state of Sr, one concludes that the ^3S, occurring at about the average, is more likely than any other to be the state of excitation of the atom after dissociating from the C state. This would indicate an electron configuration[9] of the molecule in the C state of $5s\sigma^2 6s\sigma$. The dissociation values for all the known states of SrH, obtained from products of dissociation, are listed in Table III.[10]

We wish to thank Dr. A. J. King for generous supplies of pure metallic strontium.

[8] See reference 4. The (v',4) of the D system, located at 16,272 cm^{-1}, has not yet been reported.

[9] This configuration differs from that assigned by Grundström (reference 3), but the difference might possibly be due to a typographical error.

[10] These values differ somewhat from those listed by Grundström (reference 3) though the methods used were identical.

SEPTEMBER 15, 1936 PHYSICAL REVIEW VOLUME 50

Mass-Spectrograph Analysis of Beryllium

WALKER BLEAKNEY, JOHN P. BLEWETT, RUBBY SHERR AND ROMAN SMOLUCHOWSKI, *Palmer Physical Laboratory, Princeton University, Princeton, N. J.*

(Received July 10, 1936)

A new source of ions suitable for positive ray analysis was developed in the form of a molecular beam from a hot oven. Ions were produced in the beam by electron impact and focused on the entrance slit of the mass spectrograph by suitable electric fields. The method was applied to the study of beryllium but only Be^9 was found. The experiment placed an upper limit on the existence of Be^8 of one part in ten thousand.

ALTHOUGH most of the lighter elements have been satisfactorily investigated, analyses of the isotopic constitution of beryllium have not yielded consistent information. Watson and Parker[1] have reported the existence of Be^8 in an intensity ratio $Be^9 : Be^8 \doteqdot 2000 : 1$ from a study of the band spectra of BeH. On the other hand, Olsson[2] failed to observe any Be^8H lines on heavily exposed photographs of the bands. Aston's[3] analysis by means of accelerated anode rays, using BeF, has given no conclusive results because of the difficulty of obtaining sufficient intensity. Furthermore, while Be^8 appears presumably as a disintegraion product of at least five nuclear reactions,[4] two, or possibly three, of these would be satisfied by the existence of a stable Be^8 nucleus, although an alternative explanation has recently been suggested.[4] From these considerations it would seem of some importance to be able to set an upper limit for the relative abundance of Be^8 in natural sources of beryllium. Our investigation was undertaken with this end in view.

The apparatus used is that described by Blewett.[5] The glass tube carrying the ionization chamber and electron filament was modified in order to permit the introduction of a small furnace in a manner shown in Fig. 1A. The furnace O can be inserted through either of the ground glass joints as indicated in the figure. It consists of a cylindrical spiral T, Fig. 1B, made from a strip of 1- or 2-mil tantalum, 2 cm long, 8 mm wide spot welded to two nickel rods which are supported by tungsten leads. The lip extending over the side serves to partially collimate the vapor stream. It has been found desirable to use a radiation shield N, usually of sheet nichrome, to protect the glass walls and to reduce sputtering as much as possible.

A 1-kw 120/20-volt transformer supplies the

[1] Watson and Parker, Phys. Rev. **37**, 167 (1931).
[2] Olsson, Zeits. f. Physik **73**, 732 (1932).
[3] Aston, *Mass Spectra and Isotopes*.
[4] Wells and Hill, Phys. Rev. **49**, 858 (1936).

[5] Blewett, Phys. Rev. **49**, 900 (1936).

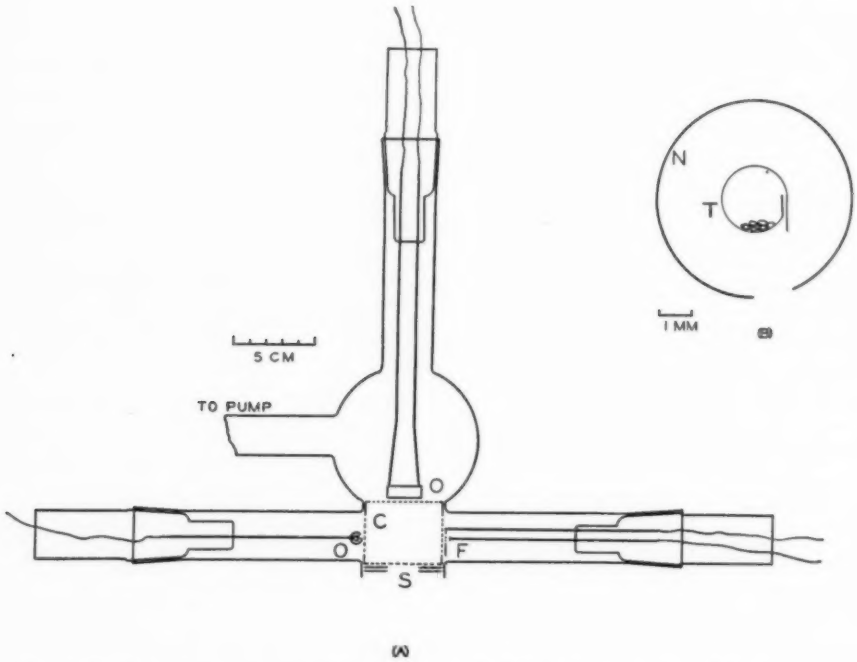

FIG. 1. A. Electrode arrangement of the ion source. B. Enlarged cross section of the furnace.

current (between 15 and 25 amperes) which passes directly through the tantalum strip. The metal under investigation is placed in contact with the furnace and vaporizes when it reaches the proper temperature. Ions are formed in the molecular beam entering the ionization chamber *C*, Fig. 1A, by electrons accelerated from the tungsten filament *F*. The ions are then accelerated into the analyzing chamber through a slit system *S* in the usual fashion.

To test the practicability of this arrangement, the furnace was packed with copper filings and heated to about 1000°C. Peaks of the order of several thousand divisions on the detecting instrument were easily obtained. It may be noted in passing that the presence of argon in the tube augmented the size of the Cu^+ peaks to an astounding degree, an effect probably caused by collisions of the second kind.[6] This supposition was substantiated by the disappearance of the effect below the ionization potential of argon.

Beryllium proved slightly more troublesome because of the degassing of the glass walls. A small electric fan, however, served to keep the walls as well as the waxed joints quite cool. Peaks as high as 13,500 divisions on our scale (2.7×10^{-11} amp.) were obtained and a search made for Be^8. The ionization efficiency was a maximum between 40 and 45 volts, so that in this range the presence of O_{16}^{++}, whose appearance potential is about 50 volts, was not possible. The background was negligible and the peaks sufficiently separated so that the tail of the mass 9 peak disappeared completely before the mass 8 position was reached. Repeated runs failed to reveal the presence of any ions at the mass 8 position. We believe this experiment places an upper limit on the existence of Be^8 of 1 part in 10,000 of Be^9. A small peak was observed at the mass 10 position, but since its size bore no definite relation to that of the mass 9, it was attributed to the presence of a small amount of BeH^+.

The success of the present method leads us to hope that it will now be possible to investigate heavier metals which have heretofore been difficult to handle by other means.

[6] Duffendack and Black, Phys. Rev. **34**, 35 (1929).

The Optical Properties of Nonpolar Liquids

HANS MUELLER, *The George Eastman Laboratory, Massachusetts Institute of Technology, Cambridge, Mass.*

(Received April 27, 1936)

A theory of the refraction, Kerr effect and light scattering for liquids with nonpolar axially symmetric molecules is developed. The molecules are assumed to possess a limited freedom of rotation. This assumption alone does not alter the classical equations. It is necessary to consider the quasi-crystalline grouping of neighboring molecules which produces an anisotropic polarization field. The anisotropy of the Lorentz forces is calculated by combining the classical cavity method with Ewald's lattice theory. It is shown that the procedure of Raman and Krishnan is not justified. With a low potential barrier the quasi-crystalline grouping gives an increase of the refraction, Kerr effect, depolarization and intensity of the Rayleigh scattered light. This is true also for an arbitrarily high potential barrier, provided the anisotropy of the Lorentz force is sufficiently large. These results agree with the observed increase of the refraction in compressed gases and in some solids, and with the observed increase of the depolarization in compressed gases and in liquids near the critical temperature. The observations in liquids are explained by considering a moderate anisotropy of the Lorentz force and a potential barrier of finite height. In this case the molar refraction is slightly smaller than that of the ideal gas. No large deviations from the Lorentz-Lorenz equation can be expected even if the anisotropy is considerable. The refraction changes with pressure and temperature and its dispersion differs from that of the gas. The depolarization and the intensity of the scattered light are considerably smaller than, and the Kerr constant is only a fraction of, the values derived from the classical equation. The classical relations between depolarization and intensity and between Kerr constant and depolarization are only approximate. The theory is applied to benzene. It is assumed that the molecules have the same polarizabilities in the liquid and gaseous state. All observations can be explained by assuming a potential barrier of about 8.8 kT and an anisotropy of the Lorentz force which is in good accordance with the results of the x-ray analysis of the liquid structure.

IT is a well-established fact that the classical theories of refraction, light scattering and the electro-optical Kerr effect fail when applied to liquids. In liquids the molecules appear to have a slightly decreased polarizability and a much smaller optical anisotropy than in the gas. Since for most substances the absorption-spectrum is essentially the same in the gaseous, liquid and solid phase, these changes cannot be due to a change of the molecular structure. They must be connected with the fact that in liquids the molecules cannot rotate and translate as freely as in a gas. In a qualitative way the apparent decrease of the optical anisotropy can be understood by considering the anisotropic Lorentz force. Raman and Krishnan[1] have given a theory of this effect, but Stuart and Volkmann[2] have criticized their assumptions and we shall point out the inadequacies of their arguments.

Recent work has shown that in a liquid the positions and orientations of the molecules are not random. The structure of a liquid can be described by considering an arbitrarily chosen molecule. Due to the dense packing and the intramolecular forces the nearest neighboring molecules tend to assume definite preferred positions with respect to the molecule considered. They form a quasi-crystalline or cybotactic group. For anisotropic molecules these groups are anisotropic. Hence the neighboring molecules exert forces on the central molecule which prevent its free rotation. Quasi-crystalline grouping and hindered rotation are closely interrelated, but the calculation is simplified by considering their effects separately.

THE INFLUENCE OF HINDERED ROTATION

We consider a molecule with axial symmetry. b_1, $b_2=b_3$ are its polarizabilities. If the molecule is polar its permanent moment μ is parallel to the axis of symmetry. Following the method of Debye[3] we can assume that the axis of each molecule has at every instant a definite preferred direction. The energy $V(\Theta)$ is required to deflect the axis by an angle Θ from its preferred position. For nonpolar symmetric molecules, e.g., CO_2, C_6H_6, the potential hill is symmetric with respect to two minima at $\Theta=0$ and $\Theta=\pi$. For more

[1] C. V. Raman and K. S. Krishnan, Proc. Roy. Soc. **A117**, 589 (1928); Phil. Mag. **5**, 498 (1928).

[2] H. A. Stuart and H. Volkmann, Zeits. f. Physik **83**, 461 (1933).

[3] P. Debye, Physik. Zeits. **36**, 100, 193 (1935).

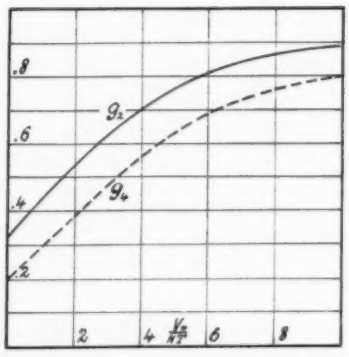

FIG. 1. The functions $g_2(V_0/kT)$ and $g_4(V_0/kT)$ for a symmetric potential barrier $V=V_0(1-\cos^2\theta)$.

complex molecules and probably for most polar molecules $\Theta=0$ gives the only minimum. Using classical statistics one finds the average polarizabilities β of the molecule. If the field is acting parallel to the preferred direction

$$\beta_1=b_2+(b_1-b_2)g_2+(g_2-g_1^2)\mu^2/kT \qquad (1)$$

and for a field normal to the preferred direction

$$\beta_2=\beta_3=\tfrac{1}{2}[(b_1+b_2)-(b_1-b_2)g_2 +(1-g_2)\mu^2/kT]. \qquad (1')$$

Here we have introduced a set of functions

$$g_n(V/kT)=\frac{\int_0^\pi \exp(-V/kT)\cos^n\Theta\sin\Theta d\Theta}{\int_0^\pi \exp(-V/kT)\sin\Theta d\Theta}. \qquad (2)$$

If $V=V_0(1-\cos\Theta)$, g_n can be expressed in terms of Langevin's function $L(x)=\operatorname{cotgh} x-1/x$, $g_1=L(V_0/kT)$, $g_2=1-2L(V_0/kT)kT/V_0$. For a symmetric potential hill $g_{2n+1}=0$. The simplest example of a symmetric potential barrier is $V=V_0(1-\cos^2\Theta)$ which gives

$$g_2=\left(\tfrac{1}{2}x^{-1}\exp x/\int_0^{x^{\frac{1}{2}}}\exp t^2dt\right)-\tfrac{1}{2}x^{-1},$$

$$x=V_0/kT, \quad \text{and} \quad g_4=g_2-(3g_2-1)/2x.$$

The latter two functions are plotted in Fig. 1. g_2 has the limiting values $\frac{1}{3}$ for free rotation and 1 for no rotation. g_4 varies between 0.2 and 1.

In the classical theory it is assumed that the field acting on any molecule is parallel to the applied field E and has the value $E+4\pi I/3$, where I is the polarization. Since all angles between the field and the preferred directions occur with equal probability the average molar polarization P can be calculated in the usual way, giving

$$P=(\epsilon-1)M/(\epsilon+2)\rho=(4\pi/3)A\tfrac{1}{3}(\beta_1+2\beta_2)$$
$$=(4\pi/9)A[(b_1+2b_2)+(1-g_1^2)\mu^2/kT].$$

Hence with the classical assumption the molar refraction $R=(4\pi/9)A(b_1+2b_2)$ will not be changed whatever the form of the potential barrier may be. Furthermore, if the potential hill is symmetric, the dipole-contribution also will not be altered. Hindered rotation reduces the dipole term only if $V(\Theta)$ is asymmetric. We shall show below that analogous conclusions hold also for the Kerr constant and the scattering of light.

Experiments, however, show that neither polar nor nonpolar liquids satisfy the Lorentz-Lorenz equation. According to Stuart and Volkmann[2] the differences between the theoretical and the measured values of the Kerr constant and the depolarization are equally large for either type of molecule. Hence Debye's theory of hindered rotation, while it may explain the dielectric constant and the Kerr effect of some special polar liquids, is not sufficient to account for the optical properties of most liquids.

Our further considerations are confined to nonpolar liquids. For these the classical assumption $F=E+4\pi I/3$ leads always to the Lorentz-Lorenz equation. Hence it is necessary to abandon this assumption and replace the isotropic by an anisotropic Lorentz force.

THE ANISOTROPIC LORENTZ FORCE IN CRYSTALS

Inasmuch as the structure of a liquid has a closer resemblance to that of a crystal than to that of a gas, it is natural to approach the problem of the inner field by considering first an ideal crystal. The theory of the Lorentz force in a lattice was developed by Ewald[4] and generalized by Born.[5] The writer[6] has given a simplified derivation.

We consider an infinite lattice whose elementary cell contains only one atom situated at the

[4] P. P. Ewald, Ann. d. Physik **49**, 1, 117 (1916).
[5] M. Born and M. Goeppert-Mayer, *Handbuch der Physik*, Vol. 24, p. 770.
[6] H. Mueller, Phys. Rev. **47**, 948 (1935).

origin of the cell. If x, y, z are the axes of the optical index ellipsoid, the Lorentz force acting on any atom can be written

$$F_x = E_x + 4\pi L_x I_x. \tag{3}$$

The "Lorentz factors" L_x, L_y, L_z can be derived from Ewald's lattice potential[7]

$$\bar{\psi} = \psi - 1/r, \qquad L_x = \Delta/4\pi(\partial^2\bar{\psi}/\partial x^2)_0.$$

Poisson's equation requires

$$L_x + L_y + L_z = 1. \tag{4}$$

The Lorentz factors depend on the shape, but not on the size of the elementary cell. Previously the author[6] has given the values of $L_x = L_y$ and L_z for tetragonal lattices. Fig. 2 gives these factors for simple hexagonal lattices. They depend on the ratio c/a, where c is the lattice spacing in the direction of the hexagonal axis, and a is the distance to the nearest neighbors normal to the axis. The results are very similar to those for tetragonal lattices.

We observe again that if c/a is moderately large $L_x = kc/a$ and $L_z = 1 - 2kc/a$. Since with $c/a > 1$ we have a layer lattice, this result has the following simple interpretation: In a layer lattice the Lorentz force can be calculated by considering the atoms continuously distributed in all layers except the layer in which the atom is situated. For a field E_z the continuous distribution gives the field $4\pi I_z$ and hence contributes 1 to the factor L_z. The dipoles in the same layer give a negative field which can readily be calculated by direct summation. Thus one finds $k = 0.359$ for tetragonal and $k = 0.370$ for hexagonal lattices. These factors agree with the slope[8] of the L_x-curves if $c/a > 1.5$.

Similarly for small values of c/a one has $L_z = k'(a/c)^2$, which means that in a chain lattice it is necessary to consider the discontinuous structure along only a single chain of atoms. k' is therefore given by a simple infinite sum and has the values 0.3826 and 0.3313 for tetragonal and hexagonal lattices respectively. This is a good approximation if $c/a < 0.6$. If c/a differs little from unity one can use a similar approximation by calculating the field of the dipoles within a rectangular box. The validity of the latter method was demonstrated in a previous paper.[6]

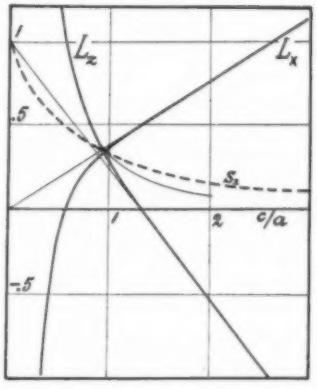

FIG. 2. The Lorentz factors for simple hexagonal lattices and the approximations for small and large values of c/a. Dotted curve: Raman and Krishnan's approximation.

In evaluating the field of the dipoles in a single layer or chain one again can consider the atoms at a large distance as continuously distributed. Hence the Lorentz factors are determined if we know the distribution of the few nearest neighbors only. Even in a crystal the atoms more than a few atomic distances away can be looked upon as forming a continuum.

This result justifies the well-known cavity method for calculating the inner field[9] and furnishes the basic principle for evaluating the Lorentz force in liquids.

Fig. 2 illustrates another important point. Following a suggestion of Havelock,[10] Raman and Krishnan[1] assume that for an anisotropic structure an ellipsoidal cavity can be found which has the property that the atoms within give no contribution to the Lorentz force. This assumption is incorrect because L can take negative values, whereas the cavity method leads always to positive values. Without justifying themselves Raman and Krishnan postulate furthermore that the hypothetical ellipsoid has an axial ratio c/a. Hence they assume a Lorentz factor

[7] The lattice potential ψ is the electrostatic potential of a charge distribution consisting of discrete unit positive charges at the lattice points and a uniform constant negative charge density $-1/\Delta$, where Δ is the volume of the elementary cell. If the charge at the origin is missing the potential is $\bar{\psi} = \psi - 1/r$ and the derivative must be taken for the values $x = y = z = 0$.

[8] In the paper mentioned (reference 6) we estimated from the graph for tetragonal lattices $2k = 0.72$. The direct summation gives 0.718.

[9] This result shows also that in general it is advisable to use an anisotropic cavity for an anisotropic crystal.

[10] T. H. Havelock, Proc. Roy. Soc. **A80**, 31 (1908).

$$s=s_z=\frac{1-\epsilon^2}{\epsilon^2}\left(\tfrac{1}{2}\epsilon \ln\frac{1+\epsilon}{1-\epsilon}-1\right), \qquad (5)$$

where ϵ is the eccentricity $\epsilon^2=1-(a/c)^2$. If $a>c$ one takes $\epsilon^2=(a/c)^2-1$ and obtains

$$s_z=\frac{1+\epsilon^2}{\epsilon^2}\left(1-(1/\epsilon)\tan^{-1}\epsilon\right). \qquad (5')$$

s_x and s_y are determined by the relations $s_x=s_y$ and $s_x+s_y+s_z=1$. In Fig. 2 the dotted curve gives the values of s_z. Raman and Krishnan's assumption $s_z=L_z$ is obviously untenable.

The use of the s factors is however justified if the cavity method is correctly applied. The cavity can have any size as long as it includes at least the nearest 20 or 30 neighboring atoms. We find then $F_x=E_x+4\pi s_x I_x+F_x'$. Comparison with (3) gives

$$F_x'=4\pi(L_x-s_x)I_x=4\pi\gamma_x I_x, \qquad (6)$$

where $\gamma_x+\gamma_y+\gamma_z=0$, hence $\gamma=\gamma_z=-2\gamma_x=-2\gamma_y=L_z-s_z$.

F' is the field of the finite number of dipoles within an ellipsoidal cavity, the axes of which are parallel to the optical axes of the crystal. The field F' does not depend on the size of the ellipsoid, but only on its eccentricity. Consequently the field of the dipoles within a uniformly polarized shell, bordered by two concentric ellipsoids of equal eccentricities is zero at the center.

The above results hold also for molecular lattices. In a forthcoming paper it will be shown that they are also valid for "diffuse" lattices in which the atoms or molecules oscillate about their equilibrium positions.

The Lorentz Force in Liquids

From the work of Stewart,[11] Warren,[12] Bernal and Fowler,[13] Debye,[3] Frenkel[14] and others, the following assumptions concerning the structure of liquids seem reasonable. For rod- or disk-shaped molecules the preferred positions of the nearest neighboring molecules are arranged in a lattice with axial symmetry. In many liquids the x-ray analysis[12] points to a simple hexagonal lattice.[15] The preferred orientation of the molecule considered and of its nearest neighbors will have the direction of the symmetry axis of the lattice. The position and orientation of any distant molecule is arbitrary.

The environment of a molecule can be divided into three regions:

1. The cybotactic region, with a pronounced lattice structure. Within it all molecules have the same preferred orientation. The dimensions of this zone must be much smaller than the wavelength of light. We assume that it includes at least 20 to 30 molecules and that it has the shape of an ellipsoid of rotation whose eccentricity ϵ is smaller than the eccentricity of the ellipsoid representing the shape of the molecule.

2. The continuous region. This includes all distant molecules whose positions and orientations are independent of those of the molecule upon which we fix our attention. As far as this molecule is concerned the distant molecules act as if forming a continuous distribution of matter. This region, extending to infinity, starts at a certain boundary, which is assumed to be an ellipsoid, larger but of the same eccentricity as the one limiting the cybotactic zone.

3. The intermediate region between 1 and 2. Here the molecules are only slightly influenced by the intramolecular forces exerted by the central molecule. This region may be divided into a series of concentric ellipsoidal shells of constant eccentricity ϵ. Every molecule within one shell will be influenced in the same manner by the central molecule.

The molecule upon which we fix our attention may be any arbitrary molecule. The symmetry axis of its cybotactic lattice can take on any direction with equal probability. We assume that no outer influence, not even that of a strong electric field, can change the distribution of the preferred directions to any marked degree.[16] The preferred orientation of a molecule changes slowly with time, but this change is assumed to

[11] G. W. Stewart, Trans. Faraday Soc. **29**, 982 (1933).
[12] B. E. Warren, Phys. Rev. **44**, 969 (1933).
[13] J. D. Bernal and R. H. Fowler, J. Chem. Phys. **1**, 515 (1933).
[14] J. Frenkel, Acta phys. chem. **3**, 663 (1936).

[15] This is the simplest possible assumption, but it is not essential for our calculation.
[16] Investigations of the light scattering and the x-ray diffraction of liquids in a strong electric field have furnished no evidence to the contrary.

be negligible during the period of a light wave.[17]

Under the influence of an electric field E the liquid acquires an average polarization I in the direction of E. Within a cybotactic group, however, the polarization is not in the direction of the field. Hence we introduce the concept of the "local polarization J." J varies continuously throughout the liquid. It depends on the local preferred direction.

The results of the preceding section give for the Lorentz force in a liquid

$$F_z=E_z+4\pi s_z I_z+4\pi\gamma_z J_z. \tag{7}$$

$4\pi s_z I_z$ is the field of the distant molecules which act as if they were a continuum. $4\pi\gamma_z J_z$ is according to Eq. (6) the field of the dipoles in the cybotactic group. The dipoles in the intermediate range give no field, because, as we have seen, the field of a uniformly polarized ellipsoidal shell is zero at the center. The three equations (7) give the components of F parallel and normal to the preferred axis. Hence

$$J_x=N\beta_2 F_x;\quad J_y=N\beta_2 F_y;\quad J_z=N\beta_1 F_z, \tag{8}$$

where β_1 and β_2 are the average polarizabilities of the molecule defined by Eq. (1). $N=\rho A/M$ is the number of molecules per cc, ρ, the density, A, Avogadro's number and M the molecular weight. Introducing Eq. (8) in Eq. (7) gives

$$F_z=l_z(E+4/3\pi I)_z, \tag{9}$$

where, since $I=(n^2-1)E/4\pi$,

$$\begin{aligned} l_x=l_y&=[1-3/2(s-\tfrac{1}{3})(n^2-1)/(n^2+2)]/\\ &\qquad(1+2\pi\gamma N\beta_2),\\ l_z&=[1+3(s-\tfrac{1}{3})(n^2-1)/(n^2+2)]/\\ &\qquad(1-4\pi\gamma N\beta_1). \end{aligned} \tag{10}$$

By combining Eqs. (9) and (7) one gets three equations for J_x, J_y and J_z. Finally, since I is obviously the average value of the local polarization J, $I=\bar{J}$, one can eliminate J and calculate the molar refraction R_L of the liquid.

$$R_L=(n^2-1)M/(n^2+2)\rho=\frac{4}{3}\pi A\frac{\tfrac{1}{3}[\beta_1/(1-4\pi\gamma\beta_1 N)+2\beta_2/(1+2\pi\gamma\beta_2 N)]}{1-(4/3)\pi N(s-\tfrac{1}{3})[\beta_1/(1-4\pi\gamma\beta_1 N)-\beta_2/(1+2\pi\gamma\beta_2 N)]}. \tag{11}$$

This expression can be simplified. The denominator corresponds to the correction given by Raman and Krishnan.[18] But since the boundary of a cybotactic group has a smaller eccentricity than the molecule, our value of $(s-\frac{1}{3})$ is much smaller than theirs. In fact this correction is so small that it can be neglected in most cases. Therefore we take $s=\frac{1}{3}$, which means that the cybotactic groups are approximately spherical. Even if they have elliposidal shape, the assumption $s=\frac{1}{3}$ does not alter the results by more than a fraction of one percent, because a change of s alters the value of $\gamma=L_z-s$ in such a way, that l_x, l_z and R_L remain almost unchanged.

If we introduce

$$\begin{aligned} &p=b_1/b_2,\quad b=\tfrac{1}{3}(b_1+2b_2),\\ &B=[1-g_2(1-p)]/(p+2),\\ &x=12\pi Nb(L_z-\tfrac{1}{3})=9(L_z-\tfrac{1}{3})\rho R_0/M,\\ &R_0=4/3\pi Ab. \end{aligned} \tag{12}$$

Eq. (11) takes the simple form

$$\begin{aligned} R_L/R_0&=B/(1-xB)\\ &\quad+(1-B)/(1+\tfrac{1}{4}x(1-B)). \end{aligned} \tag{13}$$

R_0 is the molar refraction of the gas, x depends on the anisotropy of the quasi-crystalline structure and B on the freedom of rotation. Since b_1, b_2 and R_0 can be obtained from measurements in the gaseous state, Eq. (13) contains only two unknown parameters L_z and g_2. They are characteristic of each liquid. g_2 varies with the temperature and the density. We do not expect a temperature dependence of L_z, except near the critical temperature of the liquid.

[17] The characteristic frequencies of mutual vibration of the molecules are in the far infrared. C. H. Cartwright, Phys. Rev. **49**, 470 (1936).

[18] Raman and Krishnan's relation is obtained if we put $s=L_z$, hence $\gamma=0$ and $\beta_1=b_1$, $\beta_2=b_2$. The latter relations imply that the molecules have entirely lost their freedom of rotation ($g_2=1$) Raman and Krishnan's equation gives results of the correct order of magnitude because it contains two errors which partly compensate each other. The anisotropy of their Lorentz field is too small ($s<L_z$, see Fig. 1), whereas the effect of hindered rotation is taken too large.

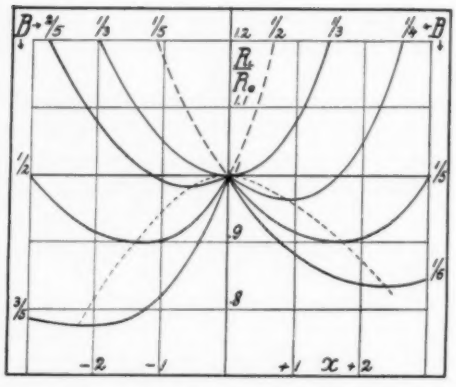

FIG. 3. The molar refraction of liquids. The variable $x=9(L_z-1/3)\rho R_0/M$ depends on the anisotropy of the Lorentz force, the parameter B on the potential barrier and the optical anisotropy of the molecule. The dotted curve gives the minima of the curves.

THE MOLAR REFRACTION OF LIQUIDS. BENZENE

The classical work of L. Lorenz led to the conclusion that the molar refraction is the same in the liquid and gaseous state. This fact has frequently been mentioned as an argument against anisotropic Lorentz forces. But more accurate measurements have shown that the refraction of a liquid is usually slightly smaller than that of its vapor, and that it varies with temperature and pressure. In addition the dispersion of R_L is larger than the dispersion of R_0.

Although these differences are relatively small, they are nevertheless too large to be explained by changes of the polarizabilities of the molecule.[19] Our theory accounts for all these changes without postulating any alteration in the polarizabilities.

In Fig. 3 R_L/R_0 is plotted as a function of x for various values of B. Since x is of the order of magnitude of $9(L-\frac{1}{3})(n^2-1)/(n^2+2)$ its absolute value is probably never larger than 3. From Fig. 2 it follows that x is positive for disk-shaped and negative for rod-shaped molecules. The parameter B varies between $\frac{1}{3}$ for $g_2=\frac{1}{3}$, and $p/(p+2)$ for $g_2=1$. Since for most molecules $\frac{1}{3}<p<3$ it is sufficient to vary B between the limits 0.15 and 0.6. Rod-shaped molecules usually have $p>1$ and hence $B>\frac{1}{3}$, while for disk-shaped molecules $B<\frac{1}{3}$.[20]

The curves in Fig. 3 have a minimum $9B(1-B)/(3B+1)$ for $x=2(1-3B)/3B(1-B)$ and R_L/R_0 is 1 for $x=0$ and for $x=(B+1)(1-3B)/B(1-B)$. If the molecules can rotate freely or almost freely the anisotropy of the Lorentz force demands $R_L>R_0$. It is probable that this condition exists in compressed gases, which would explain the increase of the molar polarization of CO_2 with pressure.[19] If the anisotropy is very large we always get $R_L>R_0$, even if no rotation exists. The Lorentz force reaches its largest anisotropy in the crystalline state. Hence it is not surprising that the molar polarization of solid benzene is larger than that of its vapor.[19]

The case $R_L<R_0$ occurs only if we have hindered rotation together with a moderate anisotropy of the Lorentz force. These are exactly the conditions existing in liquids. We notice that in all cases of practical importance $R_L/R_0>0.9$. Hence the approximate validity of the Lorentz-Lorenz equation cannot be advanced as an argument against anisotropic Lorentz forces.

Since we have no direct information concerning the values of g_2 and L_z we are not able to predict the refraction of a liquid. Inversely, however, we can find approximate values of these parameters from the observed values of R_L.

We will discuss the procedure for benzene. According to Stuart[21] the polarizabilities are $b_1=63.5\,10^{-25}$, $b_2=b_3=123.1\,10^{-25}$ hence $p=0.516$. In Fig. 4 R_L/R_0 is given as a function of x for various values of g_2. Wasastjerna[22] has determined $R_0=27.20$ (D-line) and $R_L=26.18$ (room temperature), hence $R_L/R_0=0.962$. Fig. 4 shows that this value can be understood only if g_2 is larger than 0.775. If we assume a potential $V_0(1-\cos^2\theta)$ this indicates, according to Fig. 1,

[19] The work of Fajans and Joos (Zeits. f. Physik **23**, 1 (1924)) and the theory of photoelasticity (H. Mueller, Phys. Rev. **47**, 947 (1935)) show that such changes must occur in solids, but in liquids they cannot play an important part as shown by the fact that the molar polarization of CO_2 increases with pressure (F. G. Keyes and J. G. Kirkwood, Phys. Rev. **36**, 754 (1930)) and that the polarization of solid benzene is larger than that of benzene vapor (C. P. Smyth, J. Am. Chem. Soc. **55**, 453 (1932)).

[20] This is not true in some exceptional cases, e.g., formic acid and acetic acid. For these substances our theory predicts $R_L>R_0$.

[21] H. A. Stuart, *Molekülstruktur* (Berlin 1934), p. 173. These polarizabilities are determined from the Kerr effect of the vapor. Cabannes' measurement of the depolarization of the scattered light gives $p=0.505$.

[22] J. A. Wasastjerna, Soc. Sc. Fennica, Comm. Math. Phys. **2**, No. 13 (1924). The corresponding values of the molar polarization are $P_L=26.61$ $P_0=27.01$, hence $P_L/P_0=0.985$. The ratio p_0 of the static polarizabilities is probably larger than p. $P_{\text{solid}}=28.5$.

that the potential barrier must be higher than 5.2 kT.

A value for x and a closer estimate of g_2 can be obtained if we consider the dispersion. A change of wave-length does not affect g_2 and L_z, since they depend only on the liquid structure, but it does change the value of R_0 and hence of x. The slope of the curves R_L/R_0 for $g_2=$ const. is related to the difference between the dispersions of R_L and R_0. According to Wasastjerna[22] $R_F-R_C=0.74$ for liquid benzene, and $R_F-R_C=0.68$ for the vapor. From these data one estimates $d(R_L/R_0)/dx=0.12/x$. Lines corresponding to these slopes are shown in Fig. 4. We see that there is only one solution for which $R_L/R_0=0.962$ and for which the slope suits the observed difference of dispersions, namely $x=1.8$ and $g_2=0.875$. This corresponds to a potential hill of about 8.8 kT, a value of the same order of magnitude as those given by Debye[3] and Andrade.[23]

With $\rho=0.881$, $R_0=27.2$, $M=78.05$, we calculate from $x=9(L_z-\frac{1}{3})\rho R_0/M$ (Eq. 12) $L_z=0.98$. If we assume a simple hexagonal structure of the cybotactic group we find from Fig. 2 that this corresponds to $c/a=0.56$. According to the considerations of de Boer[24] a hexagonal structure seems a good approximation. He reports that recent x-ray work gives $c=3.5$ to 3.6A. To account for the observed density we must have $M/A\rho=ca^2 2^{\frac{1}{2}}/2$ or $c/a=0.50$ to 0.53, which is a surprisingly good verification of our result.

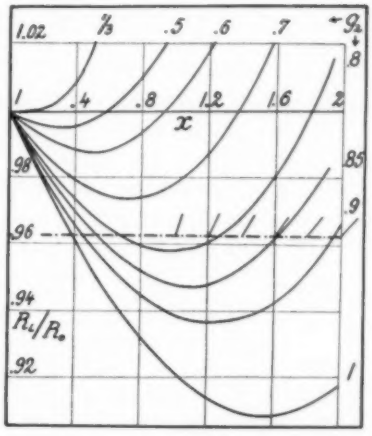

FIG. 4. The molar refraction of benzene. The dotted line gives the observed value. The short lines indicate the slopes $d(R_L/R_0)/dx$ required by the observed dispersions.

In view of the fact that the value of p is accurate to only about 3 percent and that a small part of the change of dispersion may be due to the shift of the absorption lines,[25] the above results are somewhat inaccurate. The true solution probably lies within the ranges $1.4<x<1.8$ and $0.82<g_2<0.9$.

With this solution we can now estimate the order of magnitude of the temperature- and the pressure variation of R_L. If we assume $L_z=$ const. and abbreviate $R_L/R_0=r$, $\varphi=V_0(\rho)/kT$ we have

$$1/R_0\frac{\partial R_L}{dT}=-\frac{1}{\rho}\frac{d\rho}{dT}\left[x\frac{\partial r}{\partial x}+\frac{\partial r}{\partial g_2}\frac{dg_2}{d\varphi}\varphi\frac{dV_0}{d\rho}\frac{\rho}{V_0}\right]-\frac{\partial r}{\partial g_2}\frac{dg_2}{d\varphi}\frac{\varphi}{T}, \tag{14}$$

$$1/R_0\frac{\partial R_L}{\partial p}=-\frac{1}{\rho}\frac{d\rho}{dp}\left[x\frac{\partial r}{\partial x}+\frac{\partial r}{\partial g_2}\frac{dg_2}{d\varphi}\varphi\frac{dV_0}{d\rho}\frac{\rho}{V_0}\right]. \tag{15}$$

With the values $(1/\rho)(d\rho/dT)=-1.21\ 10^{-3}$, $(1/\rho)(d\rho/dp)=9.5\ 10^{-11}$, $x\partial r/\partial x=0.12$, $\partial r/\partial g_2=-0.44$ (the latter value estimated from Fig. 4) $dg_2/d\varphi=0.018$ (from Fig. 1), $\varphi=8.8$, $T=290$ we get roughly $(1/R_0)\partial R_L/\partial T=2$ to $3\ 10^{-4}$. The experimental value is $1.22\ 10^{-4}$. The theoretical value of $(1/R_0)\partial R_L/\partial p$ depends largely on $V_0(\rho)$. If we assume[23] $V_0=c\rho^t$ close agreement with the observed value $-0.98\ 10^{-11}$ is obtained for $t=3$. But this result depends very much on the value of $dg_2/d\varphi$ and hence on the choice of the potential barrier. At any rate the order of magnitude of $\partial R_L/\partial T$ and $\partial R_L/\partial p$ is correct.

To sum up, the value of the molar refraction of liquid benzene, its dispersion, and its pressure and temperature dependence can be explained by assuming hindered rotation and cybotactic grouping. The characteristic quantities of C_6H_6

[22] E. N. da C. Andrade, Phil. Mag. **17**, 497 (1934).
[24] J. H. de Boer, Trans. Faraday Soc. **32**, 13 (1936).
[25] P. Pringsheim, *Handbuch der Physik*, Vol. 23/1, p. 246.

are $g_2=0.88$ and $x=1.8$ or $L_z=0.98$ approximately. These quantities can be determined without making any special assumptions concerning the type of grouping or the form of the potential barrier. The assumptions are introduced only to correlate the parameters with quantities which have a simple physical meaning, and to show that their values are reasonable.

The Intensity and Depolarization of the Scattered Light

The theory of the unmodified scattered light for liquids was developed independently by King,[26] Gans[27] and Ramanathan.[28] Free rotation and isotropy of the Lorentz force were assumed. In their original forms the three theories gave different results, but the later papers of Ramanathan and Didlaukies[29] have eliminated these discrepancies. However, the large amount of experimental data available do not verify the theory.[30]

We will follow Ramanathan's general formulation of the theory, but correct it by taking into account the influence of hindered rotation and the anisotropic polarization field. If the incident light of intensity 1 is plane polarized with an electric vector E, the intensity of the light scattered by a unit volume at a distance 1 cm in the direction normal to the plane of E is given by

$$I_p=\tfrac{1}{2}(2\pi/\lambda)^4N[\gamma(\mu_p)_{av}{}^2+(\mu_p{}^2)_{av}-(\mu_p)_{av}{}^2],$$
$$I_n=\tfrac{1}{2}(2\pi/\lambda)^4N(\mu_n{}^2)_{av}. \qquad (16)$$

I_p and I_n are the scattered light components having electric vectors parallel and normal to E, respectively. λ is the wave-length in vacuum, N the number of molecules per cc, $\gamma=NkT\beta$, k Boltzmann's constant and β the isothermal compressibility at the absolute temperature T. μ_p is the component of the induced dipole moment in the direction of E and μ_n is its component normal to E. $(\mu)_{av}{}^2$ is the square of the average and $(\mu^2)_{av}$ the average of the square. To find these averages we introduce three Cartesian systems of coordinates (Fig. 5): A fixed system p, n_1, n_2 whose directions coincide, respectively, with E, with the direction of propagation of the incident beam and with the direction of observation. The second system x, y, z has the z axis parallel to the preferred direction of a molecule with the x axis in the plane (pz). The position of this system is given by the angles ϑ, φ. Since the preferred directions are distributed at random the probability of finding a molecule with the preferred axis in the range $d\vartheta$, $d\varphi$ is $\sin\vartheta d\vartheta d\varphi/4\pi$. The third system of coordinates 1, 2, 3 coincides with the axes of the ellipsoid of polarization of the molecule. The orientation of the symmetry axis 1 with respect to the axis z is given by the polar coordinates Θ, ψ, the axis 2 being in the plane $(z1)$. The probability that the molecule has this orientation is $\exp(-V/kT)\sin\theta d\theta d\psi/\int\exp(-V/kT)\sin\theta d\theta d\psi$. The field acting on a molecule is given by (9). By calculating successively E_x, E_y, E_z; F_1, F_2, F_3; μ_1, μ_2, μ_3; μ_x, μ_y, μ_z one finds

$$\mu_p=(E+4/3\pi I)\{\begin{aligned}&l_x[(b_1\sin^2\theta+b_2\cos^2\theta)\cos^2\psi\sin^2\vartheta+(b_1-b_2)\cos\theta\sin\theta\cos\vartheta\sin\vartheta\cos\psi\\&\quad+b_2\sin^2\psi\sin^2\vartheta]+l_z[(b_1\cos^2\theta+b_2\sin^2\theta)\cos^2\vartheta\\&\quad+(b_1-b_2)\cos\theta\sin\theta\cos\vartheta\sin\vartheta\cos\psi],\end{aligned} \qquad (17)$$

$$\mu_{n_1}=(E+4/3\pi I)\{\begin{aligned}&l_x[(b_1-b_2)\sin\theta\sin\vartheta\cos\psi(\cos\theta\sin\vartheta\cos\varphi-\sin\theta\cos\vartheta\cos\varphi\cos\psi\\&\quad+\sin\theta\sin\varphi\sin\psi)-b_2\sin\vartheta\cos\vartheta\cos\varphi]\\&+l_z[(b_1\cos^2\theta+b_2\sin^2\theta)\sin\vartheta\cos\vartheta\cos\varphi\\&\quad+(b_1-b_2)\sin\theta\cos\theta\cos\vartheta(\sin\varphi\sin\psi-\cos\vartheta\cos\varphi\cos\psi)].\end{aligned} \qquad (18)$$

These expressions must be introduced in

$$(\mu_p{}^2)_{av}=\frac{\int\mu_p{}^2\exp(-V/kT)\sin\theta\sin\vartheta d\theta d\vartheta d\varphi d\psi}{\int\exp(-V/kT)\sin\theta\sin\vartheta d\theta d\vartheta d\varphi d\psi} \qquad (19)$$

[26] L. V. King, Proc. Roy. Soc. **A104**, 333 (1923).
[27] R. Gans, Zeits. f. Physik **17**, 353 (1923).
[28] K. R. Ramanathan, Proc. ind. Assoc. f. cult. sc. **8**, 181 (1923); Indian J. Phys. **1**, 413 (1927).
[29] M. Didlaukies, Ann. d. Physik **5**, 205 (1930).
[30] The difficulties have been discussed by J. Cabannes: *La diffusion moléculaire de la lumière* (Paris, 1929), pp. 204–300.

and the analogous expression for $(\mu_n^2)_{av}$. $(\mu_p)_{av}$ is of course identical with the average polarization per molecule I/N and $(\mu_n)_{av}=0$. The integration of (19) gives

$$(\mu_p^2)_{av}=[(E+4\pi I/3)^2/15]\begin{cases} l_z^2[b_1^2(2g_2+g_4)+b_2^2(3-5g_2+2g_4)+4b_1b_2(g_2-g_4)] \\ \quad +l_x^2[b_1^2(3-5g_2+2g_4)+b_2^2(3+3g_2+2g_4)+2b_1b_2(1+g_2-2g_4)] \\ \quad +2l_xl_z[2b_1^2(g_2-g_4)+b_2^2(1+g_2-2g_4)+b_1b_2(1-3g_2+4g_4)] \end{cases} \quad (20)$$

$$(\mu_n^2)_{av}=[(E+4\pi I/3)^2/15]\begin{cases} l_z^2[b_1^2(2g_2-g_4)+b_2^2(1-g_4)+2b_1b_2(g_4-g_2)] \\ \quad +l_x^2[b_1^2(1-g_4)+b_2^2(1+g_2+g_4)+b_1b_2(-1-g_2+2g_4)] \\ \quad +l_xl_z[b_1^2(2g_4-2g_2)+b_2^2(-1-g_2+g_4)+b_1b_2(-1+3g_2-4g_4)] \end{cases} \quad (20')$$

where g_2 and g_4 are the functions of the potential barrier defined in Eq. (2). If we take again $s=\frac{1}{3}$, the definitions (10) give

$$l_x=1/(1+x(1-B)/4), \quad l_z=1/(1-xB),$$

where x and B are defined in (12).

If there is no anisotropy of the Lorentz force, $x=0$, $l_x=l_z=1$, we get the classical relations

$$(\mu_p^2)_{av}=[(E+4\pi I/3)^2/15][3b_1^2+8b_2^2+4b_1b_2],$$
$$(\mu_n^2)_{av}=[(E+4\pi I/3)^2/15](b_1-b_2)^2.$$

This is true for any value of g_2 and g_4. Hence hindered rotation alone does not alter the classical theory.

If the incident light is not polarized, one has $I_p'=I_p+I_n$, $I_n'=2I_n$ and hence the total intensity of the scattered light is $I_0=I_p+3I_n$, and its depolarization $\Delta=2I_n/(I_p+I_n)$. By introducing (20) in (16) and using the definitions (12) we get

$$I_0=\tfrac{1}{2}(\pi/\lambda^2)^2((n^2-1)^2/N)\cdot i; \qquad i=[\gamma-1+(M_1+3M_2)3/5]; \quad (21)$$

$$\Delta=6M_2/[5(\gamma-1)+3(M_1+M_2)], \quad (22)$$

where

$$M_1=(l_z^2m_1+l_x^2m_2+2l_xl_zm_3)(R_0/R_L)^2/(p+2)^2,$$
$$M_2=(l_z^2m_3+l_x^2m_4-l_xl_zm_5)(R_0/R_L)^2/(p+2)^2 \quad (23)$$

and

$$\begin{aligned} m_1&=3+g_2(p^2+4p-5)+2g_4(p-1)^2, \\ m_2&=(3p^2+2p+3)+g_2(-5p^2+2p+3)+2g_4(p-1)^2, \\ m_3&=1+2g_2(p^2-p)-g_4(p-1)^2, \\ m_4&=(p^2-p+1)+g_2(1-p)-g_4(p-1)^2, \\ m_5&=(1+p)+g_2(2p^2-3p+1)-2g_4(p-1)^2. \end{aligned} \quad (24)$$

For $x=0$ we obtain the classical relations

$$\Delta=6\delta^2/(5\gamma+7\delta^2)$$

where $\delta^2=(p-1)^2/(p+2)^2=(b_1-b_2)^2/(b_1+2b_2)^2$

and $$i=\gamma+13\delta^2/5,$$

which lead to

$$i=6\gamma(1+\Delta)/(6-7\Delta). \quad (25)$$

For the case of an anisotropic Lorentz field it is not possible to retain these relations by introducing for example a quantity analogous to the anisotropy factor δ. In particular Eq. (25) is not justified.[31]

The significance and use of the results can best be illustrated by applying them to benzene. Since $p=0.516$ is given, one constructs first a table of B and m_i for a series of values of g_2. We assume again a potential $V_0(1-\cos^2\theta)$ and obtain for each g_2 the corresponding[32] value of g_4 from Fig. 1. Next one tabulates l_x, l_z and $(R_L/R_0)^2$ as functions of x and g_2 and using (23) gets $M_1(x, g_2)$ and $M_2(x, g_2)$. Finally (21) and (22) serve to find the intensity factor $i(x, g_2)$ and the depolarization $\Delta(x, g_2)$. The results are plotted in Figs. 6 and 7. They are constructed

[31] The determinations of Avogadro's number from the light scattering in liquids presupposes the validity of Eq. (25). This relation is true only if $3M_1-4M_2=5$. In our theory $(3M_1-4M_2)/5$ is a function of g_2 and x. The calculation for benzene shows that this function is very similar to R_L/R_0 shown in Fig. 4. Its value never deviates much from 1. The fact that the light scattering method has furnished approximate, but not accurate values of Avogadro's number is therefore not an argument against but rather for the anisotropy of the Lorentz force.

[32] Fig. 1 shows that (g_2-g_4) remains almost constant for $V_0/kT<5$ and decreases very slowly for higher potential barriers. We have verified the same behavior for other forms of the potential. Hence for small values of g_2 and also for $g_2=1$ our curves do not depend on the choice of V. Between $g_2=0.8$ and $g_2=0.95$, however, the results vary for different potential barriers.

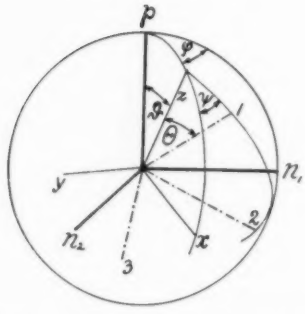

FIG. 5. The 3 coordinate systems used in calculating light scattering and Kerr effect. p, n_1, n_2 is fixed in space; n_1 direction of propagation of incident light; z direction of preferred orientation; l momentary direction of symmetry axis of molecule.

with $\gamma=0.026$, which corresponds to the density and the compressibility of benzene at 18°.

If there were no anisotropy of the Lorentz force we should find $i_0=12.0\ 10^{-2}$ and $\Delta_0=0.57$ whereas the observations at 15° give[33] $i=8.2\ 10^{-2}$ and $\Delta=0.42$. These observed values can be completely understood if $g_2>0.8$, as Figs. 6 and 7 show. Our previous results from the refraction, that g_2 is about 0.88 and that x is between 1.4 and 1.8 are thereby given considerable added support.[34]

Recently Turner[35] has shown for benzene that the variation of the intensity of the scattered light with the wave-length is not strictly proportional to $(n^2-1)^2/\lambda^4$. Our theory does not require this proportionality, because i depends on x and hence on R_0 and the wave-length. From $\lambda=5460$A to $\lambda=4350$A R_0 increases by about 3 percent, hence x changes by 0.054. For $x=1.8$, $g_2=0.88$ the slope of the curve is about $\partial i/\partial x=0.2$, hence $\Delta i=(\partial i/\partial x)\Delta x=0.011$ or an increase of i of about 14 percent. Turner's data give between these wave-lengths an increase of i of about 20 percent.

From the slope of the curves in Fig. 7 it follows that the depolarization should vary by less than 0.01 in the range of the visible spectrum. Within experimental errors of this magnitude the observations have shown no dispersion of the depolarization.

If the potential barrier is low the anisotropy of the Lorentz force gives a larger depolarization than the classical theory. Hence the "apparent" optical anisotropy[36] of the molecules can be larger than for the gas. This will occur in liquids at high temperatures and in gases at high pressures. In fact Rao[37] has shown that near the critical temperature the apparent anisotropy is from 3 to 4 times larger than for the gas, and in gases Volkmann[38] has found an increase of δ^2 with pressure.

Summing up, the theory accounts for all anomalies of the intensity and the depolarization of the scattered light. It is perhaps surprising that the theory of Gans,[27] which is based on statistical considerations, does not lead to our results. This is due to the fact that Gans assumes that the isotropic micro-distribution corresponds to a state of minimum energy. In liquids it seems more natural to assume that in small volume-elements the optical anisotropy fluctuates around a finite value.

THE KERR EFFECT IN LIQUIDS

The measurements of the electro-optical Kerr effect demonstrate the failure of the classical theory of Langevin and Born in the most impressive manner.[39] The Kerr constant K_L of liquids is always much smaller than its theoretical value K_0. The work of Briegleb,[40] and

[33] Calculated from Cabannes' value $R=10.7\ 10^{-6}$. Cabannes' remark, that C_6H_6 scatters more than it should, is based on the implication that (25) is correct. (25) gives $i=7.3\ 10^{-2}$. Actually benzene scatters much less than it should according to the classical theory. Hence we do not think that Rocard's theory can be accepted. See J. Cabannes, *La diffusion moléculaire de la lumière*, pp. 237 and 296.

[34] Figs. 4 and 6 are not appreciably altered if one takes $p=0.500$ or if a different form of the potential barrier is chosen. The curves in Fig. 7 however are very sensitive to such changes and a better agreement for Δ could not be expected.

[35] A. F. Turner, Diss. University of Berlin (1934), Physik. Ber. **16**, 1860 (1935). The observed increase of i for wave-lengths $\lambda>5460$A could only be explained if our curves had a large curvature at their minima or if p changes with λ.

[36] The "apparent" optical anisotropy is the value of δ^2 which is obtained from the relation $\Delta=6\delta^2/(5\gamma+7\delta^2)$.

[37] R. S. Rao, Ind. J. Phys. **2**, 7 (1924). Rao, Stuart and Volkmann, reference 2, believe that the large increase is not real but caused by experimental difficulties. In view of Volkmann's latest results, reference 38, δ must have a maximum where $\delta^2>\delta_0^2$.

[38] H. Volkmann, Ann. d. Physik **24**, 457 (1935).

[39] C. V. Raman and K. S. Krishnan, Phil. Mag. **3**, 713 (1927) claim the validity of the classical theory for liquids. But they compare the Kerr constants with the "apparent" anisotropy determined from the depolarization in liquids. Hence their considerations are not a verification of Langevin's theory. They only demonstrate the approximate validity of the relation of Gans between K_L and Δ.

[40] G. Briegleb, Zeits. f. physik. Chemie **14**, 97 (1931); **16**, 249 (1932).

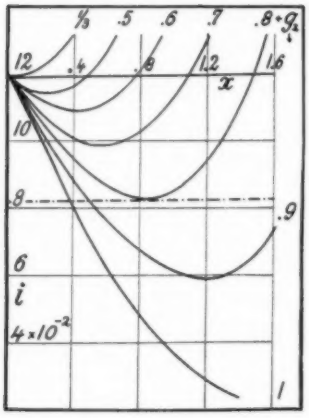

FIG. 6. The intensity factor i for the scattered light for benzene. The dotted line corresponds to the observed value.

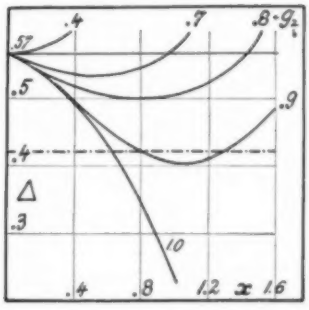

FIG. 7. The depolarization of the scattered light for benzene. The dotted line gives the observed depolarization.

Stuart and Volkmann[2] makes it seem almost impossible to correlate the Kerr constants of liquids with the optical properties of the molecule.

There exist two possibilities for the formulation of a new theory. One might assume that the cybotactic groups behave like small anisotropic crystals. Even if they are spherical they will be oriented by an electric field, and this orientation produces uniaxial birefringence of the liquid. However it can easily be seen that this assumption gives much too large values of the Kerr constant.[41] Although the groups have a smaller optical anisotropy than the molecules, they would orient themselves much more easily, because the energy of orientation is proportional to their volume, while the temperature energy kT is the same as for a single molecule. Supposing the groups contain only 50 molecules and are spherical a calculation carried out on this basis gives for benzene $K_L > 10K_0$, while the experiment gives $K_L < \frac{1}{2}K_0$.

Hence we conclude that the molecules in a quasi-crystalline group are not held together rigidly. Even if the potential barrier is so high that rotation is practically impossible the molecules still have a considerable freedom of translation. They can travel from one preferred position to another. The cybotactic lattice is a rather diffuse structure and does not act like a solid.[42] It is of course possible that the electric field changes somewhat the distribution of the preferred orientations, but we have no experimental data to estimate this effect.[16] It must be small and we shall neglect it altogether.

We calculate therefore the Kerr effect in the usual manner[43] by considering the orienting action of the field on the single molecules. We introduce again the three systems of coordinates (Fig. 5). The axis p is in the direction of the static field E_0 between the plates of the Kerr condenser, n_1 is in the direction of the light beam. The two other systems are defined as in the preceding section. Due to the field E_0 the molecules have an additional potential energy

$$U = \tfrac{1}{2}[a_1 F_{01}^2 + a_2 F_{02}^2 + a_3 F_{03}^2], \qquad (26)$$

where a_1, a_2, a_3 are the static polarizabilities of the molecule, F_{01}, F_{02}, F_{03} the components of the Lorentz force of E_0. In the system x, y, z the components of this field are $F_{0x} = f_x(E_0 + 4\pi I_0/3)_x$, where we place $f_x = 1/(1+x(1-B_0)/4)$, $f_z = 1/(1-xB_0)$, $B_0 = [1-g_2(1-p_0)]/(p_0+2)$, $p_0 = a_1/a_2$, in analogy to the definitions of l_z, l_z, B and p.

For a light wave whose electric vector E_p is parallel to the field E_0 the average polarizability is

$$\gamma_p = \int \mu_p \exp(-(V+U)/kT) \sin\theta \sin\vartheta d\theta d\vartheta d\varphi d\psi / (E_p + (4/3)\pi I_p) \int \exp(-(U+V)/kT) \times \sin\theta \sin\vartheta d\theta d\vartheta d\varphi d\psi. \qquad (27)$$

[41] If the groups are large and not spherical the Kerr effect turns out to be exceedingly large and has a large relaxation time. This is the case in liquid crystals and in colloids.

[42] This statement does not invalidate our calculation of the Lorentz force, because it can be shown that Ewald's theory is applicable to "diffuse" lattices, in which every atom oscillates about a preferred position.

[43] P. Debye, *Handbuch der Radiologie*, Vol. 6.

μ_p is given by Eq. (17). For a light wave whose electric vector E_n is normal to the field E_0 the average polarizability of a molecule is also given by (27) if we replace μ_p by μ_n where

$$\frac{\mu_n}{(E_n+(4/3)\pi I_n)}=\begin{cases} l_x[(b_1-b_2)\sin\theta\cos\theta\sin\vartheta\cos\varphi(\sin\varphi\sin\psi-\cos\vartheta\cos\varphi\cos\psi) \\ \quad+(b_1\sin^2\theta+b_2\cos^2\theta)(\cos^2\vartheta\cos^2\varphi\cos^2\psi+\sin^2\varphi\sin^2\psi \\ \quad-\cos\vartheta\sin\varphi\cos\varphi\sin\psi(1+\cos\psi))+b_2(\cos^2\vartheta\cos^2\varphi\sin^2\psi+\sin^2\varphi\cos^2\psi \\ \quad+2\cos\vartheta\sin\varphi\cos\varphi\sin\psi\cos\psi)]+l_z[(b_1\cos^2\theta+b_2\sin^2\theta)\sin^2\vartheta\cos^2\varphi \\ \qquad+(b_1-b_2)\sin\theta\cos\theta\sin\vartheta\cos\varphi(\sin\varphi\sin\psi-\cos\vartheta\cos\varphi\cos\psi)]. \end{cases}$$

The rest of the calculation follows the usual method.[43] One uses $\exp(-U/kT)=1-U/kT$, finds the term proportional to E_0^2, and from $\gamma_p=\gamma+d\gamma_p$ one determines the indices of refraction $n_p=n+dn_p$, $n_n=n+dn_n$, where $dn_p=(4/3)\pi N(n^2+2)^2 d\gamma_p/6n$.[44] The resulting Kerr constant can be written in the usual form

$$K_L=(n_p-n_n)/nE_0^2=(4/3)\pi N[(n^2+2)/2n]^2[(\epsilon+2)/3]^2\Theta_1 \tag{28}$$

but the value of Θ_1 is now given by

$$\Theta_1=1/45kT\begin{cases} l_z f_z^2[a_1b_1 2g_4+2a_2b_2(1-2g_2+g_4)+a_1b_2 2(g_2-g_4)+2a_2b_1(g_2-g_4)] \\ \quad -l_x f_x^2[a_1b_1(g_2-g_4)+a_2b_2(1-g_4)+a_1b_2(g_2-g_4)+a_2b_1(1-2g_2+g_4)] \\ \quad -l_x f_x^2[a_1b_1(g_2-g_4)+a_2b_2(1-g_4)+a_1b_2(1-2g_2+g_4)+a_2b_1(g_2-g_4)] \\ \quad +l_x f_x^2[a_1b_1 2(1-2g_2+g_4)+a_2b_2(1-g_2+g_4)+a_1b_2(-1+3g_2-2g_4)+a_2b_1(-1+3g_2-2g_4] \\ \quad +3l_x f_x f_y[a_1b_1(g_2-g_4)+a_2b_2(g_2-g_4)-a_1b_2(g_2-g_4)-a_2b_1(g_2-g_4)] \\ \qquad +3l_y f_x f_y[a_1b_1(g_2-g_4)+a_2b_2(g_2-g_4)-a_1b_2(g_2-g_4)-a_2b_1(g_2-g_4)]. \end{cases} \tag{29}$$

n is the index of refraction of the liquid, ϵ its dielectric constant and N the number of molecules per cc. g_2 and g_4 are again the functions of the potential V defined in Eq. (2). If there is no anisotropy of the Lorentz force $x=0$, $l_x=l_z=f_x=f_z=1$ and Eq. (29) reduces to the classical result $\theta_1=(a_1-a_2)(b_1-b_2)2kT/45$. This is true independent of the values of g_2 and g_4. Hence the hindered rotation alone does not alter the classical equation.

For most nonpolar molecules the difference between molar polarization and refraction is small, hence $a_1+2a_2=b_1+2b_2$. If we assume furthermore[45] $p=p_0$, then $f_x=l_x$ and $f_z=l_z$ and the Kerr constant can be written

$$K_L=\frac{4}{3}\pi N\frac{(n^2+2)^2}{6n^2}\frac{(\epsilon+2)^2}{9}\frac{(b_1-b_2)^1}{15kT}\cdot\chi, \tag{30}$$

where

$$\chi=K_L/K_0=[l_x^3\chi_1+l_z^3\chi_2+l_x l_z(l_x+l_z)\chi_3/2]/(p-1)^2, \tag{31}$$

$$\chi_1=1+2(p-1)g_2+(p-1)^2 g_4,$$

$$\chi_2=(p^2-p+1)-(2p^2-3p+1)g_2+(p-1)^2 g_4, \tag{32}$$

$$\chi_3=-(p+1)+(2p^2-5p+3)g_2-2(p-1)^2 g_4.$$

K_0 is the value of the Kerr constant calculated from the classical equation by using the observed values of N, n and ϵ of the liquid and the polarizabilities b_1, b_2 of the molecule as found from measurements in the gas. The theoretical value of χ is a function of x and g_2. This function is plotted in Fig. 8 for benzene, $p=0.516$.

Fig. 8 shows that the Kerr constant depends on the structure of the liquid to a much higher degree than any of the other optical properties. If the potential barrier is small the Kerr constant rapidly increases[46] with the anisotropy of the Lorentz force.

The curves indicate that in liquids the Kerr

[44] Our expressions for dn_p and dn_n do not satisfy the relation $dn_p/dn_n=-2$, but the deviations are probably too small to be measurable.

[45] This assumption may introduce a quite appreciable error in our results.

[46] No data on compressed gases or liquids near the critical temperature seem to be available. Such measurements would be very valuable. They would furnish the proper interpretation of Rao's results. See reference 37.

effect can be greatly reduced, eventually vanish and even reverse its sign. This marked structure sensitivity of the Kerr constant is confirmed by the experiments of Briegleb.[40]

For $\lambda=5460$A McComb[47] finds for benzene the Kerr-constant $B=Kn/\lambda=0.63\ 10^{-7}$; Briegleb measured $B=0.408\ 10^{-7}$. Since all experimental errors tend to reduce B, we shall use the larger value. We find then $K_L=2.29\ 10^{-12}$ and $K_0=5.38\ 10^{-12}$ from the experimental values of n, ρ, ϵ, b_1, b_2. Hence $\chi=0.426$.

Reference to Fig. 8 shows that this is only possible if again $g_2>0.83$. The Kerr effect checks with our previous result that $V_0=8.8kT$. Although in this case x appears somewhat smaller than previously this is not serious in view of our assumptions.

A rise of temperature decreases V_0/kT and g_2 and hence increases the value of χ. Since

$$(1/K_L)(dK_L/dT)=(1/K_0)(dK_0/dT)+(1/\chi)(d\chi/dT)$$

we conclude that the negative temperature coefficient of the Kerr constant should be smaller than that given by the classical theory. This is verified by the results of Hansen.[48] His data furnish $(1/K_L)(dK_L/dT)=-1.6\ 10^{-3}$, while we calculate $(1/K_0)(dK_0/dT)=-4.4\ 10^{-3}$. A rough estimate shows that $(1/\chi)(d\chi/dT)=+2.8\ 10^{-3}$ is compatible with the theory.[49]

If one assumes that (b_1-b_2) is proportional to $(n^2-1)/(n^2+2)$ the classical theory leads to the Havelock relation $Bn\lambda/(n^2-1)^2=h$, where h is Havelock's constant. According to our theory h must be replaced by $h\chi$. Hence the Havelock "constant" should depend on the wave-length. However this variation is small. For benzene we estimate a change of χ of about 5 percent between $\lambda=4000$A and 6000A. Within experimental errors of this order of magnitude the Havelock relation has been verified.

The classical theory gives a relation between the depolarization of the scattered light and the Kerr constant. This relation of Gans cannot be verified in our theory, because there is no simple relation between M_1, M_2 and χ. Actually for benzene the relation is only approximately correct.

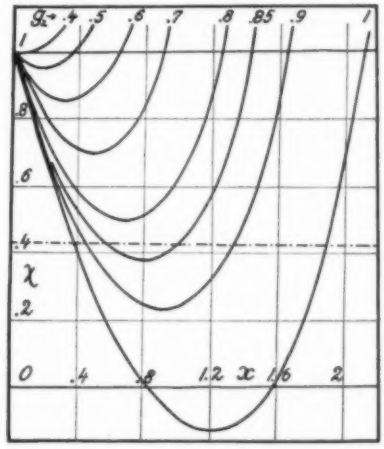

FIG. 8. The Kerr constant for liquid benzene. The dotted line corresponds to the largest observed value.

CONCLUSIONS

The value of the molar refraction of liquid benzene, its dispersion, temperature—and pressure dependence, the intensity and depolarization of the scattered light and its frequency-dependence, the Kerr constant and its temperature and frequency variation, all lead to essentially the same anisotropy of the Lorentz force and the same height of the potential barrier, when interpreted in the light of the present theory. It is probable that still better agreement could be reached by modifying some of our assumptions. Since the potential barrier is very high we must expect that wave-mechanics would give somewhat different curves. A refinement of the theory does not seem worth while before more extensive and more accurate data are available.

It appears then that hindered rotation and cybotactic grouping are sufficient to explain all deviations from the classical theory. The present theory holds only for nonpolar liquids with axial symmetry, but it can be generalized for more complex molecules. For polar molecules it must be modified.

The writer acknowledges the help of Mr. Jakob Leeder in calculating the Lorentz factors for the hexagonal lattice, and is indebted to Dr. A. F. Turner for illuminating discussions concerning the problems of light scattering.

[47] H. E. McComb, Phys. Rev. **29**, 525 (1909).
[48] From Landolt-Börnstein, II. Erg. bd., Vol. 2.
[49] It is probable that in some liquids, especially near the critical temperature, the temperature coefficient of the Kerr effect should be positive.

The Scattering of Fast Neutrons by Heavy Nuclei

CHARLES H. FAY, *Research Laboratory of Physics, Harvard University, Cambridge, Mass.*

(Received June 27, 1936)

The experimental work of Dunning has shown that for fast neutrons the capture cross sections of heavy nuclei are small compared to their cross sections for elastic scattering. While it cannot be concluded from this that polarization effects (i.e., contributions to the elastic scattering from quasi-stationary states of the nucleus-neutron system) are negligible, it seemed worth while to investigate the results of a treatment neglecting polarization. We use the effective potential for a neutron in the field of a heavy nucleus developed by Van Vleck. The values of the constants of the inter-particle interactions are adjusted slightly from those found by Feenberg from binding energy calculations. The problem reduces to that of a neutron in the field of a potential well whose depth is a slowly varying function of the neutron velocity. The scattering problem is solved by the method of partial cross sections. Anomalous resonances due to the attractive potential are found in the higher partial cross sections. Although these resonances have anomalously high peaks it is shown that on account of their sharpness they contribute little to the cross section for a neutron beam having a broad velocity distribution. The cross section is found to vary markedly with both velocity and atomic number. Even for a broad velocity distribution corresponding to Dunning's experimental source oscillations remain in the cross section as a function of atomic number. However, the existing experimental points fit the curve within the experimental error. That the experimental results are in no case much larger than those given by the theory would perhaps indicate that contributions due to polarization effects are small. Possible experimental work to test the theory is mentioned.

INTRODUCTION

EXPERIMENTAL work on the scattering and absorption of fast neutrons has been carried out by several investigators.[1, 2, 3] Perhaps the most comprehensive investigation of the scattering of fast neutrons has been made by J. R. Dunning and his co-workers. Using as a source the neutrons emitted by the nuclear reaction between beryllium and alpha-particles from radon and its equilibrium products, Dunning has obtained values for the collision cross section of several heavy nuclei. He has shown further that even for nuclei known experimentally to capture fast neutrons, as evidenced by the production of gamma-rays or of artificial radioactivity, the capture cross section is of the order of less than ten percent of the cross section for elastic scattering. The experimental collision cross sections fit a $Z^{\frac{2}{3}}$ law within the experimental error, Z being the atomic number.

It is to be emphasized that we are here interested in fast neutrons, of kinetic energy greater than one-half million electron volts. The experimental results for slow neutrons,[3, 4] or neutrons having approximately thermal velocities, are much more complicated. For these slow neutrons abnormally large collision cross sections are found for certain nuclei. In these cases the cross section for elastic scattering is negligible in comparison with that for neutron capture.

Bohr[5] has shown since the inception of this work that these results can be explained only by consideration of the numerous and closely spaced energy levels of the nucleus. The chance of the neutron giving up some of its kinetic energy to other degrees of freedom of the many-particle system is very good; robbed of most of its velocity, the neutron stays long enough in the nucleus to make the probability of capture large. Breit and Wigner[6] have independently dealt with the considerations discussed by Bohr in more explicit mathematical detail. They consider the effect of a single quasi-stationary level of the combined system of neutron and nucleus which has an energy in the thermal region, and show that it is reasonable that the breadth of the level due to radiation damping is large in comparison to that due to re-emission of a neutron. The ratio of the absorption to the extra scattering due to the level is correspondingly large. Of course the effect is only important near resonance, i.e., when the

[1] Chadwick, Proc. Roy. Soc. **A136**, 702 (1932); **A142**, 1 (1933).
[2] Curie-Joliot, J. de phys. et rad. **4**, 21 (1933); **4**, 278 (1933).
[3] Dunning, Phys. Rev. **45**, 586 (1934); Dunning, Pegram, Fink, and Mitchell, Phys. Rev. **48**, 265 (1935).
[4] Amaldi, d'Agostino, Fermi, Pontecorvo, Rasetti and Segrè, Proc. Roy. Soc. **A149**, 522 (1935).
[5] N. Bohr, Nature **137**, 344 (1936).
[6] Breit and Wigner, Phys. Rev. **49**, 519 (1936).

energy of the system is near that of the quasi-stationary level.

According to Bohr the nucleus plus neutron system has such quasi-stationary levels, more closely spaced than those at thermal energies, in the energy range corresponding to fast neutrons. Here the absorption due to such levels may be small in comparison to the scattering, and it is impossible to conclude from the experimental absence of large absorption that the extra scattering due to the existence of these levels, or, in other language, to polarization effects, may be neglected.

In the light of the above remarks the simple treatment of the problem dealt with in this paper is not to be taken too seriously. The work was well begun, however, before Bohr's paper made clear the possibility of large polarization effects, and it was thought of some interest to complete it. At the present stage of nuclear theory a more refined treatment appears impractical. It should be said that the vices of our treatment are inherent in the use of the statistical model. Its results may be worse than those for binding energy calculations with the statistical model, but only because scattering calculations are generally more sensitive to approximations than energy calculations.

Extension of Van Vleck's Treatment of the Interaction Between a Neutron and a Heavy Nucleus

J. H. Van Vleck[7] has considered the interaction of a neutron and a heavy nucleus on the basis of a statistical treatment of the particles of the nucleus. He employs the types of inter-particle interaction found necessary to the theory of the binding energy of nuclei. Binding energy considerations lead to neutron-proton interaction of the Majorana[8] (exchange) type. The Wigner[9] (ordinary) potential makes the binding energy of heavy nuclei increase too rapidly with atomic weight. Similarly neutron-neutron interaction of the spin coupling type[7] is required; in other language than that of the vector model this corresponds to one part Wigner to two parts Majorana interaction.[10]

[7] Van Vleck, Phys. Rev. **48**, 367 (1935).
[8] E. Majorana, Zeits. f. Physik **82**, 137 (1933).
[9] Wigner, Phys. Rev. **43**, 252 (1933).
[10] Feenberg and Knipp, Phys. Rev. **48**, 906 (1935).

The complete Hamiltonian is thus of the form

$$H=H_0-(h^2/8\pi^2M)\nabla_n^2+\sum_{j=1}^{Z}J(r_{np_j})P^M(n,p_j)+\sum_{i=1}^{N}N(r_{nn_i})\mathbf{s}_n\cdot\mathbf{s}_{n_i}, \quad (1)$$

where H_0 is the nuclear Hamiltonian, M is the mass of the neutron (or more properly the reduced mass of neutron and nucleus if the origin of coordinates is chosen as the center of gravity of the nucleus), $J(r_{np_j})P^M(n,p_j)$ is the Majorana interaction between the neutron and the jth nuclear proton, and $N(r_{nn_i})\mathbf{s}_n\cdot\mathbf{s}_{n_i}$ is the interaction between the neutron and the ith nuclear neutron. $P^M(n,p_j)$ is the Majorana exchange operator permuting the coordinates of the neutron and the jth proton, $\mathbf{s}_{n_i}$ is the vector spin matrix for the ith nuclear neutron, Z is the atomic number, and N the number of neutrons in the nucleus. H_0 of course contains terms similar to the last two in Eq. (1), so that the Hamiltonian is symmetric in the neutrons.

We shall neglect nuclear neutrons not in closed shells, so that the last term of Eq. (1) will not contribute directly to a self-consistent field effective potential. However, when exchange is taken into account it does enter. From the Dirac vector model,[11] which shows that the exchange effect for identical particles a and b is formally equivalent to insertion of a spin coupling factor $-(\frac{1}{2})(1+4\mathbf{s}_a\cdot\mathbf{s}_b)$, the exchange potential due to neutron exchange is here

$$-\sum_{i=1}^{N}(1/2)P^M(n,n_i)(1+4\mathbf{s}_n\cdot\mathbf{s}_{n_i})N(r_{nn_i})\mathbf{s}_n\cdot\mathbf{s}_{n_i},$$

or

$$-\sum_{i=1}^{N}(3/8-(1/2)\mathbf{s}_n\cdot\mathbf{s}_{n_i})N(r_{nn_i})P^M(n,n_i),$$

in virtue of the matrix identity $16(\mathbf{s}_a\cdot\mathbf{s}_b)^2+8\mathbf{s}_a\cdot\mathbf{s}_b-3=0$. Thus the Hartree-Fock equation satisfied by an approximate one-particle wave function for the neutron is

$$\begin{aligned}-(h^2/8\pi^2M)\nabla_n^2\psi(\mathbf{x}_n)+\sum_{j=1}^{Z}\int\int\int\varphi_j^*(\mathbf{x}_p)\\ \times J(r_{np})\varphi_j(\mathbf{x}_n)\psi(\mathbf{x}_p)d\tau_p\\ -(3/8)\sum_{i=1}^{N}\int\int\int\psi_i^*(\mathbf{x}_{n_n})N(r_{nn_n})\\ \times\psi_i(\mathbf{x}_n)\psi(\mathbf{x}_{n_n})d\tau_{n_n}=W\psi(\mathbf{x}_n),\end{aligned} \quad (2)$$

[11] Cf. Van Vleck, Phys. Rev. **45**, 405 (1934).

where $\varphi_j(\mathbf{x})$, $\psi_i(\mathbf{x})$ are one-particle wave functions for the jth proton and ith nuclear neutron respectively, and W is the kinetic energy of the free neutron.

We need an approximate expression for

$$\sum_{j=1}^{Z} \varphi_j^*(\mathbf{x}_p)\varphi_j(\mathbf{x}_n),$$

the Dirac density matrix[12] for the protons in the nucleus. This may be obtained by supposing that phase space is as full as permitted by the Pauli principle within the volume $r<R$, $p<P$, and empty elsewhere. Necessarily $(4\pi/3)^2P^3R^3=Zh^3/2$. We assume further that the proton wave functions are adequately represented locally by plane waves, that is, that the local momentum does not vary too rapidly with position within the nucleus, and that all momenta $p<P$ are equally probable. Then

$$\sum_{j=1}^{Z} \varphi_j^*(\mathbf{x}_p)\varphi_j(\mathbf{x}_n) \doteq (2/h^3)\int\int\int_p \exp\left[(2\pi i/h)(\mathbf{x}_p-\mathbf{x}_n)\cdot\mathbf{p}\right]d\mathbf{p}, \quad |\mathbf{x}_p+\mathbf{x}_n|/2<R; \quad \doteq 0, \quad |\mathbf{x}_p+\mathbf{x}_n|/2>R,$$

the integration being over a sphere of radius P. This gives

$$\sum_{j=1}^{Z} \varphi_j^*(\mathbf{x}_p)\varphi_j(\mathbf{x}_n) \doteq (\sin k_p r_{np} - k_p r_{np}\cos k_p r_{np})/\pi^2 r_{np}^3, \quad |\mathbf{x}_p+\mathbf{x}_n|/2<R; \quad \doteq 0, \quad |\mathbf{x}_p+\mathbf{x}_n|/2>R, \tag{3}$$

where $k_p=2\pi P/h=(9\pi Z/4R^3)^{\frac{1}{3}}$.

A similar expression holds for

$$\sum_{i=1}^{N} \psi_i^*(\mathbf{x}_{n_n})\psi_i(\mathbf{x}_n),$$

the Dirac density matrix for the nuclear neutrons, with k_p replaced by $k_n=(9\pi N/4R^3)^{\frac{1}{3}}$. It is convenient to assume R the same for both expressions; since N is roughly equal to Z and k_n involves N in a low power a further simplification may be attained by replacing k_n by k_p. With these simplifications our result is what we would have obtained had we considered only neutron-proton interaction with a $J(r)$ equal to $J(r)-3N(r)/8$; Eq. (2) becomes

$$\nabla_n^2\psi(\mathbf{x}_n)+k^2\psi(\mathbf{x}_n)=(8\pi^2M/h^2)\int\int\int[J(r')-(3/8)N(r')][(\sin k_p r'-k_p r'\cos k_p r')/\pi^2 r'^3]\times\psi(\mathbf{x}_n+\mathbf{x}')d\tau', \quad r_n<R; \quad =0, \quad r_n>R, \tag{4}$$

where we have written $k^2=8\pi^2MW/h^2$. In obtaining Eq. (4) we have replaced the conditions on Eq. (3) by the condition that the Dirac density is zero when the neutron is outside the nucleus and has the given value inside, a procedure justified by the small range of the neutron-proton and neutron-neutron interactions in comparison with R. Consideration of edge effects would prove a useless refinement in view of the fact that we have neglected them in obtaining Eq. (3).

We proceed to the problem of solving Eq. (4) for $r_n<R$. It is of the type

$$\nabla^2u(\mathbf{x})+k^2u(\mathbf{x})=\int\int\int f(r')u(\mathbf{x}+\mathbf{x}')d\tau'.$$

Now this apparently troublesome integro-differential equation may be reduced to an ordinary homogeneous differential equation, as Feenberg[13] has very kindly shown. Namely, if we try a plane wave solution, $u=\exp i\mathbf{k}'\cdot\mathbf{x}$, we find it a solution provided

$$-k'^2+k^2=\int\int\int f(r')\exp i\mathbf{k}'\cdot\mathbf{x}'d\tau'.$$

Now on account of the spherical symmetry of $f(r')$ the integral is independent of the direction of the vector $\mathbf{k}'$. Since any solution of $\nabla^2u+k'^2u=0$ can be constructed from plane wave solutions (having of course the same magnitude of $\mathbf{k}'$), this solution is also a solution of the integro-differential equation. Thus we may solve Eq. (4) by solving

$$\nabla^2\psi+k'^2\psi=0, \quad r<R; \quad \nabla^2\psi+k^2\psi=0, \quad r>R, \tag{5}$$

with

$$k'^2=k^2-(8\pi^2M/h^2)\int\int\int(J(r)-3N(r)/8)\times[(\sin k_p r-k_p r\cos k_p r)/\pi^2r^3]\times\exp i\mathbf{k}'\cdot\mathbf{x}d\tau. \tag{6}$$

[12] Dirac, Proc. Camb. Phil. Soc. **26**, 376 (1930).

[13] Private communication to J. H. Van Vleck. Van Vleck had previously obtained the result for an s wave function by explicit calculation, which we extended to p and d functions.

The problem is thus reduced to that of a neutron in the field of a potential well, the depth of the well being a function of the velocity of the neutron on account of the appearance of k' in the integral in Eq. (6).

Feenberg[10] has succeeded in fitting the observed binding energies of light nuclei by taking $J(r)$ and $N(r)$ of the same functional form, $J(r)=A\exp(-\alpha r^2)$, $N(r)=B\exp(-\alpha r^2)$. Integration of Eq. (6) with these gives

$$k'^2=k^2-(8\pi^2M/h^2)(A-3B/8)[E(w_+)-E(w_-)+(4\alpha/\pi k'^2)^{\frac{1}{2}}(\exp(-w_+^2)-\exp(-w_-^2))], \quad (7)$$
$$w_\pm=(k'\pm k_p)/2\alpha^{\frac{1}{2}},$$
$$E(w)=(2/\pi^{\frac{1}{2}})\int_0^w \exp(-x^2)dx.$$

Calculation with (7) shows that the potential well becomes gradually shallower as the neutron velocity is increased, as would be expected from the nature of exchange forces.

Before considering the scattering problem it will be well to examine the numerical magnitudes involved. Feenberg[10] gives as values of A, B, and α best fitting the binding energies of light nuclei

$$A=-74mc^2,\qquad 3B/4=26mc^2,$$
$$\alpha^{-\frac{1}{2}}=2.17\cdot10^{-13}\text{ cm}. \quad (8)$$

We assume the Gamow value $R=7.8\cdot10^{-13}$ cm for Pb and that R is proportional to $Z^{\frac{1}{3}}$. The latter assumption has an extremely important effect; namely, since Z and R enter the expression for k' only in $k_p=(9\pi Z/4R^3)^{\frac{1}{2}}$ the depth of the well is independent of Z, in line with the fact that the binding energy per particle is approximately constant for heavy nuclei. (We neglect the slight variation of reduced mass with Z.) Now from $M=1.670\cdot10^{-24}$ g we find $k=0.220\cdot10^{13}\,(W(\text{MEV}))^{\frac{1}{2}}$ cm^{-1}. Also $k_p=1.069\cdot10^{13}$ cm^{-1}. With these values k' has the value $1.060\cdot10^{13}$ cm^{-1} for $k=0$. We see that even for W as high as 7 MEV (million electron volts) k is considerably less than k', that is, the depth of the potential well is very large (of the order of 24 MEV) compared to the kinetic energy of the neutron. Since 7 MEV is about the upper limit of kinetic energy for the fast neutrons from a beryllium-radon source, these neutrons are not fast in the sense in which one speaks of fast electrons in discussing their scattering by atoms. The Born approximation,[14] so useful in many scattering problems, is inapplicable here. The problem may be solved in terms of known functions by the method of partial cross sections, which though tedious in its computational application leads in our case to resonances no simpler treatment could well be expected to fit.

The Method of Partial Cross Sections

The method of partial cross sections[15] depends on the fact that the wave equation for the motion of a particle in a central field is separable in polar coordinates, possessing particular solutions which are products of functions of the radius and spherical harmonics, in which more complicated solutions may conveniently be expanded. We wish to express a function representing an incoming monochromatic plane wave plus an outgoing radial wave, a reasonable idealization of the usual experimental arrangement for the study of scattering, in terms of these particular solutions. On account of the axial symmetry we shall need only the particular solutions of the form $f_l(r)P_l(\cos\theta)$. Our wave equation is of the form

$$\nabla^2\psi+(k^2-U(r))\psi=0. \quad (9)$$

If $U(r)$ vanishes not less rapidly than $1/r^2$ for large r and behaves no worse than $1/r$ at the origin $f_l(r)$ satisfying the boundary condition at the origin exists and has the asymptotic form $(1/kr)\sin(kr-l\pi/2+\varphi_l)$ for large r. The plane wave $\exp(ikz)=\exp(ikr\cos\theta)$ is an asymptotic solution of Eq. (9) and has the asymptotic expansion

$$\exp(ikr\cos\theta)$$
$$\doteq(1/kr)\sum_{l=0}^{\infty}(i)^l(2l+1)\sin(kr-l\pi/2)P_l(\cos\theta)$$

for large r. We write therefore

[14] See, e.g., Mott and Massey, *The Theory of Atomic Collisions*, Chapter VII.

[15] Cf. Mott and Massey, reference 14, Chapter II.

$$\exp(ikr\cos\theta)+f(\theta)\exp(ikr)/r$$

$$\doteq(1/kr)\sum_{l=0}^{\infty}(i)^l(2l+1)\sin(kr-l\pi/2)P_l(\cos\theta)$$

$$+\sum_{l=0}^{\infty}A_l(2l+1)P_l(\cos\theta)\exp(ikr)/kr \quad (10)$$

$$=(1/kr)\sum_{l=0}^{\infty}B_l(2l+1)\sin(kr-l\pi/2+\varphi_l)P_l(\cos\theta).$$

Equating the coefficients of $\exp(ikr)$ and of $\exp(-ikr)$ gives

$$A_l=\exp(2i\varphi_l)-1,$$

so that

$$f(\theta)=(1/k)\sum_{l=0}^{\infty}(2l+1)(\exp(2i\varphi_l)-1)P_l(\cos\theta). \quad (11)$$

From (11) we have

$$I(\theta)=|f(\theta)|^2=(1/k^2)\sum_{l=0}^{\infty}\sum_{l'=0}^{\infty}(2l+1)(2l'+1) \quad (12)$$
$$\times\sin\varphi_l\sin\varphi_{l'}\cos(\varphi_l-\varphi_{l'})P_l(\cos\theta)P_{l'}(\cos\theta),$$

the scattered current per unit solid angle when the incoming wave is normalized to unit current density. It is seen to be determined by the φ_l's, the so-called phase shifts of the radial functions.

The total cross section Q is obtained by integrating $I(\theta)$ over all directions, and is

$$Q=\sum_{l=0}^{\infty}Q_l=(4\pi/k^2)\sum_{l=0}^{\infty}(2l+1)\sin^2\varphi_l. \quad (13)$$

Physically Q_l may be regarded as the partial cross section due to particles of angular momentum about $(l+\frac{1}{2})h/2\pi$. On this basis one would expect Q_l to be important only when the classical distance of closest approach for particles of the corresponding angular momentum is such that the particle classically traverses regions where $U(r)$ is appreciable. This is not quite true, however; in the case of an attractive potential, such as we must consider, there may be three classical turning points (radii), with virtual states similar to those met with in the theory of radioactive decay and corresponding sharp high resonances which we may refer to as anomalous for want of a better term. These anomalous resonances complicate our problem, but on account of their sharpness contribute little to the cross section for a neutron beam having a broad distribution of velocities.

Solution of Problem of Scattering by a Potential Well

We now proceed to obtain an expression for the phase shifts of the radial solutions of (5). Inside the well the lth radial function is

$$f_l(r)=c_1r^{-\frac{1}{2}}J_{l+\frac{1}{2}}(k'r);$$

outside we have

$$f_l(r)=c_2r^{-\frac{1}{2}}[\cos\varphi_lJ_{l+\frac{1}{2}}(kr)$$
$$+(-1)^l\sin\varphi_lJ_{-l-\frac{1}{2}}(kr)].$$

From the continuity of $f_l(r)$ and of its first derivative at $r=R$ we find

$$\tan\varphi_l=-(-1)^l\frac{k'J'_{l+\frac{1}{2}}(k'R)J_{l+\frac{1}{2}}(kR)-kJ'_{l+\frac{1}{2}}(kR)J_{l+\frac{1}{2}}(k'R)}{k'J'_{l+\frac{1}{2}}(k'R)J_{-l-\frac{1}{2}}(kR)-kJ'_{-l-\frac{1}{2}}(kR)J_{l+\frac{1}{2}}(k'R)}. \quad (14)$$

This may be reduced to a more convenient form by eliminating the derivatives by means of the recurrence formulas satisfied by the Bessel functions, with the final result

$$\tan\varphi_l=\frac{J_{l-\frac{1}{2}}(kR)J_{l+3/2}(k'R)-J_{l+3/2}(kR)J_{l-\frac{1}{2}}(k'R)}{(-1)^l[J_{-l+\frac{1}{2}}(kR)J_{l+3/2}(k'R)-J_{-l-3/2}(kR)J_{l-\frac{1}{2}}(k'R)]}, \quad (15)$$

a formula convenient for computation. From Eqs. (13) and (15) it is evident that here Q/R^2 is a function of but two parameters kR and $k'R$. We have computed tables for the evaluation of phase shifts and Q/R^2 for a range of values of these parameters sufficient to cover the values met with in our problem. These tables will be loaned to anyone who desires to use them.

We wish to make an estimate of the area under an anomalous resonance peak of a Q_l/R^2 *versus*

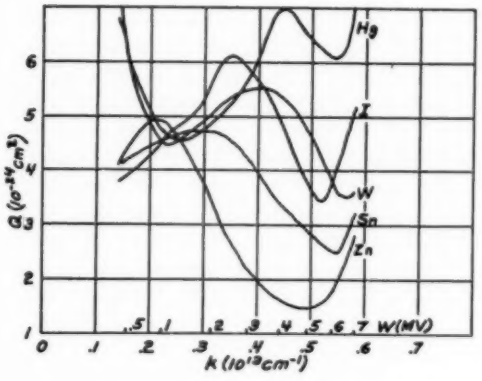

FIG. 1.

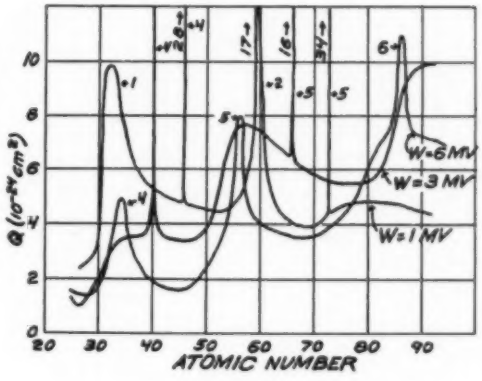

FIG. 2.

kR curve (we do not need to consider the manner of variation of $k'R$ with kR, assuming it constant over the small range involved); this we may do by using the first term of the power series expansions for $J_{l+1}(kR)$ and $J_{-l-1}(kR)$ in Eq. (15), since kR is small in comparison to l for anomalous resonance. It can be shown that

$$\tan\varphi_l \doteq (\mathfrak{R})^{2l+1}/[(2l+1)(1\cdot3\cdot5\cdots(2l-3))^2 \times((\mathfrak{R})^2-(kR)^2)], \quad (16)$$

where $\mathfrak{R}$ is the value of kR for resonance. Thus for $\tan\varphi_l=\pm1$, the points at which the curve has half its peak value,

$$(kR)^2 \doteq (\mathfrak{R})^2 \mp (\mathfrak{R})^{2l+1}/[(2l+1) \times(1\cdot3\cdot5\cdots(2l-3))^2],$$

and the peak breadth at half value is

$$\Delta(kR) \doteq (\mathfrak{R})^{2l}/[(2l+1)(1\cdot3\cdot5\cdots(2l-3))^2], \quad l\geq1.$$

Since the curve is like a $\sin^2$ curve the area under it is approximately this half value breadth times the peak height, or

$$(Q_l/R^2)_{\max}\Delta(kR) \doteq 4\pi(\mathfrak{R})^{2l-2}/[1\cdot3\cdot5\cdots(2l-3)]^2, \quad (17)$$

a result which should be reasonably accurate for $\mathfrak{R}$ small in comparison with l. We see that in spite of the increase of peak height with increasing anomaly (decreasing $\mathfrak{R}$) the breadth decreases more rapidly, so that the area under the peak, that is, the effective contribution to the cross section for a broad distribution of velocities, decreases. It is evident that experimental detection of these anomalous resonances will require a source of neutrons of quite homogeneous velocity.

RESULTS

It was found that the best fit with the experimental data was obtained by increasing $|A-3B/8|$ of Eq. (8) by five percent; a suitable adjustment in R would have served about as well. k' is raised from $1.060\cdot10^{13}$ cm^{-1} to $1.074\cdot10^{13}$ cm^{-1} for $k=0$, or less than two percent, by this change.

Behavior of cross section with velocity. Fig. 1 illustrates the variation of cross section with neutron velocity for several elements. Although the constants are such for these elements that no highly anomalous peaks appear, the curves do show important resonances. The cross section varies so much with velocity that the effect ought to be experimentally detectable by the use of some other source than beryllium-radon, having a sufficiently different velocity distribution to lead to a measurably different cross section. It is hoped that such work will soon be undertaken by those having the necessary facilities. Of course a homogeneous source would be ideal, but its experimental realization involves difficulties not readily surmounted. It is possible that the neutron beam from beryllium bombarded with deuterons or from deuterium bombarded with deuterons may prove sufficiently homogeneous to allow the detection of narrow resonances.

Variation of cross section with atomic number. Fig. 2 indicates the behavior of the cross section

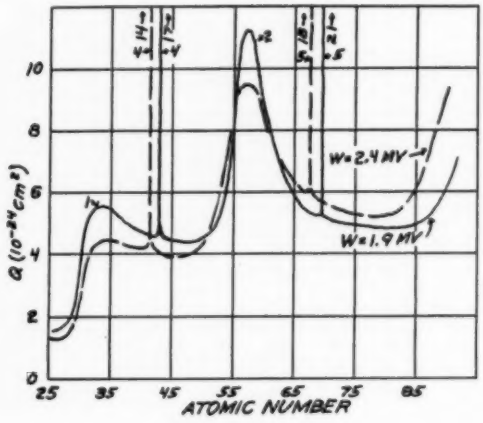

FIG. 3.

as a function of atomic number for neutron energies of 1, 3, and 6 MEV. Here of course anomalous resonances appear. The partial cross sections giving rise to the more prominent resonances are indicated, as are the heights of those peaks lying off the scale.

The most promising sources of homogeneous neutron beams give neutrons of kinetic energy around 2 MEV. Fig. 3 shows cross section as a function of atomic number for 1.86 MEV and for 2.39 MEV neutrons. It indicates what is to be expected on the basis of this theory for experimentally obtainable sources of homogeneous neutron beams, such as deuterium bombarded by deuterons.

It is evident from Figs. 2 and 3 that the cross section does not even begin to approximate a Z^4 law for any single value of neutron velocity. It would be desirable to attempt to locate some of the more anomalous peaks with a highly homogeneous neutron beam, as from their relative locations one could infer much concerning the importance of edge effects. Consideration of these in the theory would not change the nature of the resonances, but would alter their relative positions.

Results for Dunning's experimental velocity distribution. Dunning, by measuring the ranges of protons projected by neutrons from his source, has given us a fair idea of the velocity distribution of berylliium-radon neutrons. He suggests[16] a distribution of the general nature shown in Fig. 4. With this distribution we find a behavior of cross section with atomic number shown by Fig. 5. It is seen that the broader resonances indicated in Figs. 2 and 3 persist in the averaging process. The peak around $Z=34$ can be identified with resonance in the first partial cross section. The low at $Z=45$ is near the vanishing of the first partial cross section. Resonances in the first and second partial cross sections give the peak at $Z=60$. On the high velocity end the fourth partial cross section contributes somewhat to the peak at $Z=34$ and the fifth to the peak at $Z=60$.

The crosses on Fig. 5 indicate Dunning's experimental results for Cu, Zn, Sn, I, W, Hg, and Pb, the only elements in the range given for which he has made measurements with fast neutrons. Except for Cu, the agreement is within the possible experimental error, which he estimates to be about ten percent. However, his relative values are perhaps better than this, so that we are disappointed not to find the decline from Hg to Pb indicated by his results. As may be seen from the 6 MEV curve of Fig. 2, however, the rise we get comes from the high energy end of the distribution, and changes in the assumed distribution curve might reduce or eliminate the discrepancy. We cannot expect good agreement at low Z, so that the bad agreement for Cu should not be taken too seriously. It is unfortunate that Dunning has measured cross sections for slow neutrons for many elements lying at the interesting portions of our curve without investigating their cross sections for fast neutrons.

Comparison with constant depth well. It is of some interest to inquire how the scattering by the well of depth a function of the velocity com-

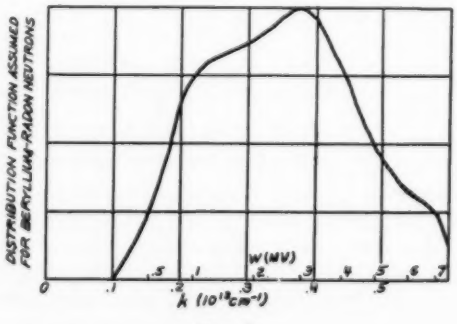

FIG. 4.

[16] I am indebted to Professor Dunning for an interesting conversation on this point.

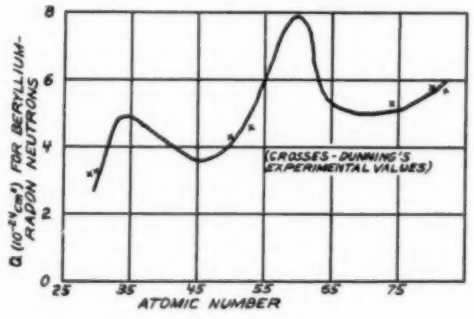

FIG. 5.

pares with a constant depth potential well. The essential difference between the two lies in the fact that k' varies more slowly with k for our well than for the constant depth well. This has the effect of making the cross section vary more slowly with velocity; resonances are broader for the well of varying depth. For this reason the results given by the constant depth well for our velocity distribution will show less oscillation with atomic number than our curve. At present there is no experimental reason for choosing one as preferable to the other, as the experimental points can be fitted equally well with the constant depth hole.

Importance of small angle scattering. The experimental work of Dunning does not measure scattering through angles of less than about 7°. The question suggested itself that possibly the theory might give such a large small angle scattering, particularly near resonances in the higher partial cross sections, that it would be necessary to take this into account in making comparisons with the experimental results. Calculation in a special case revealed that while the small angle scattering was of the order of four times the average, the contribution to the total cross section could be neglected on account of the small solid angle of the 7° cone, about 0.3 percent of the total solid angle.

Nature of polarization corrections. The experimental cross sections for fast neutron scattering are in no case much larger than those given by our theory. We may be justified in concluding from this that polarization effects are small. Contributions to the cross section from polarization may be expected simply to add to the total cross section, although it is possible that interference (nonorthogonality) is important.

It is possible to see in a general way the effect of quasi-stationary levels of the nucleus-neutron system. We should expect sharp resonances in the cross section corresponding to these levels, so that the behavior of the cross section as a function of velocity or as a function of atomic number for a homogeneous beam would be considerably more complicated. On the other hand, it is possible that the cross section as a function of atomic number for a broad velocity distribution might vary more smoothly than our result indicates, on account of the great number of resonances to be averaged over. In any event we believe that further experimental work on fast neutron scattering, a field somewhat neglected since the discovery of the exciting properties of slow neutrons, should yield results both interesting and important.

In conclusion I wish to thank Professor Van Vleck for his helpful interest in the problem.

Note on the Analysis of Photoelectric Data

ROBERT J. CASHMAN AND NOEL C. JAMISON, *Department of Physics, Northwestern University, Evanston, Illinois*
(Received July 6, 1936)

IN the development of Fowler's[1] method for the determination of photoelectric work functions, the assumption is made that "the photoelectric current I *per quantum* of light absorbed is proportional to N_B" where N_B is the number of available electrons. It has been customary, however, to plot current *per unit intensity* of incident radiation assuming a constant optical reflection coefficient; also the term $(W_a-h\nu)^{-\frac{1}{2}}$ has been assumed constant.

We have made comparisons of different methods of plotting, using data on Ba taken in this laboratory for the purpose of determining the temperature coefficient of the work function. Assuming the constancy of the terms mentioned above, a plot of current per unit intensity is shown in Fig. 1, curve A; curve B shows electrons/incident quantum plotted as ordinate. In curve C the quantity $(W_a-h\nu)^{\frac{1}{2}}\times$electrons per incident quantum is plotted as ordinate. The optical reflection coefficient varies so little over the range of frequencies used that one cannot distinguish between the fits to the theoretical curve in plots of electrons per incident quantum and electrons per absorbed quantum. It would appear from the figure that the experimental data fit the theoretical curve about equally well in the three cases. However, careful examination of large scale plots for different sets of data indicates that the least accurate fit is obtained for the plots of electrons per quantum.

According to Fowler's theory, curve C would yield the true work function. The restriction that W_a be known is not a serious one, since a change as large as 25 percent affects appreciably neither the fit nor the value of φ obtained. The value of W_a used for curve C was computed on the basis of two free electrons per atom. Waterman and Henshaw's[2] extension to Fowler's analysis was applied to the problem. Plotting electrons per quantum, the fit to their theoretical curve was as good as for curve C and the work function so obtained was the same as that found from curve C.

The values of the work functions obtained from the three curves given would necessarily be slightly different. In spite of the excellent fit to curve A, the accurate determination of work functions from such plots is not justified by existing theories. Curve B has, as a theoretical basis, DuBridge's[3] modification of Fowler's theory since his development does not yield the factor $(W_a-h\nu)^{-\frac{1}{2}}$. Should further work show conclusively that electron-per-quantum plots do not fit Fowler's curve accurately, the deviations might well be absorbed by the proportionality constant α, which DuBridge assumed to be essentially constant.

DuBridge has interpreted the proportionality factor α as "the fraction of the number of electrons which come up to unit area of surface in one second which absorb a quantum of energy when the incident light intensity is unity,"[3] or "the probability that an electron at the surface of the metal will absorb a quantum and appear outside as a photoelectron."[4] The experimental value of α for Ba based on this interpretation is 4.3×10^{-33} cm^2 sec. quantum^{-1}. Simple theoretical considerations[3] show that the optimum value of α, assuming two electrons per atom is 1.4×10^{-30}. The ratio of the α's 1/325, equals the ratio of experimental to maximum current possible according to this theory.

Fowler attached no significance to the constant of proportionality appearing in the expression for the current; however, it may be interpreted in a manner analogous to the interpretation of α. Writing Fowler's equation as

$$I=\beta\frac{\text{constant}}{(W_a-h\nu)^{\frac{1}{2}}}T^2\varphi(x),$$

where I is in electrons per quantum, β may be defined as the fraction of the number of available electrons per unit volume which will be emitted due to one incident quantum, or the probability that an available electron in unit volume of the

[1] R. H. Fowler, Phys. Rev. **38**, 45 (1931).
[2] Waterman and Henshaw, Phys. Rev. **44**, 59 (1933).
[3] L. A. DuBridge, *Actualités Scientifiques et Industrielles*, No. 268 (Paris, 1935).
[4] Marvin M. Mann and Lee A. DuBridge, Bull. Am. Phys. Soc. **11**, No. 4, Paper 24.

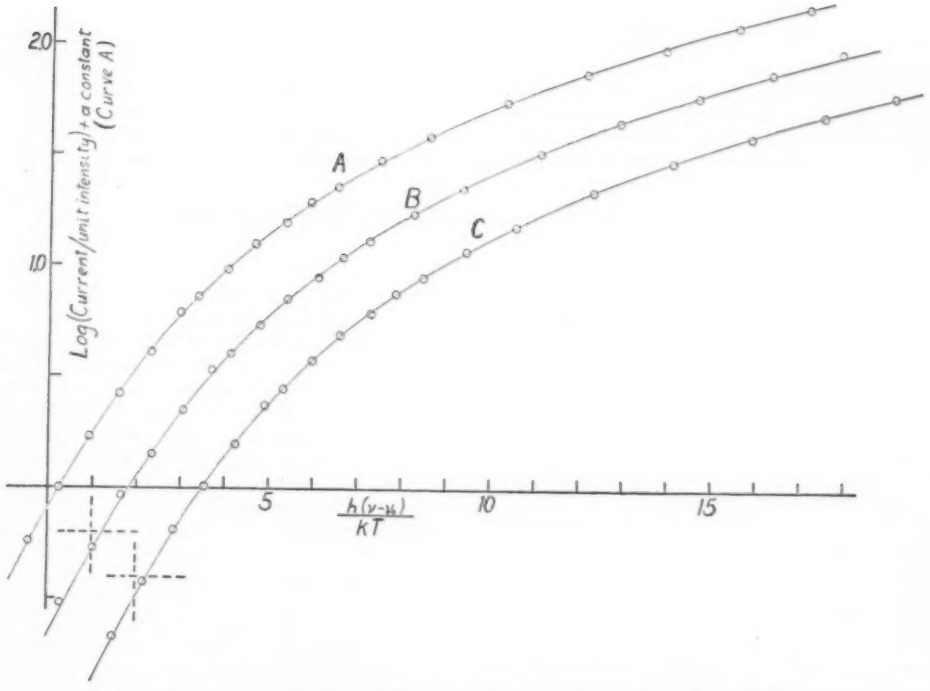

FIG. 1. Curve A: ordinates, current/unit intensity; horizontal shift, 98.58; $\varphi = 2.508$ volts. Curve B: ordinates, electrons/quantum; horizontal shift 98.85; $\varphi = 2.515$ v. Curve C: ordinates $(W_0 - h\nu)^{\frac{1}{2}} \times$electrons/quantum; horizontal shift, 98.65; $\varphi = 2.519$ v. Full lines, Fowler's theoretical curve.

metal will absorb a quantum and appear outside as a photoelectron. The experimental value of the constant β obtained for Ba was 5.0×10^{-25} cm^3 quantum^{-1}. The value of β computed on the basis of Waterman and Henshaw's analysis differs inappreciably.

A theoretical limiting value of β may be found by assuming that one electron is emitted per quantum and that the number of available electrons is equal to 1/2 the total number n of free electrons. The latter assumption is made because, according to Fowler's theory, all the energy of the absorbed quantum is added to the kinetic energy normal to the surface and but half the electrons have outward normal components. Hence

$$1 \text{ electron/quantum} = \beta e n/2.$$

Assuming two electrons per atom β becomes 6.0×10^{-23} cm^3 quantum^{-1}. The ratio of the β's 1/120, is the ratio of experimental to theoretical maximum current. Since the probability β (or α) depends on the probability of absorption, the probability of electron transmission and on the number of available electrons, at least a part of this discrepancy may be attributed to a lack of total absorption of light in that region in which photoelectrons originate.

LETTERS TO THE EDITOR

Prompt publication of brief reports of important discoveries in physics may be secured by addressing them to this department. Closing dates for this department are, for the first issue of the month, the eighteenth of the preceding month, for the second issue, the third of the month. The Board of Editors does not hold itself responsible for the opinions expressed by the correspondents.

Communications should not in general exceed 600 words in length.

A Method for the Determination of Absorption Cross Sections for Thermal Neutrons

The determination of the coefficient of back scattering of slow neutrons (absorbed by cadmium) from a thick layer enables one to calculate the ratio of the scattering and absorption cross sections, σ_s and σ_a, of the back scatterer. As the total cross section ($\sigma=\sigma_s+\sigma_a$) can be measured by direct methods, the back scattering cross section can be used to determine the absorption cross section. If the fraction of neutrons scattered backwards is denoted by S, the following relation can be derived:[1]

$$S=\frac{2\sigma_a+\sigma_s}{\sigma_s}-\left(\left(\frac{2\sigma_a+\sigma_s}{\sigma_s}\right)^2-1\right)^{\frac{1}{2}}.$$

A convenient way of measuring this back scattering consists in immersing a detector foil in a liquid and comparing the activity caused by the neutrons for the bare foil with that when the neutrons have been screened on one side, in each case subtracting the activity when the foil is screened on both sides by cadmium. The ratio R of these two activities is given by $R=2/(1-S)$, from which follows the simple equation: $(R-1)^2=\sigma/\sigma_a$. For large values of R this result becomes identical with an expression given by Amaldi and Fermi,[2] but in most cases it is not permissible to neglect the term -1 with respect to R.

In actual experiment a correction must be made for the absorption in the foil. If a fraction α is absorbed, the measured ratio is not R, but R', which is given by

$$R'=\frac{2}{1-S(1-\alpha)}, \quad \text{whence} \quad R=\frac{R'(1-\alpha)}{1-1/2\alpha R'}.$$

The cross sections occurring in these formulae are the weighted mean cross sections of the various atomic constituents in the scatterer. By varying the chemical composition of the scatterer, and especially by studying solutions and liquid or powder mixtures of various relative concentrations, it should be possible to obtain information concerning the cross sections of the different atoms. In fact, this method of mixtures, in principle, offers the possibility of determining the ratios of any two of the cross sections for scattering, capture, or collision of any of the individual atoms in the mixture. Hence, data obtained in this way, taken together with the accurate directly determined value of just one particular cross section, should permit the calculation of the absolute values of all the individual cross sections involved.

For example, if R is measured for a very dilute solution of a cadmium salt, the total cross section will hardly be different from that of water, as it is primarily due to the large hydrogen scattering. A change in R will then be due to the change in the mean capture cross section caused by the presence of the cadmium. We have performed some preliminary experiments with several liquids and solutions. In the case of a cadmium solution an effect of the correct order of magnitude was observed. Since these measurements have so far been made with a very weak source, we have not yet obtained accurate quantitative results, but the method promises to give results of considerably higher accuracy than that thus far obtained.

The experimental arrangement was as follows: A radon-beryllium source was placed at the center of a large cylindrical tank of water. A glass cylinder of 8 cm diameter was placed with its axis about 8 cm from the source and filled with the liquid or solution to be investigated. The silver detector foil was placed in a plane passing through the source, in order to have a symmetrical arrangement as regards irradiation of the foil from both sides.

In these preliminary experiments we used as detectors silver foils of 0.148 g/cm², for which α should be equal to or less than 0.10 as based on the calculations of Amaldi and Fermi. The foil was activated for two minutes. The value of R obtained in water was 7.3 ± 0.4, which is considerably less than the value $R=11$, given by Amaldi and Fermi. They used a thinner foil, placed in a plane perpendicular to a radial line from the source and activated it only one minute. We have not yet found the cause of this discrepancy.

This work is being carried out with support from the Rackham Fund of the Graduate School. We are also indebted to the Saskatchewan Cancer Commission for the radon used in these experiments, and especially to Mr. G. Wrenshall who prepared the sources.

C. T. ZAHN
E. L. HARRINGTON
S. GOUDSMIT

Department of Physics,
University of Michigan,
August 21, 1936.

[1] D. L. Bayley, B. R. Curtis, E. R. Gaerttner and S. Goudsmit, Phys. Rev. **50**, 461 (1936).
[2] E. Amaldi and E. Fermi, Ricerca Scient. **7**, 3 (1936).

The Scattering of Gamma-Rays

The experiments described by the writer in these pages some time ago[1] have been extended. The apparatus has been modified so that a single gamma-ray counter and a single electron counter are used. Figs. 1 and 2 show the relation of the scatterer and the counting tubes used in the experiments. The gamma-ray counter G has a copper wall of sufficient thickness to absorb the recoil electrons coming from the paraffin scatterer. The electron counter R has very thin walls which allow the recoil electrons to enter easily.

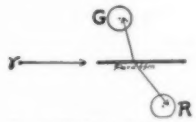

FIG. 1. Position of gamma-ray and recoil electron counters for cases A and B.

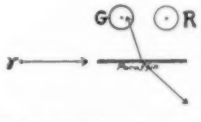

FIG. 2. Position of gamma-ray and recoil electron counters for cases C and D.

The thickness of the scatterer (paraffin $4\times1\times0.05$ cm) was such that the recoil electrons in emerging from anywhere save near its edge would suffer multiple scattering. Thus the angular positions of the counters were not especially critical. The inhomogeneity of the gamma-ray source used (84 mc of Ra C) would also tend to make the exact positions of the counters uncritical.

Observations were made with the counters in the two positions shown. In each case readings were taken both with the paraffin in place and removed. The experiment was carried on in a vacuum drum to eliminate scattering by the air. The results were as follows:

A Position 1 with scatterer in place Rate $=69.1\pm5.4$ hr.$^{-1}$
B Position 1 with scatterer removed Rate $=10.7\pm4.4$ hr.$^{-1}$
C Position 2 with scatterer in place Rate $=10.1\pm5.0$ hr.$^{-1}$
D Position 2 with scatterer removed Rate $=12.5\pm5.6$ hr.$^{-1}$

In cases C and D where both counters are on the same side of the scatterer no coincidences would be expected except between gamma-rays and associated recoil electrons which had suffered a deflection of approximately 180°; but the thickness of the scatterer is such that the great majority of these must be absorbed. The observations show that within the experimental uncertainty no increase in the coincidence rate results from the introduction of the scatterer.

The results A and B obtained with the arrangement shown in Fig. 1, however, show a decided increase in the recorded coincidences when the paraffin is introduced, indicating that there is a coincidence in time between the appearance of a recoil electron and the scattered gamma-ray which liberated it.

The residual coincidence rate of about 10 hr.$^{-1}$ is due to the finite resolving time of the circuit and to cosmic-ray showers.

ROBERT S. SHANKLAND

Case School of Applied Science,
Cleveland, Ohio,
August 24, 1936.

[1] R. S. Shankland Phys. Rev. **49**, 8 (1936).

Behavior of Slow Neutrons at Different Temperatures

In the study of slow neutrons the reflection coefficient of hydrogenated substances for thermal neutrons plays an important part because it gives information on the average number of collisions N occurring before the neutron is captured. The reflection coefficient, called the "albedo" by Amaldi and Fermi,[1] can be calculated[2] under the assumption of isotropic scattering of the neutrons at every collision and is given by

$$\beta=(\sqrt{N}-1)/(\sqrt{N}+1)=1-2/\sqrt{N}+\cdots \qquad (1)$$

(N is of the order of magnitude of 100). The quantity N is connected with the mean free path λ of the neutrons in paraffin, their mean life τ in paraffin and their mean velocity v, by the equation

$$N=v\tau/\lambda.$$

Assuming τ and λ to be independent of the velocity, as one would expect for neutron energies very small compared with the vibrational energy $h\nu$ of the hydrogen atom in paraffin, the albedo should decrease with temperature because v varies as $\sqrt{T}$.

We performed some experiments to measure β in paraffin at liquid-air temperature (90°K). The experimental procedure was similar to that used by Amaldi and Fermi.[1] We used two cylindrical paraffin blocks 12 cm in diameter and 10 cm in height. The source was at a distance of 2.5 cm from the detector and was kept at constant temperature by a small Dewar flask. The detectors were silver foils 5×5 cm with a mass of 0.06 g/cm^2 and the cadmium screens had a mass of 0.35 g/cm^2, so that their absorption in the thermal region was a total one. Activities were measured with an ionization chamber and electrometer.

At room temperature we found $\beta=0.82$ and the same result was obtained at liquid-air temperature.

This result shows that the assumptions of isotropic scattering and of constancy of λ and τ are not valid. There may be many reasons for this: first, as was shown by Fermi[2] for thermal neutrons the mean free path λ depends on the ratio $W/h\nu$ of the energy of the neutrons to the quantum of the elastic bond of hydrogen atom in paraffin, in such a way that a decrease of energy gives rise to a decrease of λ. A second fact, which must be considered, is the coherence of the directions of the motion of a thermal neutron before and after an impact, which was neglected in the deduction of (1). This coherence depends also on the ratio $W/h\nu$ and is zero only for $W\ll h\nu$. Both effects are in the sense of increasing the albedo for low temperature.

Though it is now impossible to give a quantitative explanation of the observed fact on account of multiplicity of factors involved, still the experimental result is of interest in connection with the interpretation of experiments on thermal neutrons.

E. AMALDI
E. SEGRÈ

Columbia University,
August 29, 1936.

[1] E. Amaldi and E. Fermi, Ricerca Scient. [7] **1**, 454 (1936).
[2] E. Fermi, Ricerca Scient. [7] **2**, (1936).

Crystalline Symmetry and Shear Constants of Rochelle Salt

The equations[1] for the converse piezoelectric effect in the hemihedric and hemimorphic classes of the orthorhombic system are:

Hemihedric	Hemimorphic
$e_{xx}=e_{yy}=e_{zz}=0$;	$e_{xx}=d_{31}E_z$;
$e_{yz}=d_{14}E_x$;	$e_{yy}=d_{32}E_z$;
$e_{zx}=d_{25}E_y$;	$e_{zz}=d_{33}E_z$;
$e_{xy}=d_{36}E_z$;	$e_{yz}=d_{24}E_y$;
	$e_{zx}=d_{15}E_x$;
	$e_{xy}=0$

(1)

In the hemihedric class alternating electric fields applied along X, Y, or Z can excite, respectively, the yz, zx and xy shear modes of vibration.[2] The situation is quite different in the hemimorphic class. In it longitudinal modes whose major displacements are executed along X, Y or Z may be excited by E_z, while the yz and zx shear modes are excited by E_y and E_x, respectively. Each of the above modes of vibration gives rise to a characteristic interference pattern[3] in the simple interferometer. Hence the above crystal classes are easily differentiated by observing how the amplitude of vibration of the shear or longitudinal modes varies with the direction of the applied field.

Since there has existed some doubt[4] as to whether Rochelle salt is invariably hemihedric, it is desirable to check by independent means the conclusions of Staub[5] from x-ray data. The crystallographic $\bar{a}$, $\bar{b}$ and c axes of Rochelle salt have been identified with X, Y and Z, respectively.

Twelve rectangular Rochelle specimens were studied in the interferometer at frequencies ranging from 20 to 200 kc/sec. Their crystalline symmetry was found to be hemihedric with no transitions to the hemimorphic class in the temperature range from 0 to 40°C. These results confirm those of Staub.

Representative frequency-temperature curves in Fig. 1 show negative temperature coefficients for all three shear modes. All curves show anomalies near 23.5°C (compare with the curves of Davies.[6] These anomalies may consist of discontinuities, points of inflection or the presence of maxima or minima. The presence of the maximum in the curves for the yz and xy shear modes of vibration depended upon the previous thermal and electrical treatment of the crystal. A more detailed study of this effect is being made.

The shear constants c_{44}, c_{55} and c_{66} were evaluated at 22°C from the measured frequencies of the yz, zx and xy shear modes, respectively, by means of the equation[7]

$$F_{ijmn}=\tfrac{1}{2}(C_{ij}/\rho)^{\frac{1}{2}}(m^2/x_i^2+n^2/x_j^2)^{\frac{1}{2}}, \qquad (2)$$

where $C_{23}=c_{44}$; $C_{13}=c_{55}$; $C_{12}=c_{66}$; and ρ was taken as 1.7605 g/cm³.

It was found, however, that (2) is far from accurate in Rochelle salt. The apparent elastic constant thus determined varies parabolically when plotted against the ratio of x_i to x_j. The maximum value of the constant lies at the vertex of the parabola, where $x_i=x_j$. The maximum value of the shear constants so determined are compared below with Mandel's[8] values obtained from static experiments.

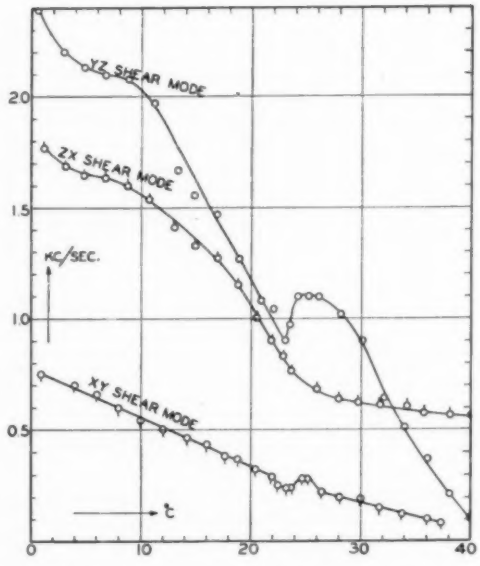

FIG. 1. Variation of frequency of the shear modes with temperature. Change in frequency in kc/sec. as ordinates; temperature in °C as abscissas. Frequency yz shear mode is 168.9 kc/sec. at 1°C, zx shear mode 28.3, xy shear mode 52.8.

	Writers	Mandel
c_{44}	8.72×10^{10} dynes/cm²	16.36×10^{10} dynes/cm²
c_{55}	2.46	3.24
c_{66}	7.95	12.43

The discrepancy between these dynamically and statically determined values is so large that the writers plan to make a redetermination of the static values.

A large coefficient of viscosity,[9] b_{44}, was apparent in the yz shear mode. This was manifested by broad tuning in large plates of the resonant fundamental frequencies. Thus at frequencies of 50 kc/sec. the amplitude of oscillation would remain strong over a frequency range as large as 10 kc/sec. With the application of static electric fields the shift of the interference fringes showed a time constant of more than one minute. The viscosity coefficients b_{55} and b_{66} must be considerably smaller than b_{44}. Evidence indicated that Eq. (2) fails in Rochelle salt partly since it does not take into account viscosity.

The writers wish to express their thanks to the Brush Laboratories for gifts of both cut and uncut Rochelle salt crystals.

R. TASCHEK
H. OSTERBERG

University of Wisconsin,
August 27, 1936.

[1] Voigt, *Lehrbuch der Kristallphysik*, p. 830.
[2] Osterberg and Cookson, Rev. Sci. Inst. **6**, 347 (1935).
[3] Osterberg and Cookson, Rev. Sci. Inst. **6**, 247 (1935).
[4] Valasek, Phys. Rev. **20**, 639 (1922).
[5] Staub, Helv. Phys. Acta **7**, 1 (1934).
[6] Davies, Phil. Mag. **16**, 97 (1933).
[7] Osterberg and Cookson, Phys. Rev. **47**, 781 (1935).
[8] Mandel, Proc. Roy. Soc. **116**, 623 (1927).
[9] Thompson, Phil. Trans. Roy. Soc. London **231**, 365 (1933).

Some Theoretical Considerations on Anomalous Diffraction Gratings

I wish to publish some theoretical considerations about the phenomena shown by certain gratings in the experiments of Wood[1] and Strong.[2] Both consider as a "typical case" the following phenomenon exhibited by their grating *C*. Let us consider the intensity of a continuous spectrum as a function of the increasing wave-length. Then: (a) at certain characteristic wave-lengths (Rayleigh's wave-lengths) the intensity falls nearly to zero and shows a sharp edge; (b) after having been nearly zero for an interval of the order of 100A (dark band), the intensity rises to abnormally high values and shows a bright band without sharp edges.

Part (a) may be explained by Rayleigh-Voigt's theory.[3] I wish to point out that the derivative of that second-order term, which carries the irregularity in the distribution of intensity, becomes infinite for Rayleigh's wave-lengths. Hence a sharp edge in the intensity must be present in every grating, but only the geometrical characteristics determine whether the irregular term is the important one for the intensity, or not.

In connection with part (b) of the phenomenon the following should be noted. (I) A suggestion of Langer related by Wood: Since the position of the bright bands depends upon the optical constants of the metal of the grating, these bands would be connected with that part of the diffracted waves which travels with different velocity along the surface of the grating. (II) Rayleigh's condition for the phenomenon (a) means that the wavelets with velocity *c* diffracted by a groove must reach the neighboring grooves in resonance with the incident wave; similarly when slower waves were diffracted by the grooves, one would expect effects of resonance for larger wave-lengths. (III) Applying the principle of Huygens to the diffraction, we must remember that an oscillator on a metallic surface sends also Sommerfeld's superficial waves,[4] which, to be noted, are polarized with their magnetic vector parallel to the surface, as the anomalously diffracted light.

Starting from these considerations I made an attempt to extend Rayleigh-Voigt's theory, including superficial waves on the grating. This extension is not quite formally satisfactory, but it seems to me to be sufficiently justified. It explains the essential features of the phenomenon (b); the width of the bright bands is due to the absorption of the superficial waves, and their distance from Rayleigh's wave-length depends upon the strong variation of the optical constants with wave-length. Wood's result that a negative image of the bands is found in the spectrum of the regularly refracted light, is easily understood from the point of view of the approximation method.

The theory was checked by a rough numerical evaluation starting from suitable data. In carrying out the calculations it appears clearly that the whole phenomenon of the bands is extremely sensitive to changes of the form of the grating. Hence one has to think that every anomalous grating will show its own type of bands. It follows also that the study of grating *C* was very useful in distinguishing phenomena (a) and (b) which seem to be due to quite different physical mechanisms. I do not think, however, that it will be easy to define the characteristics of a grating showing the same bands as grating *C*. The presence of strong bands seems to be due to accidental relations between the coefficients of Fourier's development of the profile of the grating; one can only say that the presence of narrow grooves or ridges in the profile, that is, a prevalence of high harmonics, is a necessary condition. A detailed account will be published in the *Nuovo Cimento*.

UGO FANO

Istituto Fisico della R. Università,
Rome, Italy,
July 21, 1936.

[1] Wood, Phys. Rev. **48**, 928 (1935).
[2] Strong, Phys. Rev. **49**, 291 (1936).
[3] Lord Rayleigh, Proc. Roy. Soc. **79**, 399 (1907); Voigt, Gött. Nachr. p. 41 (1910).
[4] Sommerfeld, Ann. d. Physik **28**, 665 (1909).

The Paschen-Back Effect—^2S ^2P Multiplets in Strong Fields

In an article published in the *Physical Review* on the Paschen-Back effect of ^2S ^2P multiplets Green and Loring[1] have stated that the fine structure of magnetic triplets in "strong fields" had never been experimentally established, the theory, however, having been expounded long before. The authors then explain how they have studied the phenomena for the 6708 line of Li "in reversal" and managed to resolve the *s* components.

Presumably the authors had not had information about my experimental work on the same subject carried out at the Laboratoire du Grand Electro-aimant de l'Académie des Sciences at Bellevue, under the direction of Professor A. Cotton. Nevertheless the results had been published as early as January 1935 in the *Comptes Rendus Acad. Sci.* and republished in the *Jubilee Book* of Peter Zeeman ('S Gravenhage, Martinus Nijhoff, 1935) in an article by F. Croze and P. Jacquinot.

In this work the 6708 line has been studied up to 44,000 gauss and I stated explicitly that the *s* components are resolved into two sub-components and that, moreover, the components on the short wave side give a larger separation than those on the other. The values of the separation I found are in satisfactory agreement with the values calculated after K. Darwin. The results had been obtained for the Li emission line given by a high frequency tube as described in the two notes previously quoted, and are quite the same as those obtained by Green and Loring in a 38,000-gauss field with the line "in reversal."

It was with great pleasure that I had the opportunity of reading the confirmation of my own experiments in the article by Green and Loring whom I am always personally happy to quote.

P. JACQUINOT

August 31, 1936.

[1] Green and Loring, Phys. Rev. **49**, 630 (1936)

The Nature of Energy States in Solids

Using the methods of quantum mechanics and group theory Van Vleck,[1] Penney and Schlapp[2] and Amelia Frank[3] have developed a theory for the behavior of energy levels of an atom when subjected to the electric fields of other atoms in a crystalline solid. They have treated in detail the hydrated sulphates of neodymium, praseodymium and samarium.

They applied their theory to the experimental results of Gorter and de Haas[4] on the magnetic susceptibility of Pr and Nd salts and were able to reproduce the experimental curves from 14°K to room temperatures. While the agreement here was very good, unfortunately, a number of other discrepancies made their appearance. Thus the potential field constant D in the equation $V=D(x^4+y^4+z^4)$, which one would expect to be very similar for the various rare earths due to their similar chemical and crystallographic properties, is about four times as large for neodymium as for praseodymium. Further, while one would expect Er and Nd to behave somewhat similarly since they have the same spectroscopic term only inverted, the actual susceptibility data are not alike, for the $1/\chi$, T diagram for Er gives almost a straight line while for Nd it is distinctly curved. It should be mentioned, however, that the experimental work of Gorter and de Haas is not in agreement with two room temperature points determined by Zernicke and James,[5] and Cabrara.[6] Finally, the agreement with samarium is extremely poor. Spedding and Bear[7] have also found experimentally at least five low lying levels while the maximum number permitted by theory is two in a cubic field and three in a combined cubic and rhombic field.

In view of these discrepancies I have thought it advisable to study the energy levels of the rare earths spectroscopically. In collaboration with Dr. Nutting and Mr. Hamlin, I have found that the lowest state of neodymium is split into at least three levels with a separation of 76 and 260 cm^{-1} from the lowest state. Theory as applied to the work of Gorter and de Haas demands about 0, 243 and 834. Our work is in definite disagreement with these results. However, if the experimental work of the above authors is disregarded the relative separations are the same as predicted by theory. With our separations most of the discrepancies disappear. The magnetic susceptibilities as calculated from these levels give a $1/\chi$, T diagram which is almost a straight line in good agreement with the experimental work on erbium. Further the calculated susceptibility agrees within experimental error with the room temperature values of Zernicke and James, and Cabrara. Finally the field constant D, being only one-third as big as before is in good agreement with that of praseodymium. The discrepancy in the case of samarium seems to be real and bears out the author's contention that there must be an additional electronic level lying near the basic one in that case.

In exactly the same way that Penney and Schlapp treated neodymium and praseodymium, I have treated erbium and dysprosium using the field constants as determined by Nd after correcting them for the additional screening according to Slater's method and found the basic state of Er^{+++} would be split into five levels separated by 19 cm^{-1}, 38 cm^{-1}, 83 cm^{-1} and 87 cm^{-1} from the basic state.

Nutting and Meehan have advised me by letter that they have observed levels at 0, 19, 41 and 85 cm^{-1}. This agreement is remarkable when one realizes that there are no arbitrary constants involved so that the relative splitting cannot be altered. As there is a slight leeway in the value of the screening constants used, the over-all spreading could be varied slightly and has been chosen to give the best fit. The value used, however, is well within the experimental error of determining screening constants by any other method.

The levels calculated for Dy while of the right order of magnitude were not in good agreement with the experiment, but this is not surprising for the basic state of Dy is the same as that for Sm, except that it is inverted, and if an extra level exists there one would expect it to be present in Dy also and while it would probably be farther away it would still perturb the splitting of the basic state.

The excellent agreement in the case of Nd and Er seems to indicate that Penney and Schlapp's assumption of a cubic field is justified. While the magnetic susceptibility would not be very sensitive to the existence of a rhombic term in the potential energy equation, the splitting of the levels would be extremely sensitive. From our data the rhombic term could not be more than 2 percent of the cubic term as there is absolutely no evidence of the rhombic splitting in our photographs.

From the above results it can be seen that a study of the absorption spectra offers a powerful tool for determining the position, symmetry and distance of the atoms in the first row about the ion being studied. It, therefore, complements x-ray studies in that this method is most powerful in the region where the x-ray measurements are least reliable. It also should give considerable information about the potential and electric fields which exist about an ion in a crystal or in solution.

I wish to thank Dr. Nutting and Mr. Meehan for very generously permitting me to use their values for erbium in advance of publication. I wish also to thank Professor Kirkwood for valuable assistance on the theoretical side of the problem.

This work was carried out under the George Fisher Baker Research Fellowship at Cornell University.

FRANK H. SPEDDING

Cornell University,
Ithaca, New York,
September 3, 1936.

[1] Van Vleck, *The Theory of Electric and Magnetic Susceptibility* (Oxford Press).
[2] Penney and Schlapp, Phys. Rev. **41**, 194 (1932).
[3] Amelia Frank, Phys. Rev. **48**, 765 (1935).
[4] Gorter and de Haas, Leiden Comm. 218*b*.
[5] Zernicke and James, J. Am. Chem. Soc. **48**, 2827 (1926).
[6] Cabrara, Comptes rendus **180**, 669 (1925).
[7] Spedding and Bear, Phys. Rev. **46**, 975 (1934).

On the Chemical Differences Between Nitrogen Isotopes

We wish to report on some preliminary experiments concerning the possibility of a chemical separation of the nitrogen isotopes. Although our work in this field has not yet been completed, a publication by E. Ogawa[1] causes us to publish a short summary of our conclusions at this time.

The analyses were performed with a mass spectrometer in the laboratory of Professor Bleakney in Princeton University as described by Wahl, Huffman and Hipple.[2] As these authors found indications of a small difference in vapor pressure between $N^{14}H_3$ and $N^{15}H_3$ and because distillation, if effective, would be by far the easiest way to obtain a change in the isotope rates, we first experimented on this possibility. We used the method by which Wahl and Urey investigated the vapor pressure ratios in water.[3] Distillations were carried out without boiling at different temperatures, the final residue varying between 1/15 and 1/70 of the amount of starting material. No definite trend of the vapor pressure ratio with temperature could be distinguished. As an average value for the pressure ratio $P(N^{14}H_3) : P(N^{15}H_3)$ we obtained 1.0025 in six experiments, with an average error of 0.003. It may be mentioned that Wahl, Huffman and Hipple give 1.0052 as their best figure for this proportion. It is probable that $N^{14}H_3$ is slightly more volatile than is $N^{15}H_3$, but we feel convinced that the vapor pressure ratio differs from unity only a few tenths of a percent at most. Therefore the nitrogen separation by the distillation of ammonia does not seem promising. Next we investigated the reaction of $N^{15}H_3+N^{14}H_4OH \rightleftarrows N^{14}H_3+N^{15}H_4OH$ for which Wahl, Huffman and Hipple had reported a possible but uncertain concentration of the heavy isotope in the NH_4OH. Purified air was passed through a bottle containing concentrated ammonia till only a small fraction of the original amount of ammonia was left in the solution. From the isotopic composition of the original material and the final sample we calculated the equilibrium constant from the Rayleigh formula. We found that the N^{15} possibly concentrates slightly in the liquid but the effect is so small at any rate, that it could not be recognized with certainty.

Then we turned to the exchange reaction $N^{15}H_3+N^{14}H_4^+ \rightleftarrows N^{14}H_3+N^{15}H_4^+$, already considered by Urey and Greiff.[4] We started from a concentrated solution of ammonium chloride, to which at intervals we added small amounts of sodium hydroxide solution. A current of purified air removed the NH_3 formed after each addition. At the moment we have the analysis of only one run in which we started with 0.61 mole NH_4Cl and finished with 0.052 mole. During this process the ratio of $N^{14}N^{15}$ decreased from 250.2 to 233.8. (These numbers are not corrected for diffuse background and hence the analysis of the original material does not agree with the generally accepted value). This gives for the fractionation factor the value 1.027. We hope to check this value soon with other samples we have prepared, but we have been forced to abandon this matter temporarily because it will not be possible to obtain analyses by the mass spectrometer for some time.

The last experiment described seems to be the same as one performed by Ogawa, an extract of which publication is printed in *Nature*.[5] From the figures given fractionation factors ranging from 1.7 to 1.8 can be calculated which are very much higher than ours. We feel quite certain that as large an increase in concentration of N^{15} could not remain undetected by the mass spectrometer and that Ogawa's values, which are obtained from atomic weight determinations, are too high.

The importance of finding the most favorable reaction is clearly seen from the calculations by Urey and Greiff on the efficiency of a column as depending on the separating factor of the process used.

Finally, it may be mentioned that a preliminary experiment on the exchange $HCN^{15}+CN^{14-} \rightleftarrows HCN^{14}+CN^{15-}$ indicated that N^{15} was concentrated in the HCN gas to quite an appreciable extent.

We are indebted to Dr. W. W. Lozier for the analyses made for this work, and also to the E. K. Adam's Fellowship Fund for a stipend for one of us (A. H. W. A.).

H. C. Urey
A. H. W. Aten, Jr.

Department of Chemistry,
Columbia University,
New York, N. Y.

[1] E. Ogawa, Bull. Chem. Soc. Japan **2**, 428 (1936).
[2] Wahl, Huffman and Hipple, J. Chem. Phys. **3**, 434 (1935).
[3] Wahl and Urey, J. Chem. Phys. **3**, 411 (1935).
[4] Greiff, J. Am. Chem. Soc. **57**, 321 (1935).
[5] E. Ogawa, Nature **138**, 294 (1936).

Effect of Hydrocarbons at Low Temperatures on Slow Neutrons

Investigations of the properties of slow neutrons passed through paraffin at various temperatures have established the fact that temperature equilibrium must be attained at least partially.[1–5] The somewhat remarkable character of this fact, considering the size of the energy losses and the probable mechanisms involved led the authors to investigate the phenomenon in more detail, first with paraffin and later with pure normal heptane.

The apparatus used is shown in Fig. 1. It consists of a metal Dewar (brass and monel metal walls 1 mm thick) surrounded by a large cylindrical block of paraffin in which the radon-beryllium neutron source (100–220 millicuries) was imbedded. The inside diameter of the Dewar was 14 cm and the height one meter. A soft glass Dewar (3 cm outside diameter) was mounted along the axis of the metal Dewar, to allow irradiation of the cylindrical silver targets without alteration of the temperature of the hydrocarbon. The cylindrical copper container shown was used for the heptane only, and was the same length as the silver targets (11 cm), and 4.5 cm thick, with a wall thickness of 0.3 mm. Copper-constantan thermocouples were

Table I.

Thickness of paraffin cylinder	Temperature (°K)	Activity (% 300°K activity)
1.5	300°–200°	100 ± 2
	100°– 11°	113 ± 2
2.5	70°	94 ± 2
	21°	86 ± 2
3.5	90°	103 ± 2
	55°	71 ± 2

soldered to the top and bottom of the container to measure the temperature of the hydrocarbon. The targets were silver cylinders 13 mm in diameter, 11 cm long, and 0.25 mm thick, which could be slipped tightly over the thin wall tube counter used for measuring the activities. In the work with paraffin, the copper container for the heptane was removed and replaced by cylinders of paraffin of different thicknesses.

The procedure was to cool the contents of the Dewar to 20°K by keeping liquid hydrogen around the container for approximately 20 minutes. The hydrogen was then allowed to boil away and readings were taken when the temperature of the hydrocarbon had risen to 25°K, thus insuring the absence of any liquid hydrogen in the Dewar. Readings of the silver activities were taken continuously, as the Dewar warmed, over a period of eighteen hours. The results for normal heptane are shown in Fig. 2 in which the circles show the measured activity (140 seconds period). The solid curve was calculated from the equation

$$A = \delta e^{-\gamma T^{-\frac{1}{2}}}(1 - e^{-\eta T^{-\frac{1}{2}}}),$$

in which A is the silver activity, δ, γ and η are constants, and T is the absolute temperature of the hydrocarbon. The assumptions on which the equation is based are (a) that the neutrons are at the temperature of the hydrocarbon, (b) that the proton capture cross section is proportional to the reciprocal of the neutron velocity, and (c) that the silver capture cross section obeys the same law. The constant η is evaluated from the thickness of the silver targets and the cross section, 36×10^{-24} cm², from the data of Amaldi and Fermi[6] for the capture by silver of the neutrons

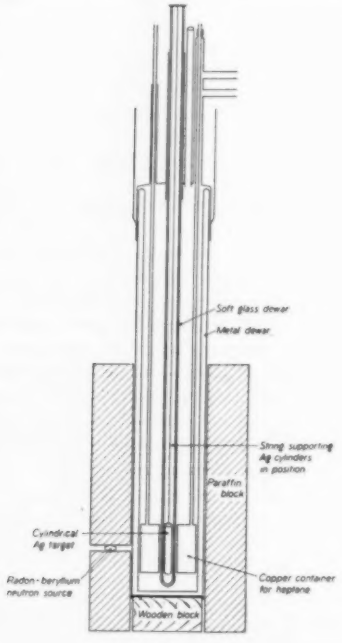

FIG. 1.

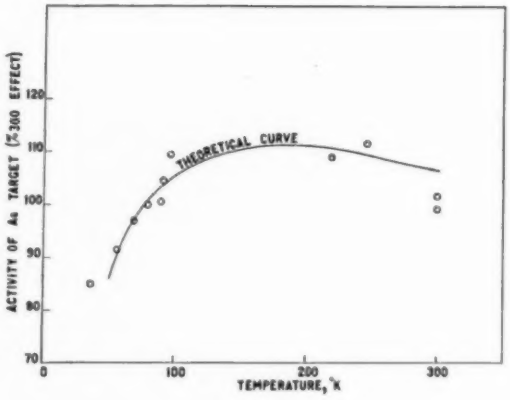

FIG. 2.

exciting the 140 seconds silver activity. The data seem to be in essential agreement with these assumptions.

The data obtained in some preliminary work with paraffin cylinders, are presented in Table I.

The 1.5 cm cylinder caused an increase in the activity, which appeared between 200° and 100°, and was relatively constant from 100° down to liquid helium temperatures (4°K); the 2.5 cm cylinder showed a small decrease, slightly dependent on temperature at 70° and below; and the 3.5 cm cylinder showed a rapid decrease between 90° and 60°. Though none of these results were obtained over as wide a range of temperatures as those for the heptane, they are all in agreement with the heptane results, and the assumptions listed above.

All of the above results apply to the thermal neutrons (those absorbed by 0.3 mm Cd) which excite the 140 seconds silver activity. A series of experiments with a 0.3 mm thick cadmium shield around the silver targets showed that at least 92 percent of the activity disappeared on interposition of the cadmium shield, roughly independent of the temperature (20°–300°K) of the surrounding hydrocarbon cylinder. The activity with the cadmium shield interposed was too small to measure accurately. This large cadmium absorption effect may be connected with the fact that the majority of the neutrons pass through approximately 2 mm of soft glass and 2 mm of brass and monel metal before striking the target.

The authors wish to express their gratitude to Professor G. N. Lewis for his invaluable advice and criticism, and to Mr. J. W. Stout for the preparation of several liters of liquid helium.

W. F. LIBBY
EARL A. LONG

Department of Chemistry,
University of California,
Berkeley, California,
September 3, 1936.

[1] Dunning, Pegram, Mitchell and Fink, Phys. Rev. **47**, 888 (1935).
[2] Moon and Tillman, Nature **135**, 904 (1935).
[3] Dunning, Pegram, Fink, Mitchell and Segrè, Phys. Rev. **48**, 704 (1935).
[4] Westcott and Niewodniczanski, Proc. Camb. Phil. Soc. **31**, 617 (1935).
[5] Moon and Tillman, Proc. Roy. Soc. **A153**, 476 (1936).
[6] Amaldi and Fermi, Ricerca Scient. [VI], **2**, 344 (1935).

Bond Effect in the Action of Protons on Neutrons

The marked ability of protons bound in hydrocarbons to slow neutrons down to thermal equilibrium with the hydrocarbon, as indicated in the preceding letter and earlier work[1–5] induced the authors to undertake a systematic investigation of different types of hydrogenous molecules to discover any dependence of this phenomenon upon the character of the molecule and the bond. The experiments with liquid hydrogen here described reveal the existence of a remarkable difference between the H_2 molecule and the hydrocarbons.

The apparatus used is shown in Fig. 1 of the preceding communication with the exception that the copper container used for the heptane was removed, leaving the space between the inner soft glass Dewar and the outer metal Dewar empty. The procedure used was to determine the activity of the silver targets (1) with the Dewar empty, (2) with the Dewar filled with liquid or solid hydrogen to a level approximately 5 cm above the top of the silver target, (3) same as the preceding but with the liquid hydrogen nearest the inner Dewar replaced by a 1.5 cm cylinder of paraffin, and (4) at room temperature, the Dewar being filled with a solution of methyl alcohol in acetic acid (21 percent alcohol by volume) which contained the same number of protons per cubic centimeter as does liquid hydrogen. Table I presents the results corrected for radon decay. The solid hydrogen was obtained by exhausting the Dewar until an equilibrium vapor pressure of 3.8 cm of mercury was obtained.

The comparison of Experiments $2a$–b either with Experiment 3 or with the experiments described in the preceding communication shows the great difference between liquid or solid hydrogen and a hydrocarbon. A comparison of Experiments 2 and 4 shows a nearly identical activity whether the Dewar is filled with hydrogen at very low temperatures or with a solution of the same proton density at room temperature. Moreover, the same result had been obtained in a preliminary experiment in a smaller Dewar in which the thickness of the liquid hydrogen layer around the soft glass Dewar was 3.5 cm instead of 5.5 cm. It would not be correct to conclude, however, that the liquid and solid hydrogen do not cool at all. The experiments indicate, rather, that the low speed neutrons have been cooled by liquid hydrogen at 20°K, and by solid hydrogen at 12°K, to a mean temperature of perhaps 150°K and that the increase in silver activity which should be thus produced has been nearly offset by the increase in capture by protons. This view is in agreement with the results of Fomin, Houtermans, Leipunsky and Schubnikow,[6] on the backward scattering of slow neutrons from liquid hydrogen and from water at room temperature.

In interpreting Experiment 3 we assume, therefore, that the 300°K neutrons which enter the Dewar have been partly cooled by the liquid hydrogen and then brought to very low velocities and consequently absorbed by the thin layer of paraffin. It must in any case be concluded that at very low temperatures paraffin has a much greater effect either in decelerating or absorbing these neutrons than cold hydrogen. Unless this difference can be ascribed to the carbon nucleus itself, and experiments with which we are now engaged should soon settle this question, the difference in behavior between very cold hydrogen and paraffin must be ascribed to the chemical bond.

TABLE I.

Experiment	Description	Activity of Ag (140 seconds)
1	Empty Dewar (300°K)	593±15
2*a*	Liquid hydrogen (20°K)	769±15
b	Solid hydrogen (12°K)	758±15
3	1.5 cm paraffin cylinder+liquid (20°K) hydrogen	579±15
4	Acetic acid solution (300°K)	776±15

Our experiments are analogous to those of Westcott and Niewodniczanski[4] on paraffin and hydrogen at 20°K. They performed two sets of experiments and found it impossible to reconcile their first set with their second. Our results agree closely with their first set.

The authors again wish to thank Professor G. N. Lewis for his interest and assistance in this work. They are also indebted to Mr. Samuel Ruben for assistance with the experimental work, and to Dr. L. R. Taussig and the University of California Hospital for donation of the radon used.

W. F. LIBBY
EARL A. LONG

Department of Chemistry,
University of California,
Berkeley, California,
September 3, 1936.

[1] Dunning, Pegram, Mitchell and Fink, Phys. Rev. **47**, 888 (1935).
[2] Moon and Tillman, Nature **135**, 904 (1935).
[3] Dunning, Pegram, Fink, Mitchell and Segrè, Phys. Rev. **48**, 704 (1935).
[4] Westcott and Niewodniczanski, Proc. Camb. Phil. Soc. **31**, 617 (1935).
[5] Moon and Tillman, Proc. Roy. Soc. **A153**, 476 (1936).
[6] Fomin, Houtermans, Leipunsky and Schubnikow, Physik. Zeits. Sowjetunion **9**, 696 (1936).

Resonance Energy of Cadmium for Neutron Capture

The experiments of Rasetti, Segrè, Fink, Dunning and Pegram[1] on the absorption of slow (thermal) neutrons by a layer of cadmium moving with a velocity relative to the neutron source have indicated that the collision cross section remains practically constant in an energy interval of about 20 percent of $3kT/2$. On the other hand Powers, Fink and Pegram[2] have reported a 7 percent increase in the absorption coefficient on lowering the neutron temperature from 300°K to 95°K.

It is of interest to consider these two sets of experimental data in terms of the Breit-Wigner formula for the cross section here involved. For this purpose the latter formula can be written in the form:

$$\sigma = 1/E^{\frac{1}{2}}\{(E \pm 1)^2 + B^2\},$$

where E and B are measured in energy units E_0; and σ, in arbitrary units. E_0 represents the resonance energy; and B, the half-width of the virtual level responsible for the capture. The plus sign refers to the case of positive resonance energy; and the minus sign, to the case of negative resonance energy.

For positive resonance energy it is easily seen that when $B<2/\sqrt{5}$ the cross section has both a minimum and a maximum value; and when $B=2/\sqrt{5}$, these two extremal values coalesce at a horizontal flex, for which $E=3/5$. For still broader resonance σ decreases steadily with increasing energy, without showing a resonance maximum. These variations in shape of the cross section curve are very clearly illustrated by a set of curves in σ and E for given values of B.

The failure in the first of the above-mentioned two sets of experiments to detect an appreciable variation of σ with E, throughout a 20 percent range around $3kT/2$, could be explained qualitatively, either if one of the extremal values of σ occurred at $E=3kT/2E_0$, approximately, or if the point $E=3kT/2E_0$ lay in the long flat portion of a curve with a horizontal flex.

It is, of course, not accurate to regard the thermal neutrons as a homogeneous group in energy, but one should rather consider them as having approximately a Maxwellian distribution, and interpret the experimental results in terms of appropriate integrals. At the present stage of experimental uncertainty it does not seem worth while to carry out such integrations; but by considering the neutrons as homogeneous one should be able to determine the order of magnitude of the resonance energy E_0 and the half-width BE_0. Each of the two sets of experiments permits an estimate of B as a double valued function of $3kT/2E_0$; and both taken together, an estimate of E_0 and B. Thus, taking $3kT/2=0.036$ volt, the two relations lead to a resonance energy of 0.05_5 volt and a half-width of about the same value. In view of the rough approximation in the method of interpretation assuming homogeneous thermal neutrons and of the wide limits of relative experimental error (due to the great difficulties connected with experiments of the type here discussed, especially the thermal experiments) the above values should be considered as giving little more than the order of magnitude of the quantities involved.

The possibility of a negative resonance energy would, of course, be excluded by the first set of experiments, since σ would have no extremal values for positive neutron energies, but would decrease more rapidly than $1/\sqrt{E}$.

Before making a more careful analysis of such data it would be desirable to have data similar to the above mentioned, in the first case with the neutron source at low temperatures, and in the second case for different temperature intervals.

E. SEGRÈ
C. T. ZAHN

Department of Physics,
University of Michigan,
Ann Arbor, Michigan,
September 3, 1936.

[1] Rasetti, Segrè, Fink, Dunning and Pegram, Phys. Rev. **49**, 104 (1936).
[2] Powers, Fink and Pegram, Phys. Rev. **49**, 650 (1936); see also Tillman, Proc. Phys. Soc. **48**, 642 (1936).